AD-A023 352

AN EXPERIMENTAL INVESTIGATION OF HIGH SUBSONIC FLOW OVER AN OFF AXIS LONGITUDINAL CAVITY WITH ANTIRESONANCE DEVICES

Kenneth Vaccaro

Air Force Institute of Technology
Wright-Patterson Air Force Base, Ohio

December 1974

KEEP UP TO DATE

Between the time you ordered this report—which is only one of the hundreds of thousands in the NTIS information collection available to you—and the time you are reading this message, several *new* reports relevant to your interests probably have entered the collection.

Subscribe to the **Weekly Government Abstracts** series that will bring you summaries of new reports *as soon as they are received by NTIS* from the originators of the research. The WGA's are an NTIS weekly newsletter service covering the most recent research findings in 25 areas of industrial, technological, and sociological interest—invaluable information for executives and professionals who must keep up to date.

The executive and professional information service provided by NTIS in the **Weekly Government Abstracts** newsletters will give you thorough and comprehensive coverage of government-conducted or sponsored research activities. And you'll get this important information within two weeks of the time it's released by originating agencies.

WGA newsletters are computer produced and electronically photocomposed to slash the time gap between the release of a report and its availability. You can learn about technical innovations immediately—and use them in the most meaningful and productive ways possible for your organization. Please request NTIS-PR-205/PCW for more information.

The weekly newsletter series will keep you current. But *learn what you have missed in the past* by ordering a computer **NTISearch** of all the research reports in your area of interest, dating as far back as 1964, if you wish. Please request NTIS-PR-186/PCN for more information.

WRITE: Managing Editor
5285 Port Royal Road
Springfield, VA 22161

Keep Up To Date With SRIM

SRIM (Selected Research in Microfiche) provides you with regular, automatic distribution of the complete texts of NTIS research reports *only* in the subject areas you select. SRIM covers almost all Government research reports by subject area and/or the originating Federal or local government agency. You may subscribe by any category or subcategory of our WGA (**Weekly Government Abstracts**) or **Government Reports Announcements and Index** categories, or to the reports issued by a particular agency such as the Department of Defense, Federal Energy Administration, or Environmental Protection Agency. Other options that will give you greater selectivity are available on request.

The cost of SRIM service is only 45¢ domestic (60¢ foreign) for each complete microfiched report. Your SRIM service begins as soon as your order is received and processed and you will receive biweekly shipments thereafter. If you wish, your service will be backdated to furnish you microfiche of reports issued earlier.

Because of contractual arrangements with several Special Technology Groups, not all NTIS reports are distributed in the SRIM program. You will receive a notice in your microfiche shipments identifying the exceptionally priced reports not available through SRIM.

A deposit account with NTIS is required before this service can be initiated. If you have specific questions concerning this service, please call (703) 451-1558, or write NTIS, attention SRIM Product Manager.

This information product distributed by

NTIS U.S. DEPARTMENT OF COMMERCE
National Technical Information Service
5285 Port Royal Road
Springfield, Virginia 22161

ADA023352

AIR FORCE INSTITUTE OF TECHNOLOGY

AIR UNIVERSITY
UNITED STATES AIR FORCE

AN EXPERIMENTAL INVESTIGATION OF
HIGH SUBSONIC FLOW OVER AN OFF AXIS
LONGITUDINAL CAVITY WITH
ANTIRESONANCE DEVICES

THESIS

GAE/AE/74D-26

Kenneth Vaccaro
Second Lieutenant
USAF

SCHOOL OF ENGINEERING

WRIGHT-PATTERSON AIR FORCE BASE, OHIO

Unclassified

SECURITY CLASSIFICATION OF THIS PAGE (When Data Entered)

REPORT DOCUMENTATION PAGE

READ INSTRUCTIONS BEFORE COMPLETING FORM

1. REPORT NUMBER GAE/AE/74D-26	2. GOVT ACCESSION NO.	3. RECIPIENT'S CATALOG NUMBER
4. TITLE (and Subtitle) AN EXPERIMENTAL INVESTIGATION OF HIGH SUBSONIC FLOW OVER AN OFF AXIS LONGITUDINAL CAVITY WITH ANTIRESONANCE DEVICES		5. TYPE OF REPORT & PERIOD COVERED AFIT THESIS 6. PERFORMING ORG. REPORT NUMBER
7. AUTHOR(s) Kenneth Vaccaro 2nd Lieutenant USAF		8. CONTRACT OR GRANT NUMBER(s)
9. PERFORMING ORGANIZATION NAME AND ADDRESS Air Force Institute of Technology Wright-Patterson Air Force Base, Ohio 45433		10. PROGRAM ELEMENT, PROJECT, TASK AREA & WORK UNIT NUMBERS
11. CONTROLLING OFFICE NAME AND ADDRESS		12. REPORT DATE December, 1974 13. NUMBER OF PAGES 98
14. MONITORING AGENCY NAME & ADDRESS(if different from Controlling Office) Air Force Flight Dynamics Laboratory Wright-Patterson Air Force Base, Ohio 45433		15. SECURITY CLASS. (of this report) Unclassified 15a. DECLASSIFICATION/DOWNGRADING SCHEDULE

16. DISTRIBUTION STATEMENT (of this Report)

Approved for public release; distribution unlimited.

17. DISTRIBUTION STATEMENT (of the abstract entered in Block 20, if different from Report)

18. SUPPLEMENTARY NOTES

Approved for public release: IAW AFR/190-17

Jerry C. Hix, CAPT USAF
Director of Information

19. KEY WORDS (Continue on reverse side if necessary and identify by block number)

Cavity Oscillations
Cavity Flow
Frequency Response (Cavity)
Antiresonance Devices
Ogive Cylinder

[redacted]

20. ABSTRACT (Continue on reverse side if necessary and identify by block number)

This study is a preliminary effort to reduce the level of the resonance and to provide a means of predicting the pressure gains and resonant frequencies associated with a forward facing cylindrical cavity in high subsonic flow. The basic model was an ogive cylinder fitted with an off-axis longitudinal cavity. Eleven different suppression devices were investigated.

Transmission line theory was used very effectively to predict the

DD FORM 1 JAN 73 1473 EDITION OF 1 NOV 65 IS OBSOLETE

Unclassified

SECURITY CLASSIFICATION OF THIS PAGE (When Data Entered)

pressure gains and resonant frequency when the flow was stagnated in the cavity and to predict the resonant frequency in flow situations. The resonant frequency occurred at or near the fundamental mode frequency of a right circular cavity.

The most effective anti-resonance device, a side relief hole, reduced the RMS pressure in the cavity by a factor as great as 23. Helmholtz resonators placed in the cavity were also shown to be effective, reducing the RMS pressure by a factor as great as 6.

iv-b

AN EXPERIMENTAL INVESTIGATION OF HIGH SUBSONIC FLOW OVER AN OFF AXIS LONGITUDINAL CAVITY WITH ANTIRESONANCE DEVICES

THESIS

GAE/AE/74D-26

Kenneth Vaccaro
Second Lieutenant
USAF

Approved for public release; distribution unlimited.

AN EXPERIMENTAL INVESTIGATION OF HIGH
SUBSONIC FLOW OVER AN OFF AXIS LONGITUDINAL
CAVITY WITH ANTIRESONANCE DEVICES

THESIS

Presented to the Faculty of the School of Engineering
of the Air Force Institute of Technology
Air University
in Partial Fulfillment of the
Requirements for the Degree of
Master of Science

by

Kenneth Vaccaro, B.S.
Second Lieutenant USAF

Graduate Aeronautical Engineering

December 1974

Approved for public release; distribution unlimited.

i-d

Preface

Relatively little research has been done on cavities that open into the flow. In the research that has been conducted, resonance in the cavity has been a major problem. This report describes my effort to reduce the level of the resonance and to provide a means of predicting the pressure gains and resonant frequencies associated with one such forward facing cavity system.

Many people provided valuable advice and assistance toward the conduct of this research. Most helpful were Dr. James T. Van Kuren of the Flight Dynamics Laboratory and my faculty adviser Dr. William C. Elrod, who together have motivated and advised my efforts. I would also like to thank Professor Milton Franke for his guidance in the transmission line theory area. Capt. William R. Conner and Mr. Daniel J. McDermott of the Flight Dynamics Laboratory deserve special notice for their assistance throughout the experimental and data reduction portions of the study. Finally, I'd like to thank my mother, whose love I could not do without, and whose upbringing has made this study even possible.

Kenneth Vaccaro

Table of Contents

		Page
Preface		ii
List of Figures		v
List of Symbols		vii
Abstract		ix
I.	Introduction	1
	Background	1
	Electric Analogy	2
	Objectives	3
II.	Description of Apparatus	4
	Models	5
	Baseline Model	5
	Cavity Suppression Devices	5
	Pressure Transducers	8
	RMS Meters	8
	Tape Recorder	9
	Auto-Correlator	9
	Frequency Analyzer	9
III.	Experimental Procedure	10
IV.	Application of Transmission Line Theory to the Study	11
	Cylindrical Cavity Approximation	11
	Transmission Line Theory	13
	Orifice Equation	17
	Transmission Line Theory Limitations	18
V.	Results--Discussion and Interpretation	19
	Predicting the Frequency Response of the Cavity	19
	Application of Theory to the Baseline Model	19
	Application of Theory to Anti-Resonance Devices	20

Table of Contents

	Page
Effectiveness of Antiresonance Devices . .	34
Root Mean Square Pressure Fluctuations.	34
Temperature Measurement	40
VI. Conclusions.	42
VII. Recommendations.	44
Applications	44
Further Investigations	44
Bibliography.	46
Appendix A: Cavity Resonance Devices	47
Appendix B: Transmission Line Models	56
Appendix C: Experimental Data (P_{rms}/q Versus X/D). .	65
Vita.	86

List of Figures

Figure		Page
1.	Schematic Diagram of Test Instrumentation	6
2.	Baseline Model Configuration.	7
3.	Circular Tube of Length L	12
4.	Baseline Model with Skewed Opening.	12
5.	Baseline Model with Corrected Length.	13
6.	Experimental Versus Calculated Fundamental Mode Resonant Frequency, Mach=0.85, Alpha = 0 . .	14
7.	Pneumatic Line System	15
8.	Baseline Model Pneumatic Line Configuration . . .	19
9.	Experimental and Theoretical Gains (P_B/P_A) for Baseline Model, Mach=0.85, X=1.565, Alpha = 0 . .	21
10.	Experimental and Theoretical Gains (P_B/P_A) for Baseline Model, Mach=0.85, X=1.565, Alpha = 6 . .	22
11.	Experimental and Theoretical Gains (P_B/P_A) for Baseline Model, Mach=0.85, X=1.565, Alpha =-6 . .	23
12.	Experimental and Theoretical Gains (P_B/P_A) for Baseline Model, Mach=0.70, X=1.565, Alpha = 0 . .	24
13.	Experimental and Theoretical Gains (P_B/P_A) for Model 1, Mach=0.85, X=1.565, Alpha = 0.	25
14.	Experimental and Theoretical Gains (P_B/P_A) for Model 2, Mach=0.85, X=1.565, Alpha = 0.	26
15.	Experimental and Theoretical Gains (P_B/P_A) for Model 3, Mach=0.85, X=1.565, Alpha = 0.	27
16.	Experimental and Theoretical Gains (P_B/P_A) for Model 4, Mach=0.85, X=1.565, Alpha = 0.	28
17.	Experimental and Theoretical Gains (P_B/P_A) for Model 5, Mach=0.85, X=1.565, Alpha = 0.	30

List of Figures

Figure		Page
18.	Experimental and Theoretical Gains (P_B/P_A) for Model 6, Mach=0.85, X=1.565, Alpha = 0.	31
19.	Experimental and Theoretical Gains (P_B/P_A) for Model 7, Mach=0.85, X=1.565, Alpha = 0.	32
20.	Experimental and Theoretical Gains (P_B/P_A) for Model 11, Mach=0.85, X=1.565, Alpha = 0	33
21.	Effectiveness of Models 1,2,3, and 4 in Reducing the RMS Pressure for Various Cavity Depths, Mach=0.85, Alpha = 0.	35
22.	Effectiveness of Models 5,6, and 7 in Reducing the RMS Pressure for Various Cavity Depths, Mach=0.85, Alpha = 0.	36
23.	Effectiveness of Models 8,9, and 10 in Reducing the RMS Pressure for Various Cavity Depths, Mach=0.85, Alpha = 0.	38
24.	Effectiveness of Models 3,7, and 11 in Reducing the RMS Pressure for Various Cavity Depths, Mach=0.85, Alpha = 0.	39
25.	Variation of Temperature for Increasing P_{rms}/q Level, Mach=0.85, Alpha = 6.	41
26-33.	Model Configurations, Anti-Resonance Devices .	48-55
34-41.	Pneumatic Line Configurations, Anti-Resonance Devices.	57-64
42-61.	Effectiveness of Models in Reducing the RMS Pressure for Different Test Conditions . .	66-85

List of Symbols

A	Line Cross-Sectional Area
Alpha, α	Angle of Attack
C	Sonic Velocity
D	Line Diameter
DC	Direct Current
DVM	Digital Volt Meter
F	Frequency
FM	Frequency Modulated
Irig B	Time Code Language
K	Flow Coefficient
L	Line Length
P, P_{rms}, P_{RMS}	Root-Mean-Square Pressure
q, Q	Dynamic Pressure
R	Line Radius
RMS	Root-Mean-Square
SYM	Symbol
T	Temperature
X	Cavity Depth
Y	Shunt Admittance/Unit Length
Z	Series Impedance/Unit Length
Z_c	Characteristic Impedance
ρ	Density
γ	Propagation Constant/Unit Length

List of Symbols

Subscripts

i	Line i
m	Mean
o	Orifice
r	Receiving End
s	Sending End

Abstract

This study is a preliminary effort to reduce the level of the resonance and to provide a means of predicting the pressure gains and resonant frequencies associated with a forward facing cylindrical cavity in high subsonic flow. The basic model was an ogive cylinder fitted with an off-axis longitudinal cavity. Eleven different suppression devices were investigated.

Transmission line theory was used very effectively to predict the pressure gains and resonant frequency when the flow was stagnated in the cavity and to predict the resonant frequency in flow situations. The resonant frequency occurred at or near the fundamental mode frequency of a right circular cavity.

The most effective anti-resonance device, a side relief hole, reduced the RMS pressure in the cavity by a factor as great as 23. Helmholtz resonators placed in the cavity were also shown to be effective, reducing the RMS pressure by a factor as great as 6.

AN EXPERIMENTAL INVESTIGATION OF HIGH SUBSONIC FLOW OVER AN OFF AXIS LONGITUDINAL CAVITY WITH ANTIRESONANCE DEVICES

I. Introduction

Background

Several applications exist within the Air Force for the use of optical equipment on aircraft during flight. In most cases it is desirable to have minimum losses along a light path from the aircraft to an external point. Often an open port is used to minimize the surface reflections, scattering, and absorption associated with a window material. The open cavity can act as an acoustic resonator and amplify internal pressure fluctuations. These pressure fluctuations may affect internal optical components.

Previous studies of open cavities in aerodynamic flows have almost exclusively been directed toward cavities which are normal to the free stream (Ref 2). Recently, however, a need has developed to look at cavities that open into the flow. An investigation of transonic flow around an ogive cylinder with a forward facing cylindrical cavity has shown that at deep cavity positions clearly unacceptable resonance levels (P_{rms}/q greater than 1.1) were present (Ref 5).

A means of predicting and controlling the resonance level is needed in order to use the longitudinal cavity configuration in aircraft.

Electric Analogy

One means of predicting the pressure gains and resonant frequencies of an open cavity is through the use of a pneumatic-electric analogy. The cavity can be modeled using existing electrical transmission line theory.

Numerous theoretical and experimental studies have been conducted using transmission line theory to accurately predict the dynamic characteristics of fluid lines. The basic theory can be found in an article by Nichols (Ref 7). Krishnaiyer and Lechner (Ref 6) found good agreement between their experimental data on blocked pneumatic lines, and calculations based on a modification of Nichol's theory. Franke, Malanowski, and Martin (Ref 3) experimented with more complicated pneumatic lines that were neither of uniform cross section along the length of the line nor necessarily blocked at the end. In this study they considered the effects of line branching in parallel and mean laminar or turbulent flow. Bird (Ref 1) formulated a computer program to calculate the pressure transfer function for an arbitrary line network where the lines were of circular cross section and each line segment was of constant radius. The program was based on Nichol's theory as modified by Krishnaiyer and Lechner. Agreement

between the theoretically based program, and experiments performed by Bird was very good. Franke, Karam, and Lymburner (Ref 4) showed that for lines of non-circular cross sections hydraulic diameters can be used with good agreement between experiment and theory.

Objectives

This study has two major objectives: first, to predict the pressure gains and resonant frequencies of a forward facing cylindrical cavity offset from the axis of an ogive cylinder using existing electrical transmission line theory; and second, to determine the effectiveness of various experimental cavity suppression devices in reducing the resonance in the cavity by a wind tunnel investigation.

II. Description of Apparatus

An investigation of the dynamic characteristics of a forward facing cavity and the effect of various resonance suppression devices on the RMS pressure fluctuations was conducted in the U. S. Air Force Flight Dynamics Laboratory Trisonic Gasdynamics Facility (Ref 10). The model used in the test was basically the same one that was used in Icardi's experiment (Ref 5).

Two types of measurements were taken during the test; the RMS pressure in the cavity, and the temperature in the cavity. The equipment used in the investigation consisted of a baseline model, 11 cavity suppression devices, 3 dynamic pressure transducers, and a thermocouple.

The outputs of the pressure transducers were processed by RMS meters and converted from analog to digital form with a Hewlett-Packard Model 9810 Desk Calculator. The calculator also plotted dynamic pressure versus depth on an attached digital control plotter. The outputs of the pressure transducers were then passed through an auto-correlator that was used to compute and display the auto-correlation function of the pressure data on a cathode-ray tube. A frequency analyzer was used to perform the discrete Fourier transform of the auto-correlation function display and present the results on its own storage cathode-ray tube. The outputs of the transducers were also recorded on magnetic tape.

The temperature recorded from the thermocouple was converted from analog to digital form through the use of the Hewlett-Packard 9810 Calculator. A schematic diagram of the test instrumentation is presented in Fig 1.

Models

Baseline Model (Model 0). The baseline model shown in Fig 2. was an ogive cylinder with a forebody fineness ratio of four. The ogive cylinder was fitted with an off-axis longitudinal cylindrical cavity. In Icardi's original experiment the diameter of the cavity was varied through the use of inserts of various diameters. In this investigation only a 0.5625-in.-ID insert was used.

The cavity depth was varied through the use of a moveable piston that was remotely positioned by a 27 VDC motor mounted in the model. The position of the piston was sensed by a linear potentiometer mechanically linked to the piston. The piston was sealed with a rubber O-ring to prevent leakage. Three Kulite pressure transducers and one thermocouple were mounted on the face of the piston.

Cavity Suppression Devices. Eleven suppression type devices were tested to determine the influence of each on the RMS pressure fluctuations in the cavity. Models 1,2, 3, and 4 were all Helmholtz resonators with various geometries, intended to not only reduce the resonance, but to facilitate packaging into an aircraft nose section. Model 1 was a conventional Helmholtz resonator with a cylindrical volume.

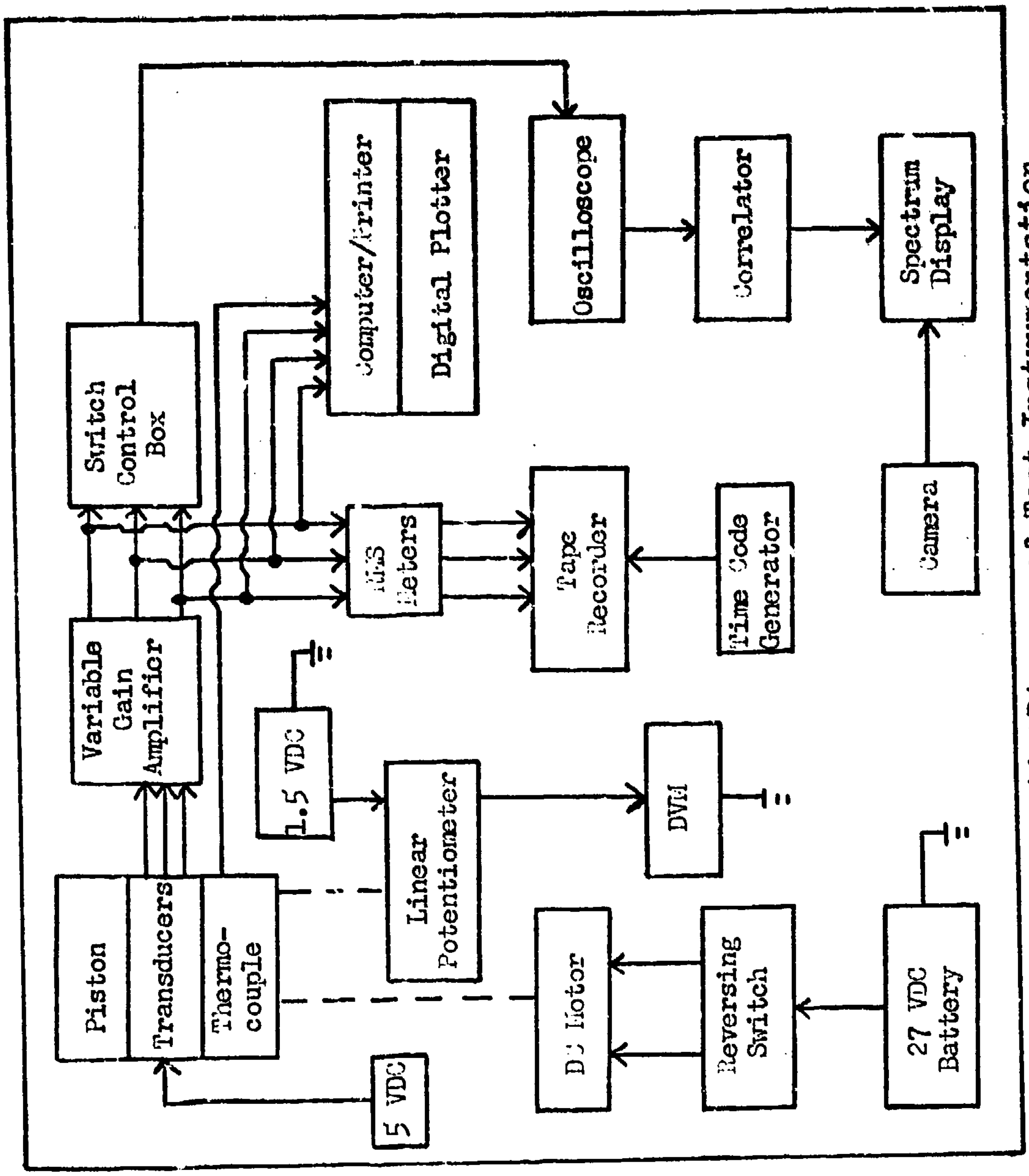

Fig. 1. Schematic Diagram of Test Instrumentation

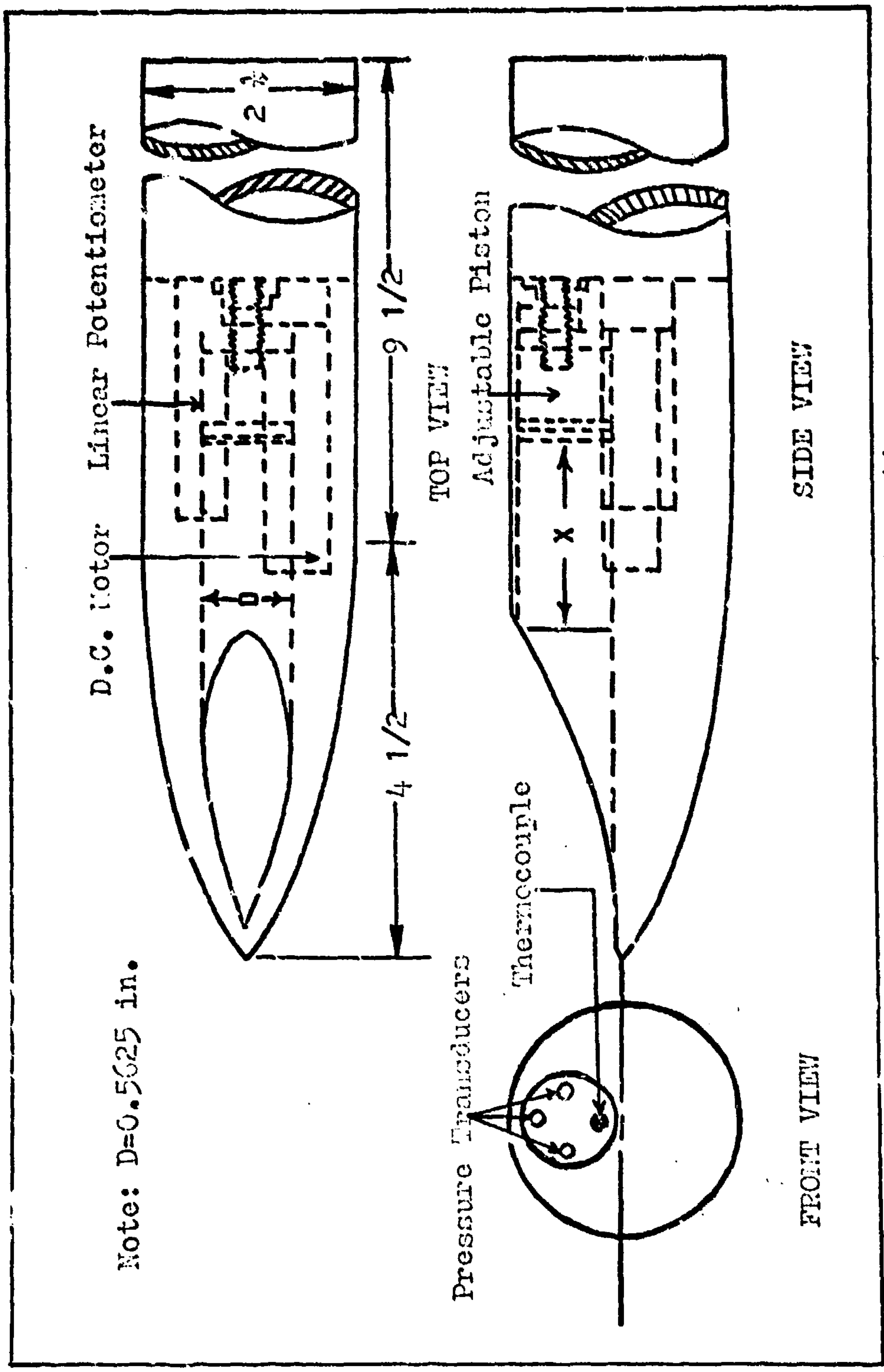

Fig. 2. Baseline Model Configuration

Model 2 had a cylindrical-segment volume. Models 3 and 4 had a combined cylindrical annular and cylindrical-segment volume. Models 5,6, and 7 consisted of the baseline model with side relief holes of various diameters. The diameters were respectively 1/8 in., 1/4 in., and 3/8 in. Model 8 consisted of the baseline model, a side relief hole of 3/8 in., and a scoop attachment to the side relief hole. Model 9 consisted of the baseline model with a 1/4 in. thick polystyrene foam lining. Model 10 consisted of the baseline model with a porous fence of approximately 0.30 porosity lined around the opening of the cavity. Model 11 consisted of a combination of models 3 and 7. Diagrams of each of the devices are presented in Appendix A.

Pressure Transducers

Three Kulite model XCQL-14-093-25 high response, variable reference, pressure transducers were used to measure the pressure variations on the base of the cavity. The transducers have a frequency response of at least 20 kHz and are self compensating for temperature.

RMS Meters

Three Hewlett-Packard model 3400A RMS volt meters were used to process the pressure data. Their output is the root-mean-square of the variations in the input signal with an integration time of two seconds.

Tape Recorder

The pressure data was recorded on magnetic tape with an Ampex model CP100, 14 channel, FM, tape recorder. It has a maximum input of 1.4 volts/channel and a frequency response good to 10 kHz. A standard FM time code generator using Irig B was used to mark the tape for later data correlation. The outputs of the transducers were visually monitered on an oscilloscope to insure that they remained within the range of the recorder.

Auto-Correlator

The auto-correlation of the pressure data was performed by the Hewlett-Packard Model 3721A Correlator. The correlator features the simultaneous computation and display of 100 points of the function selected. The correlator has an input amplifier bandwidth of 0 to 250 kHz. The input range is 40 mV, to 4 V RMS.

Frequency Analyzer

The Fourier transform of the auto-correlation function was performed by a 3720A Spectrum Display, a special purpose analyzer for use with the 3721A Correlator. The frequency range of the display is 0.005 Hz to 250 kHz. The ratio of full scale signal to noise level, for any fixed gain, is better than 50 dB.

III. Experimental Procedure

In order to establish a basis for comparing the effectiveness of the suppression devices extensive testing was first conducted on the baseline model. For each Mach number the model was first positioned at 0 degrees angle of attack. The piston was driven from the lip of the cavity to its maximum depth at a rate of 1 inch/minute. As the piston moved, the RMS pressure variations in the cavity were plotted versus the cavity depth. The piston was then repositioned at the lip of the cavity. Next, the piston position was varied and at each interval of 0.125 in. the RMS pressure was recorded from the RMS meters and the temperature was noted. Also, at each position a power-spectral-density was obtained by photographing the display on a CRT. The pressure data was then recorded on tape. The outputs of the transducers were monitored on an oscilloscope to insure that the AC and DC levels remained within the range of the tape recorder. The AC levels were controlled by varying the transducer gains and the DC levels adjusted by changing the transducer reference pressures.

The model was then tested using the same procedure but at angles of attack of 6 and -6 degrees. The model was tested at Mach numbers of both 0.85 and 0.70.

The 11 suppression devices were tested using the same procedure as outlined above for the baseline model.

IV. Application of Transmission Line Theory to the Study

Transmission line theory was used to predict the pressure gains and the resonant frequencies of the forward facing cavity making use of a computer program written by Bird for circular lines (Ref 1). The theory assumes that the diameters of the lines are small in comparison to the lengths of the lines and the wavelength of the sound. This assumption assures that only plane wave oscillations are present in the cavity. The theory also assumes that there is no mean flow in the system. Even with the no mean flow assumption, the theory has been shown to be effective in predicting the pressure gains and resonant frequencies when flow was present in the system (Ref 4).

To apply the theory, the cylindrical cavity, which was truncated at one end, was first approximated as a right cylindrical cavity by making a length correction to the overall cavity length. The approximated model was then used in the transmission line analysis.

Cylindrical Cavity Approximation

When an air column is set into resonant vibration by blowing, stationary waves are set up in the column due to the combined effects of the direct and end reflected waves.

A circular tube open at one end and closed at the other (Fig 3) has a natural resonant frequency of (Ref 8:2)

$$F_{1,2,3} = N(C/4L) \qquad N=1,3,5 \tag{1}$$

where C is the sonic velocity, L is the length of the tube, and F_1 is the fundamental frequency, F_2 is the second harmonic, F_3 is the third harmonic, etc.

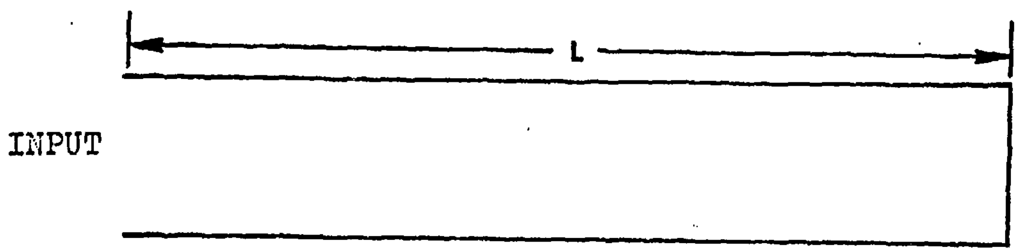

Fig. 3. Circular Tube of Length L

The model used in the study had a cylindrical cavity with a skewed opening at the forward end (Fig 4).

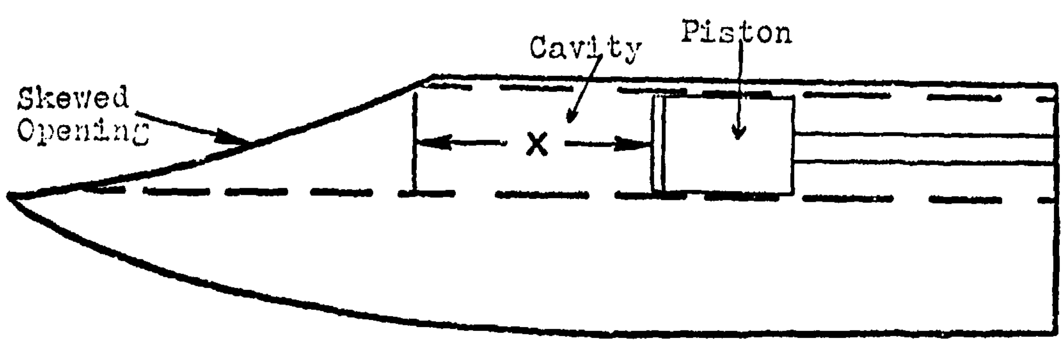

Fig. 4. Baseline Model with Skewed Opening

A length correction of 1.026 in. when added to the cavity depth X (Fig 5) produced close correlation between the

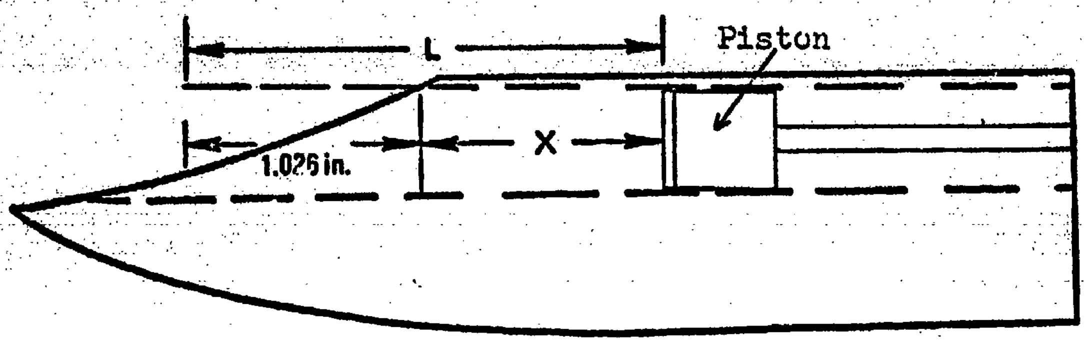

Fig. 5. Baseline Model with Corrected Length

observed experimental resonant frequencies and the resonant frequencies calculated using the corrected cavity length L=X+1.026 in. in Eq 1. Fig 6 shows a comparison of observed versus calculated resonance frequencies for various cavity depths at a Mach number of 0.85 and angle of attack of 0 degrees. Throughout the entire test the corrected length L varied at most by 0.03 in. from the value of X+1.026 in.

In the experiment only the fundamental mode was excited to a significant level. The second harmonic was present but at a RMS pressure level 30 to 40 dB lower than the fundamental mode RMS pressure level.

Transmission Line Theory

The transmission line theory used in the analysis was

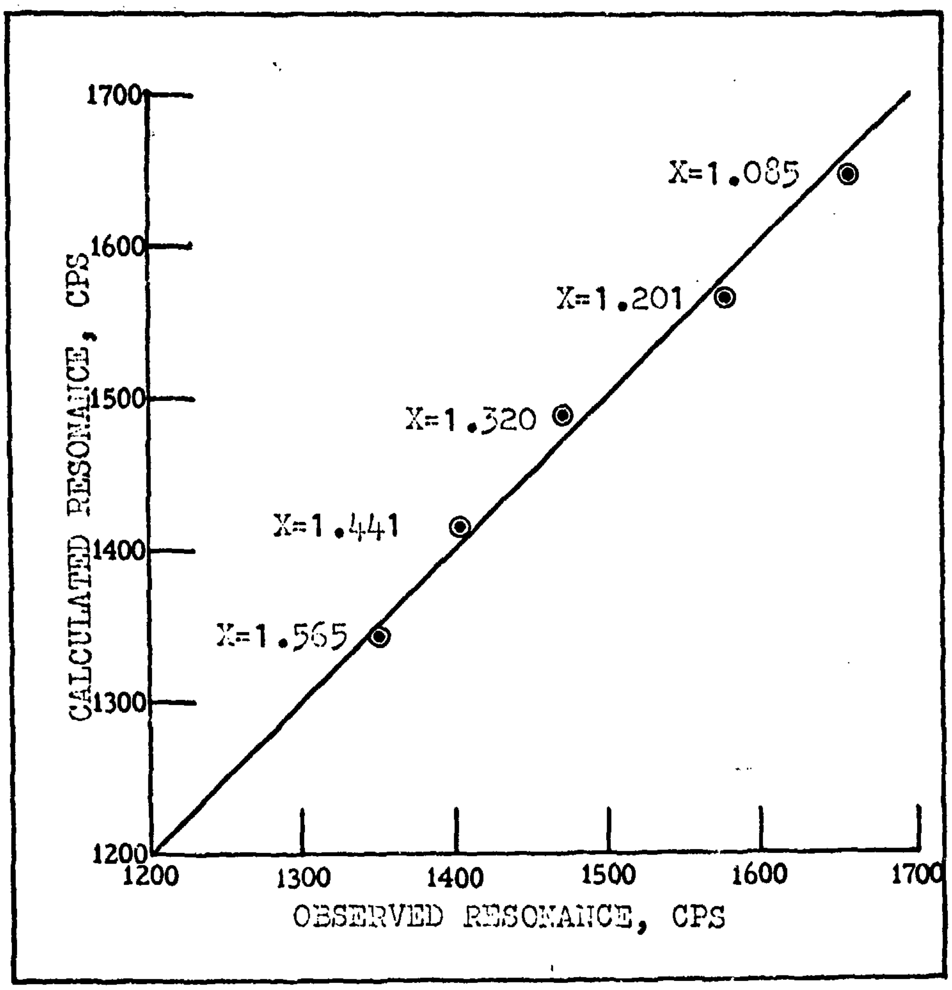

Fig. 6. Experimental Versus Calculated Fundamental Mode Resonant Frequency, Mach=0.85, Alpha=0

applied through the use of a computer program written by Bird for circular lines (Ref 1). The corrected cavity length L was used as the overall system length in the program.

To apply the theory, the cavity length was first separated into a series of line sections. A simplified pneumatic line system is shown in Fig 7. For use in Bird's program this simplified line system would be broken into

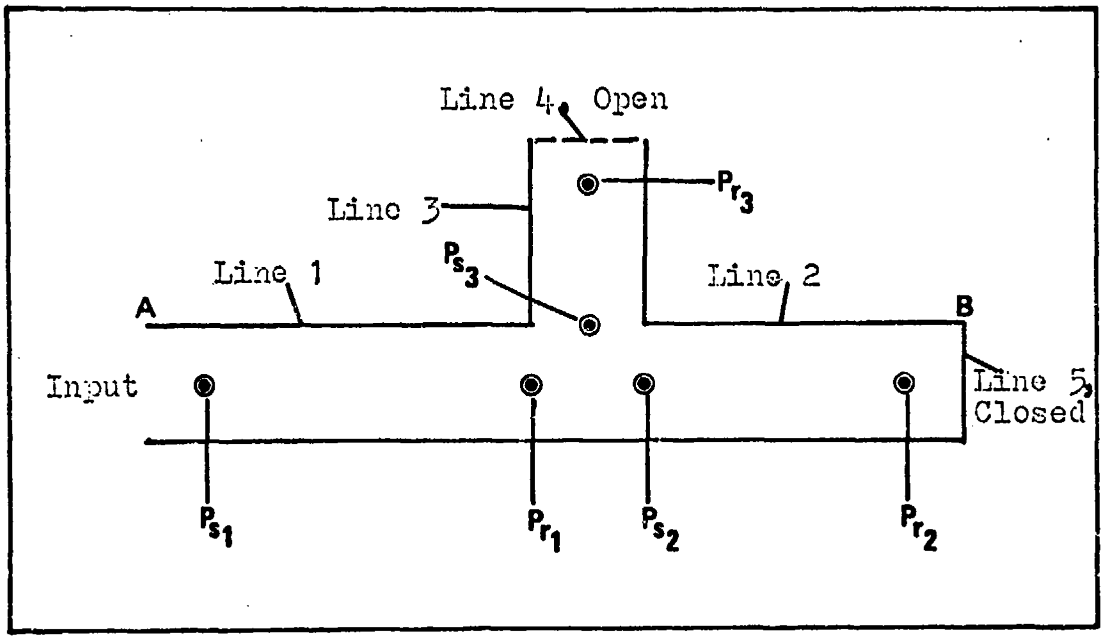

Fig. 7. Pneumatic Line System

5 line sections. The computation which is needed to compare the experimental results with the line theory is the pressure transfer function or the pressure gain between points B and A.

If the impedance Z_r at the end of a line i is known, the

input impedance of line i of length L is given by

$$Z_s = Z_c \frac{(Z_r + Z_c) + (Z_r - Z_c)\exp(-2\gamma L)}{(Z_r + Z_c) - (Z_r - Z_c)\exp(-2\gamma L)} \tag{2}$$

where the characteristic line impedance Z_c and the propagation constant γ are calculated using the equations for the shunt admittance Y and the series impedance Z given by Krishnaiyer and Lechner. The impedance Z_r at the end of an open line is calculated using orifice Eq 6 which is discussed in the next section. In Bird's program an open end is treated as a line section of zero length with a diameter equal to the diameter of the line leading to the open end. The impedance Z_r at the end of a closed line is equal to ∞ and is treated as a line section of zero diameter and zero length.

On each line section the input impedance $Z_s(L_i+1)$ of line i+1 is the output impedance $Z_r(L_i)$ of the preceding line i. In order to calculate the impedance at a junction the pressure is assumed to be uniform at the junction. Thus, the impedance Z_{r_1} is given by

$$\frac{1}{Z_{r1}} = \frac{1}{Z_{s2}} + \frac{1}{Z_{s3}} \tag{3}$$

Then, with the impedance known anywhere along the line network, the pressure gain can be calculated for each individual line using

$$\left|\frac{P_r}{P_s}\right|_i = \frac{2Z_c Z_r \exp(-\gamma L)}{Z_c(Z_r + Z_c) + (Z_r - Z_c)Z_c \exp(-2\gamma L)} \tag{4}$$

Finally, the magnitude of the transfer function $|P_B/P_A|$ can be calculated from the product of the individual line transfer functions using

$$\left|\frac{P_B}{P_A}\right| = \prod_{i=1}^{n} \left|\frac{P_r}{P_s}\right|_i \tag{5}$$

where the product is taken across all line sections between points B and A.

Orifice Equation

The impedance of an orifice is based on the steady flow orifice resistance. It is assumed that the DC flow characteristics of the orifice can be used to predict the AC flow characteristics and that the load impedance is purely a resistance which does not vary with frequency. The resulting impedance of the orifice is assumed to be given by

$$Z_o = \sqrt{\frac{2\rho\Delta P_m}{A_o^2 K^2}} \tag{6}$$

where ΔP_m is the change in pressure across the orifice, A_o is the cross-sectional area of the orifice, and K is an experimentally determined flow coefficient (0.6 is used in this investigation). The density is assumed constant across the orifice.

Transmission Line Theory Limitations

Two major limitations exist in the application of transmission line theory to this study. First, the theory is dependent only on line gepmetry, mean input pressure, atmospheric pressure, and temperature. Therefore, there is no way at present of adding in angle of attack effects and Mach number changes. Second, the theory can only be used to analyze the resonance devices that consisted of modifications to the line geometry itself. As a result, model 8 (scoop attachment), model 9 (foam insert), and model 10 (porous fence) could not be modeled using a transmission line approach.

V. Results--Discussion and Interpretation

The results presented in this chapter are grouped into two sections. The first section deals with predicting the frequency response of the cavity. The second section deals with the effectiveness of the various suppression devices in reducing the RMS pressure fluctuations.

Predicting the Frequency Response of the Cavity

Transmission line theory was used to predict the frequency response of the baseline model, models 1 thru 7, and model 11. The corrected cavity length, L=X+1.026 in., was used in all cases as the overall length of the cavity.

Application of Theory to the Baseline Model. The baseline model was separated into two line sections as shown in Fig 8.

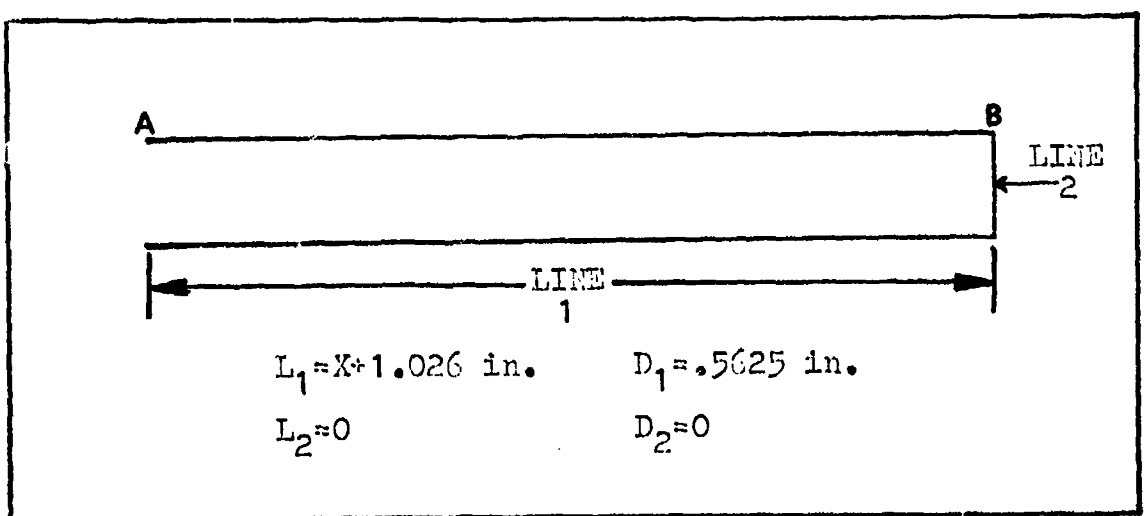

Fig. 8. Baseline Model Pneumatic Line Configuration

Comparisons between theory and experiment for different test conditions in the form of gain, (P_B/P_A), versus frequency curves are shown in Figs 9 thru 12. The X's represent the experimental points and the curves represent the theory. Since the input RMS pressure at point A was not measured, an approximate method had to be used to plot the experimental points on the figures. This was accomplished by first making one experimental point fall on the theoretical curve and then normalizing all other points with respect to the first point. Figure 9 shows very good correlation between theory and experiment. Figures 10 and 11, when compared with Fig 9, show that angles of attack of 6 and -6 degrees had little or no effect on the pressure gains and resonant frequency of the cavity. Similarly, comparing Fig 12 with Fig 9, shows that changing the Mach number from 0.85 to 0.70 had little effect on the frequency response of the cavity.

Application of Theory to Anti-Resonance Devices. Models 1 thru 7 and model 11 were examined in a similar manner as the baseline model. The same approximate method used to plot the experimental points for the baseline model was used for the anti-resonance devices. Hydraulic diameters were used when the lines were of non-circular cross section. The internal breakdown of each model into line sections is shown in Appendix B.

Figures 13,14,15, and 16 show a comparison between theory and experiment for the four Helmholtz resonators,

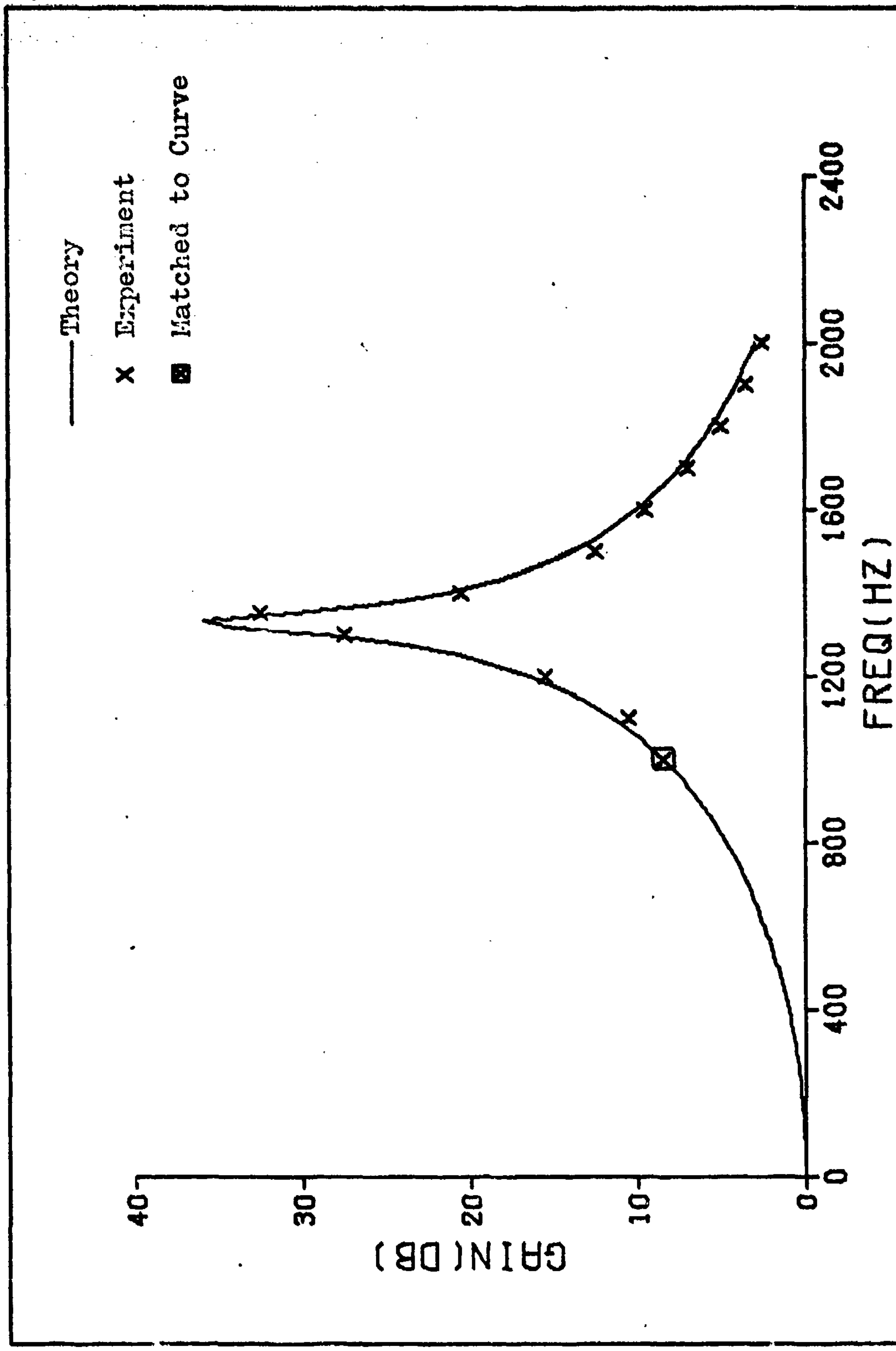

Fig. 9. Experimental and Theoretical Gains (P_B/P_A) for Baseline Model, Mach=0.85, X=1.565, Alpha =0

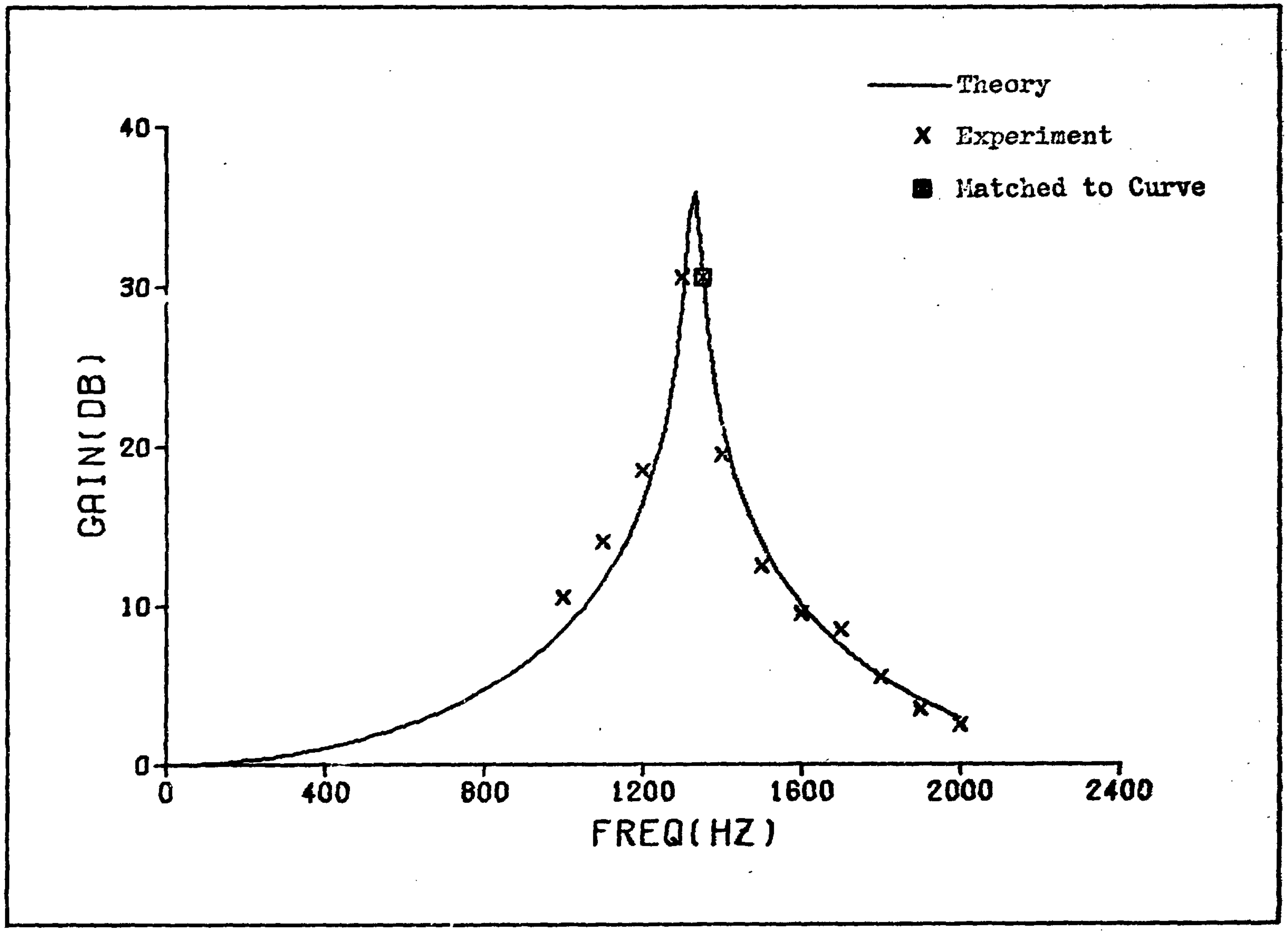

Fig. 10. Experimental and Theoretical Gains (P_B/P_A) for Baseline Model, Mach=0.85, X=1.565, Alpha =+6

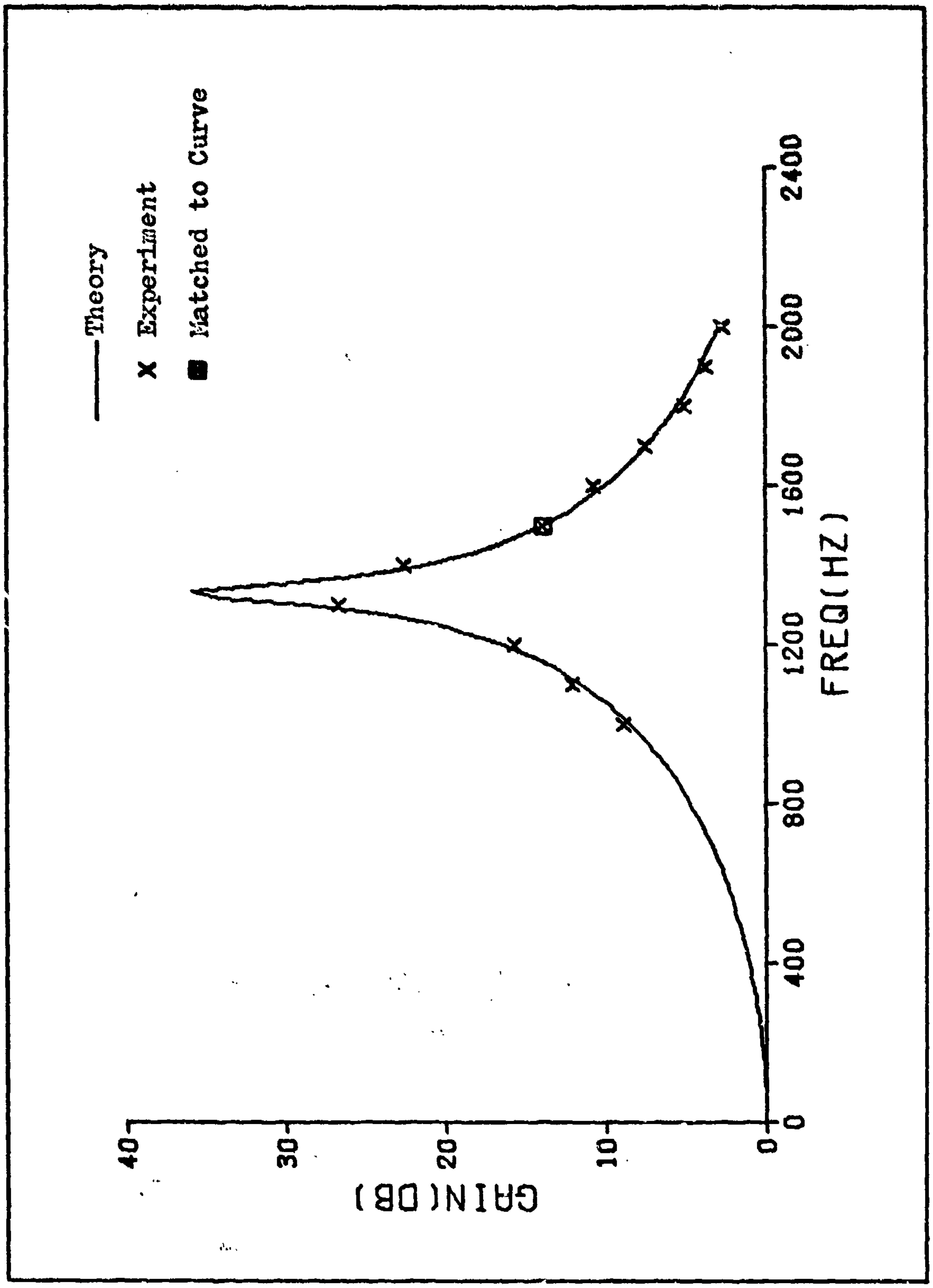

Fig. 11. Experimental and Theoretical Gains (P_B/P_A) for Baseline Model, Mach=0.85, X=1.565, Alpha =-6

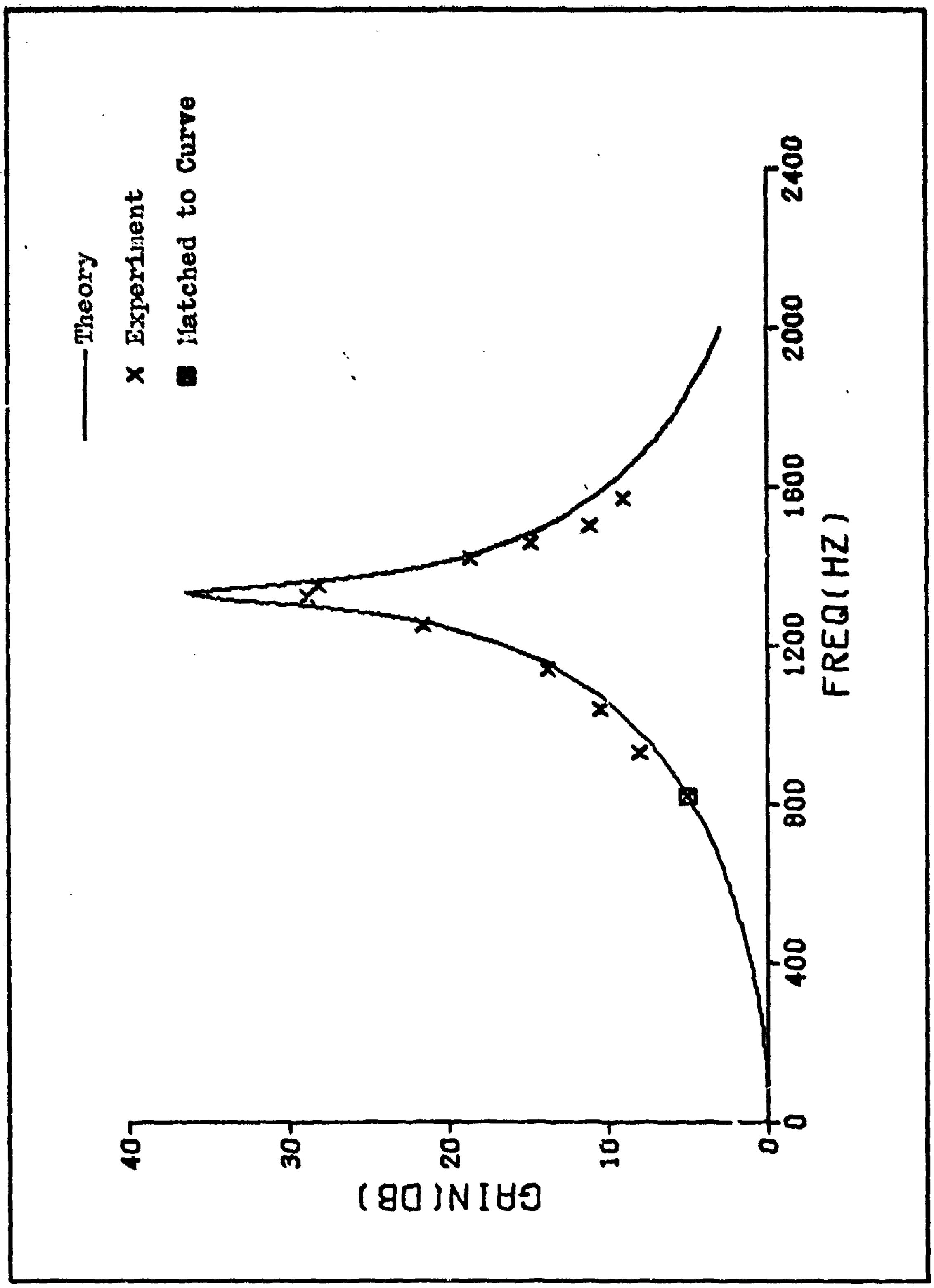

Fig. 12. Experimental and Theoretical Gains (P_B/P_A) for Baseline Model, Mach=0.70, X=1.565, Alpha=0

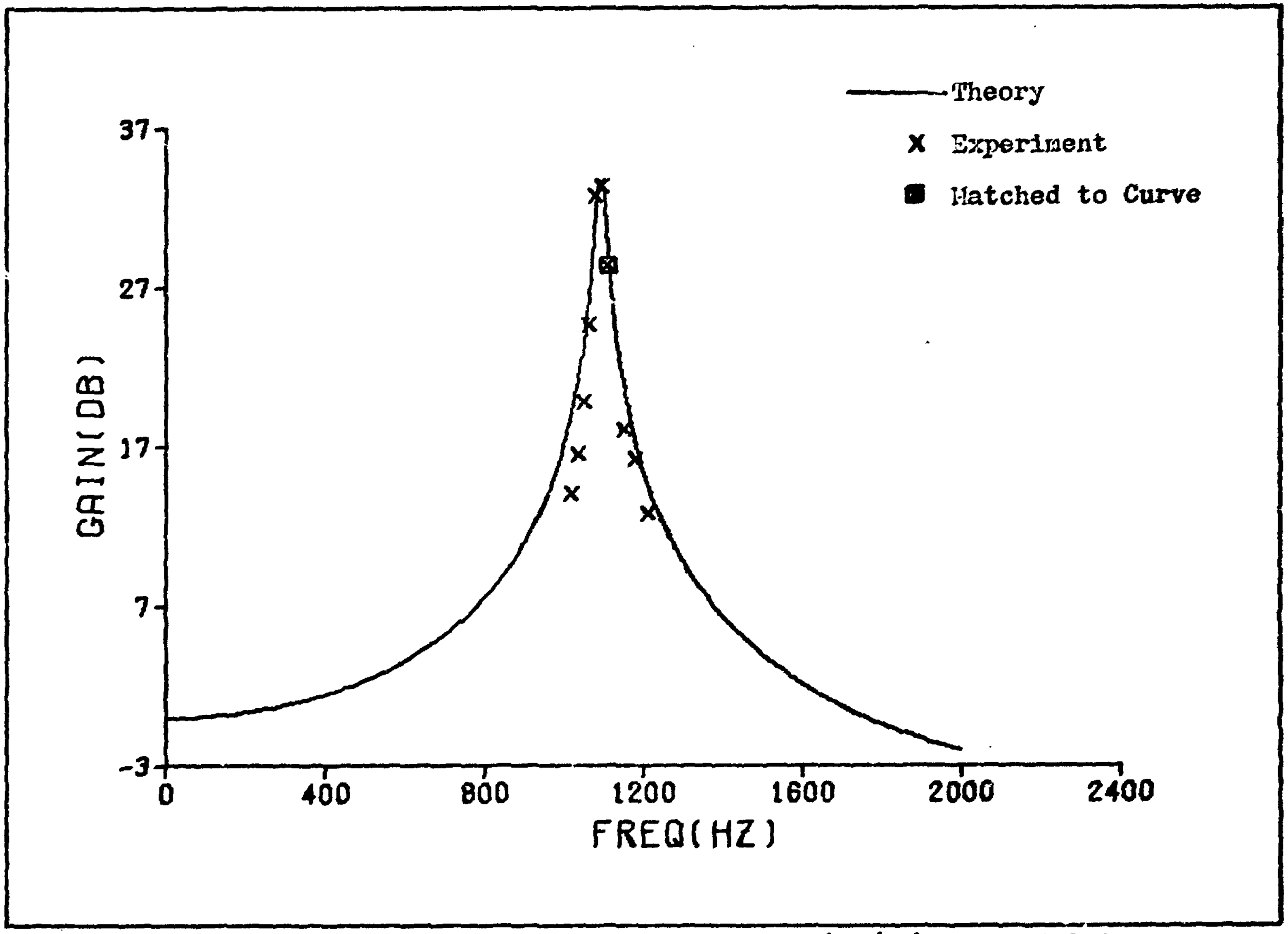

Fig. 13. Experimental and Theoretical Gains (P_B/P_A) for Model 1, Mach=0.85, X=1.565, Alpha = 0

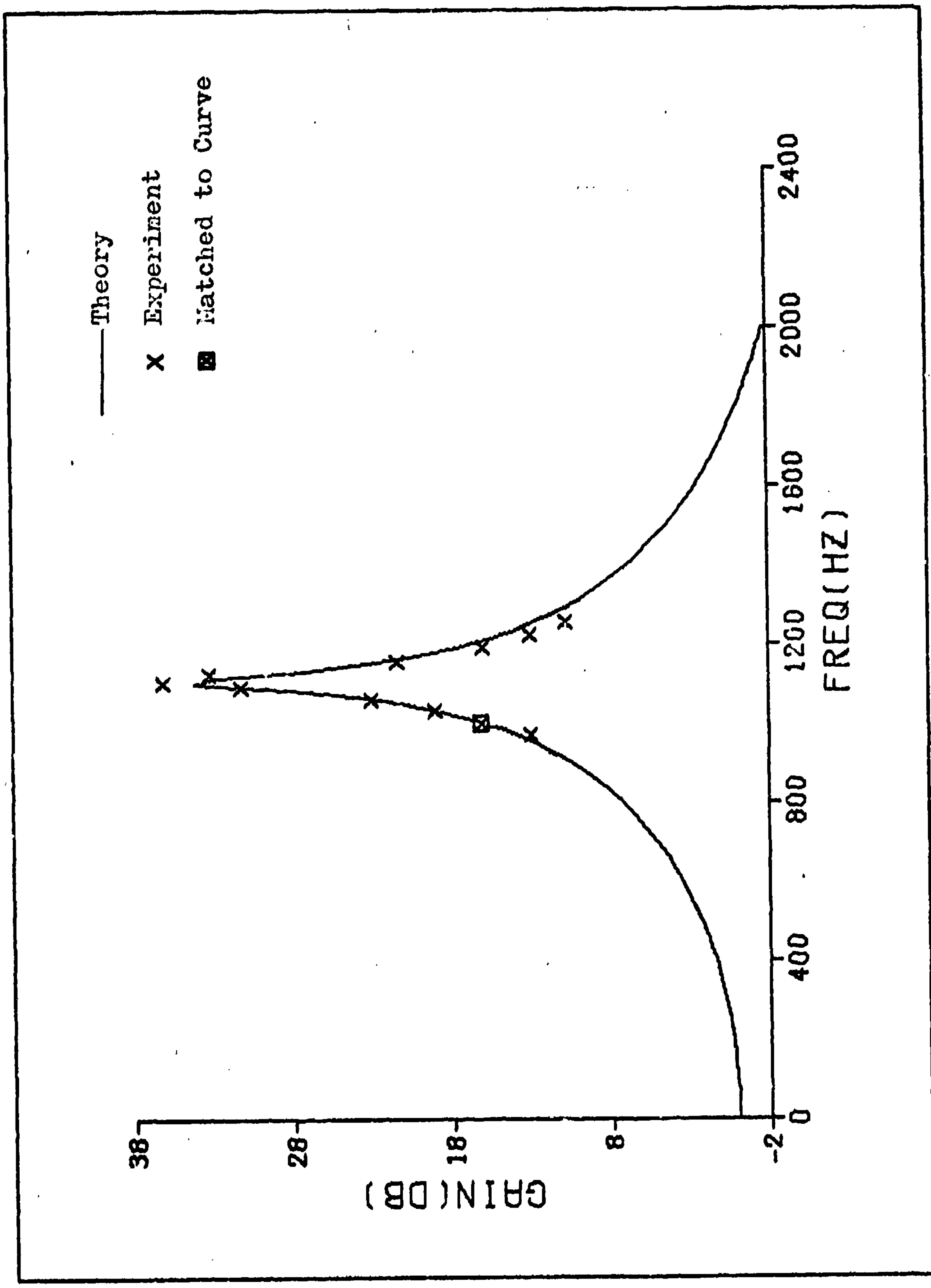

Fig. 14. Experimental and Theoretical Gains (P_T/P_A) for Model 2, Mach=0.85, X=1.565, Alpha = 0

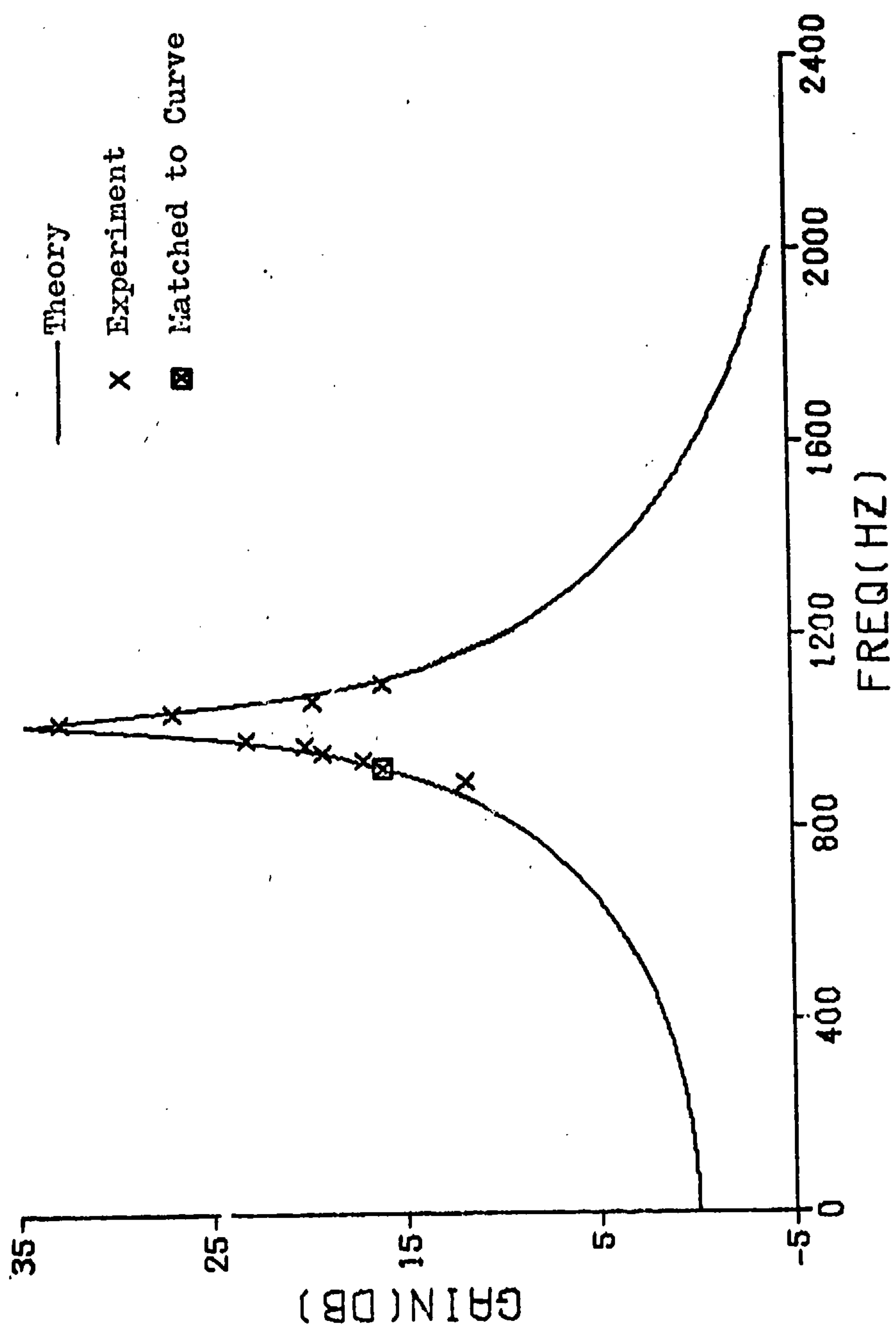

Fig. 15. Experimental and Theoretical Gains (P_B/P_A) for Model 3, Mach=0.85, X=1.565, Alpha = 0

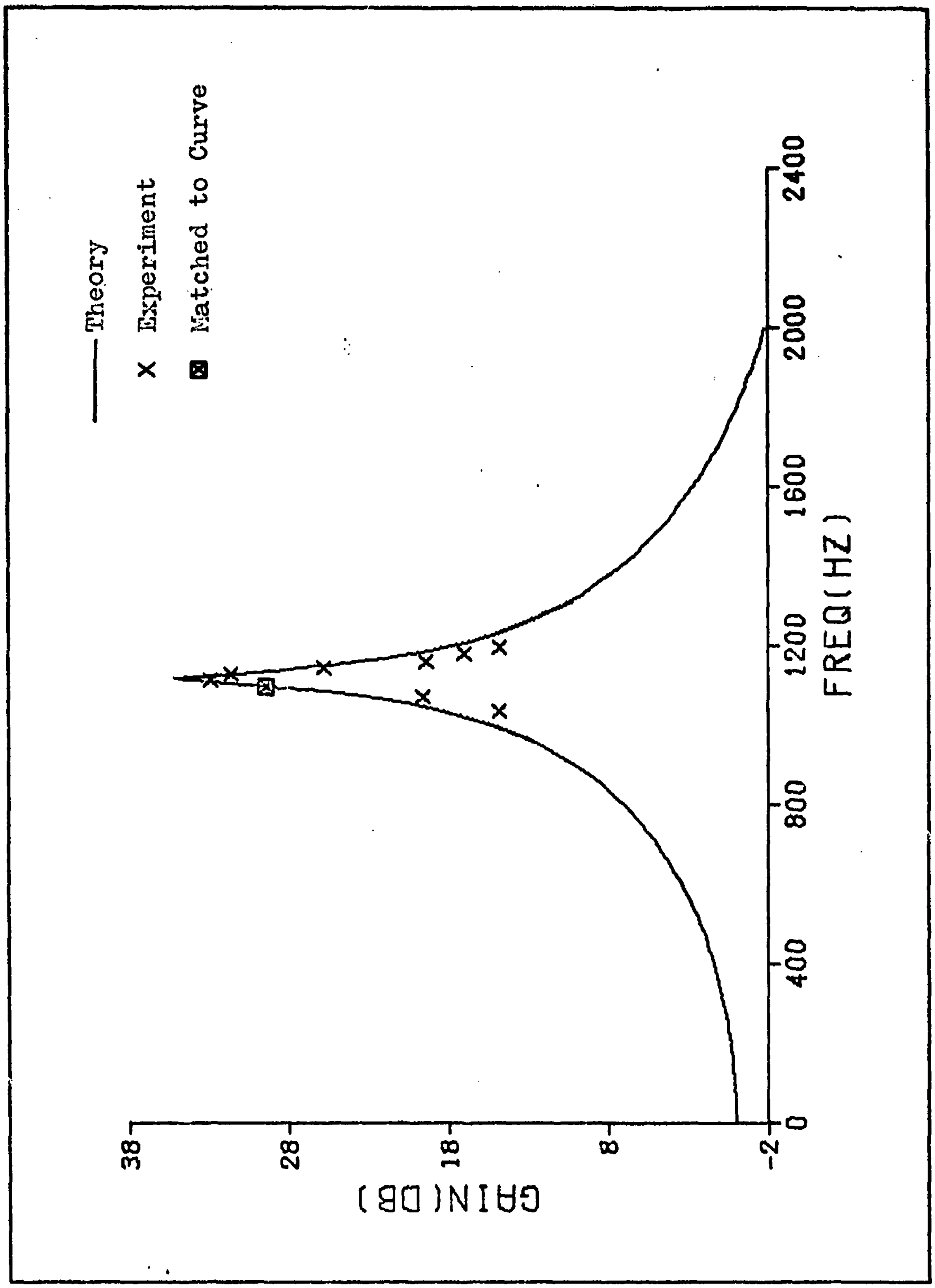

Fig. 16. Experimental and Theoretical Gains (P_B/P_A) for Model 4, Mach=0.85, X=1.565, Alpha = 0

models 1,2,3, and 4 respectively. The theory and experimental data, as in the case of the baseline model, showed very good correlation. The relief hole models (models 5,6, and 7) and model 11, a combination of a relief hole and a Helmholtz resonator, were not simulated as well by theory as the other 5 models. This is quite evident when the figures for models 5,6,7, and 11 (Figs 17,18,19, and 20) are compared with the figures already presented for the other models. The resonant frequency was still predicted very accurately, but there were significant deviations between the theoretical and experimentally determined gains. The reason the pressure gains were not predicted accurately in these last four models was that two assumptions of the theory were violated. First, the constant density assumption of the theory was violated due to high speed flow that was introduced into the cavity at free stream Mach numbers of 0.85 and 0.70. Second, the theory and experiment did not agree closely because of inaccuracies in the mean input pressure value which was not measured but was assumed to be equal to the tunnel stagnation pressure. This approximation is good when the flow in the cavity is stagnated, which was the case in models 0 thru 4. But, because there was cavity flow in models 5,6,7, and 11, the stagnation pressure was not a good approximation of the mean input pressure.

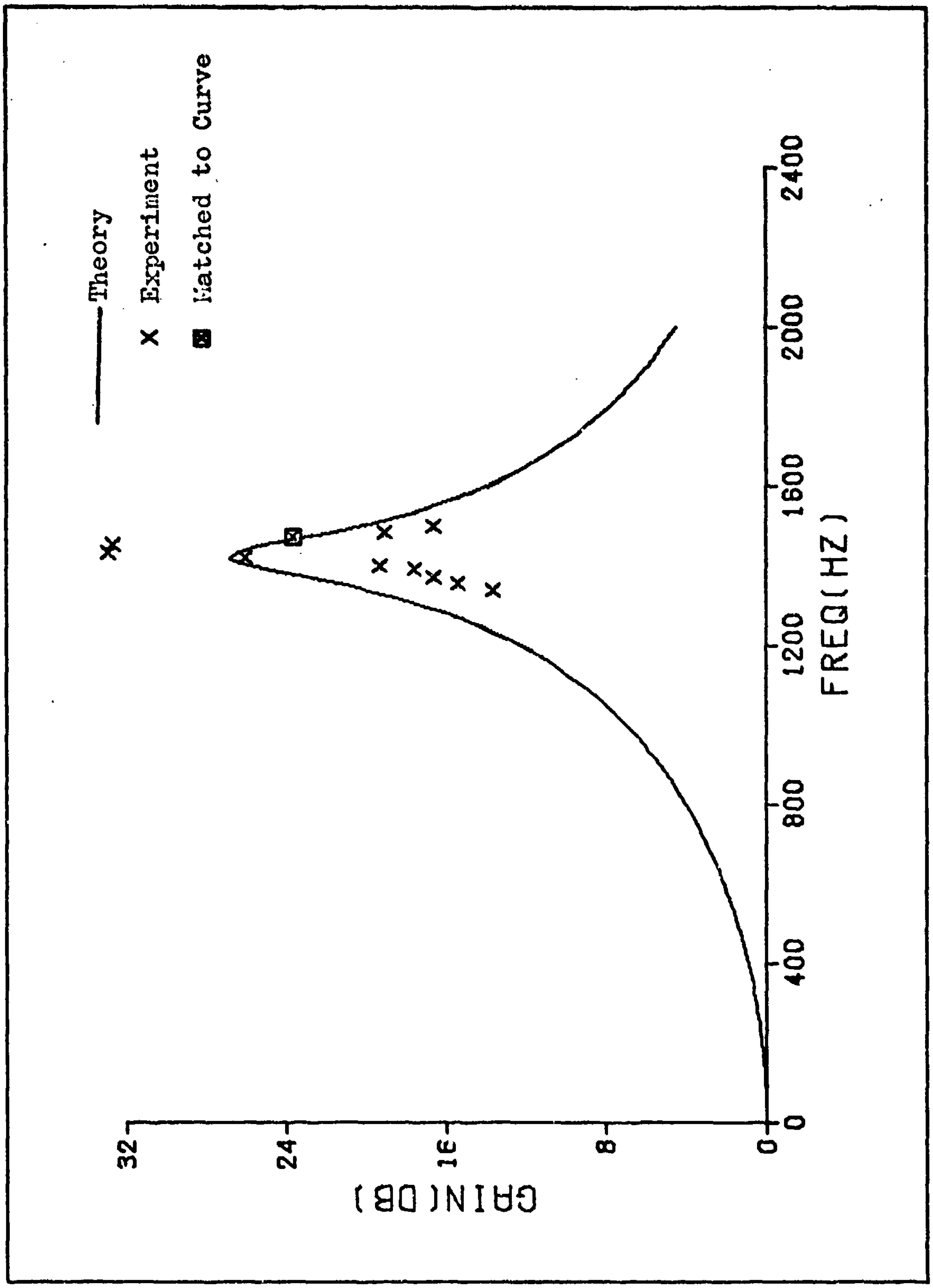

Fig. 17. Experimental and Theoretical Gains (P_B/P_A) for Model 5, Mach=0.85, X=1.565, Alpha = 0

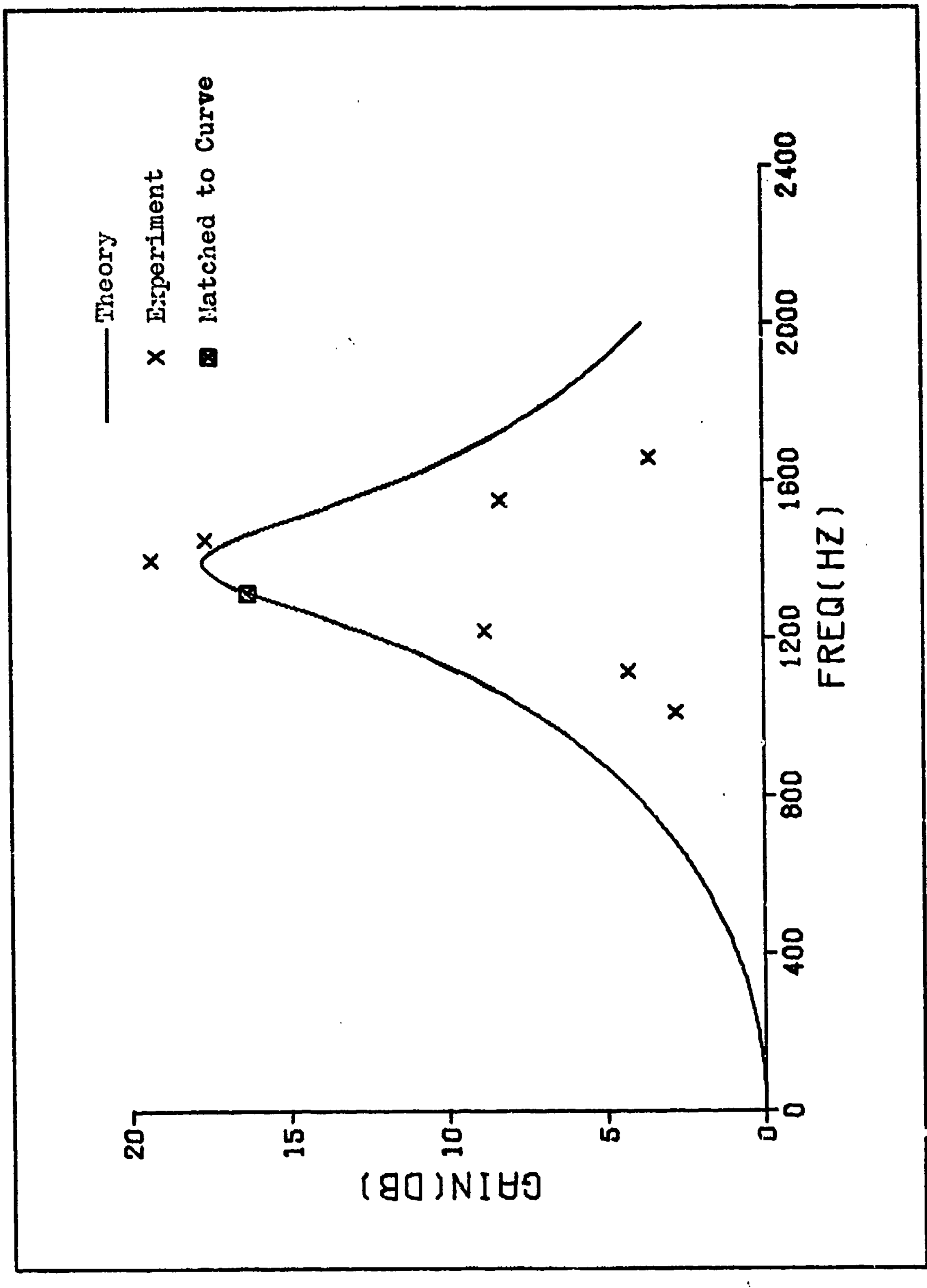

Fig. 18. Experimental and Theoretical Gains (P_B/P_A) for Model 6, Mach=0.85, X=1.565, Alpha = 0

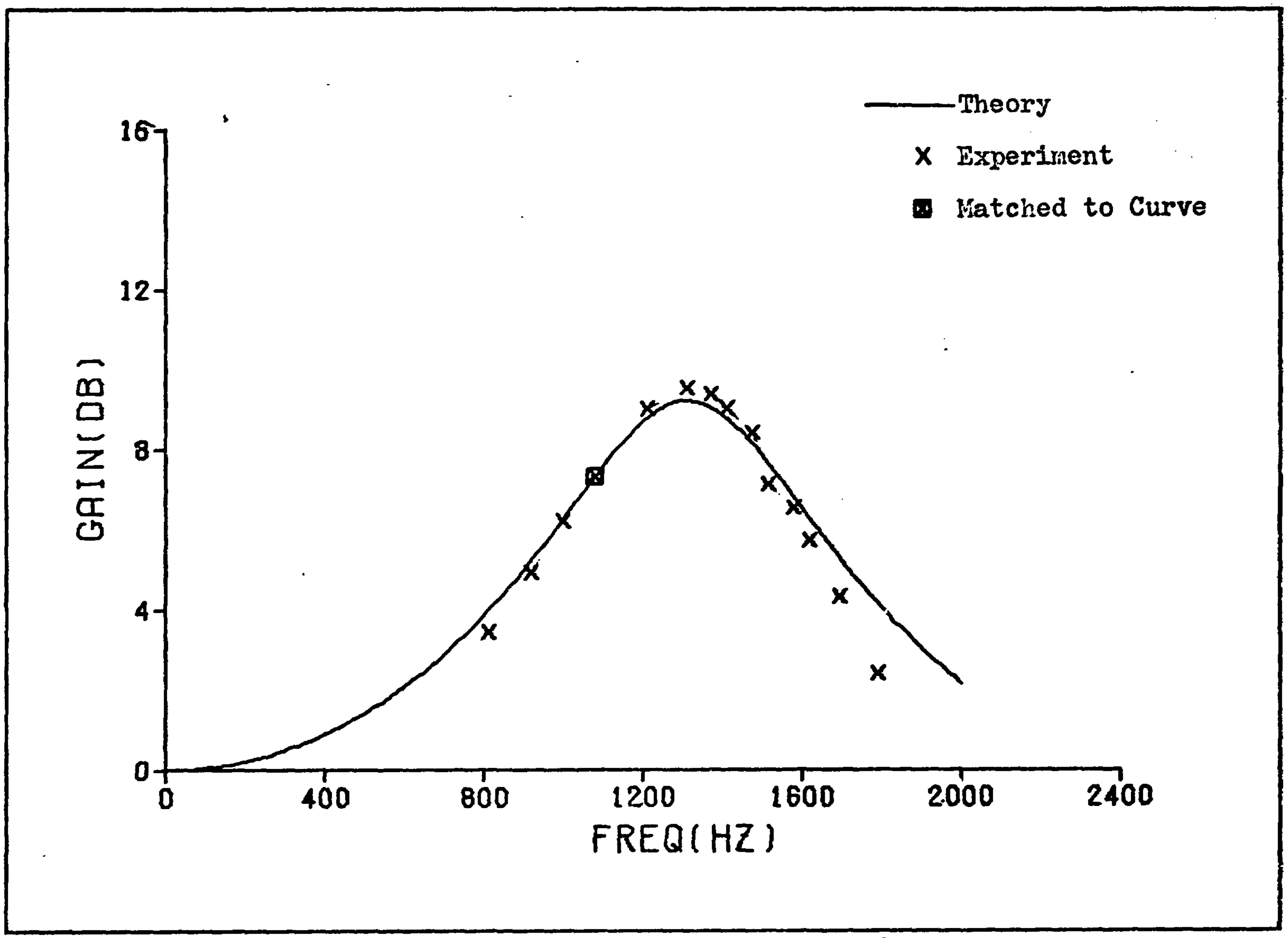

Fig. 19. Experimental and Theoretical Gains (P_B/P_A) for Model 7, Mach=0.85, X=1.565, Alpha = 0

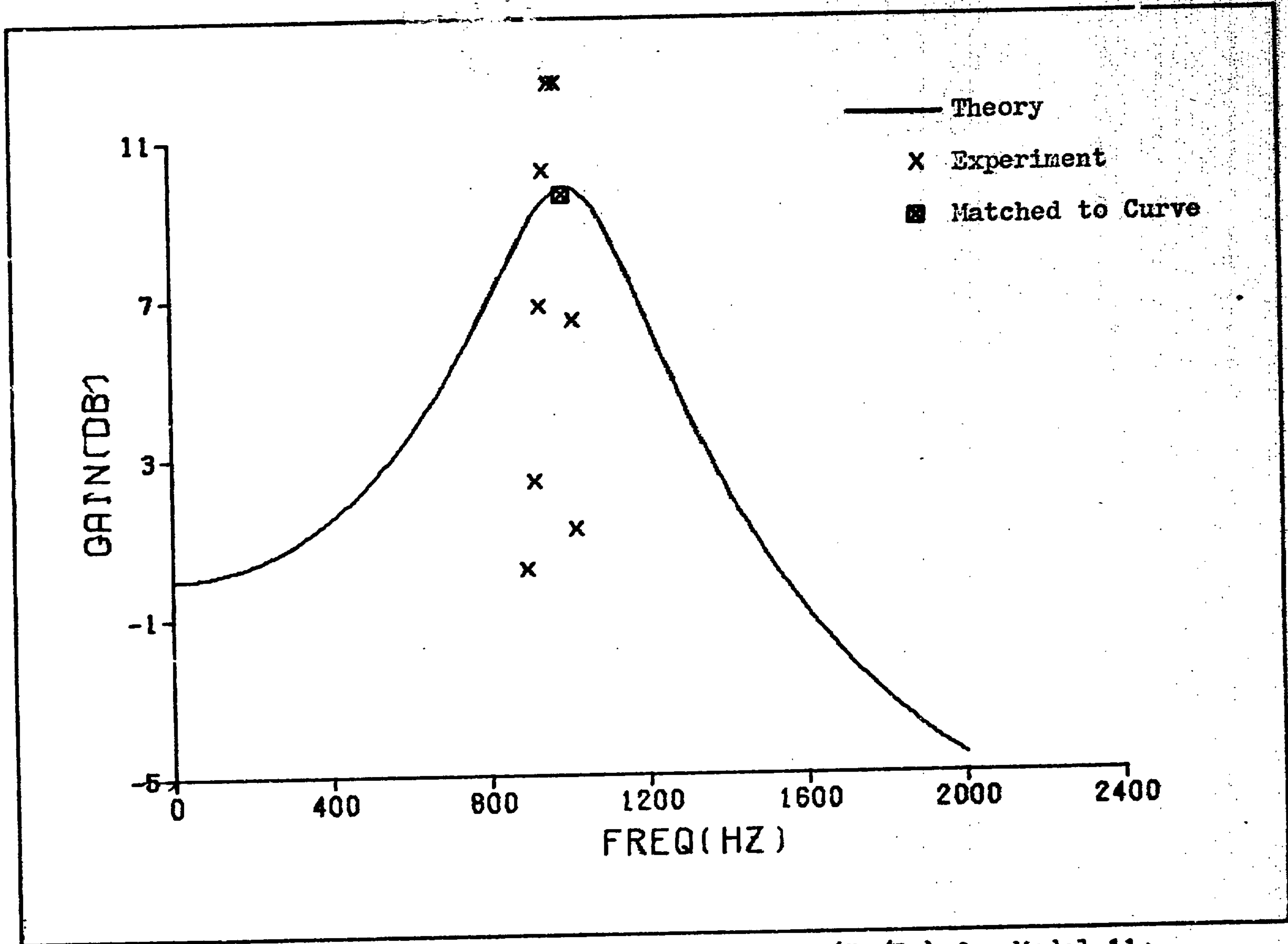

Fig. 20. Experimental and Theoretical Gains (P_B/P_A) for Model 11; Mach=0.85, X=1.565, Alpha = 0

Effectiveness of Anti-Resonance Devices

The measurement that was used to determine the effectiveness of the various models in reducing the resonance level was the RMS pressure measured at the rear of the cavity. The temperature, measured at the rear of the cavity, is also presented in this section.

Root Mean Square Pressure Fluctuations. The results of the pressure measurements are presented as plots of the RMS pressure divided by the tunnel dynamic pressure (P_{rms}/q) versus the nondimensionalized cavity depth (X/D). The curves for a Mach number of 0.85 and angle of attack of 0 degrees are typical of the data taken throughout the test and are presented in Figs 21 thru 24. In all cases the RMS pressure increased with cavity depth, this being attributed to the fact that the flow mechanism that excited the fundamental mode of the cavity was coupled more strongly to the cavity at the deeper positions.

Figure 21 shows the effect of the various Helmholtz resonators on the RMS pressure level. All of the resonators reduced the level by reflecting back part of the incident wave. Models 3 and 4, the Helmholtz resonators with combined cylindrical-segment and cylindrical annular volumes were the most effective, reducing the RMS pressure by a factor as great as 6 at the deepest cavity position.

Figure 22 shows the effect of side relief holes of various diameters on the resonance level. The side relief holes, due

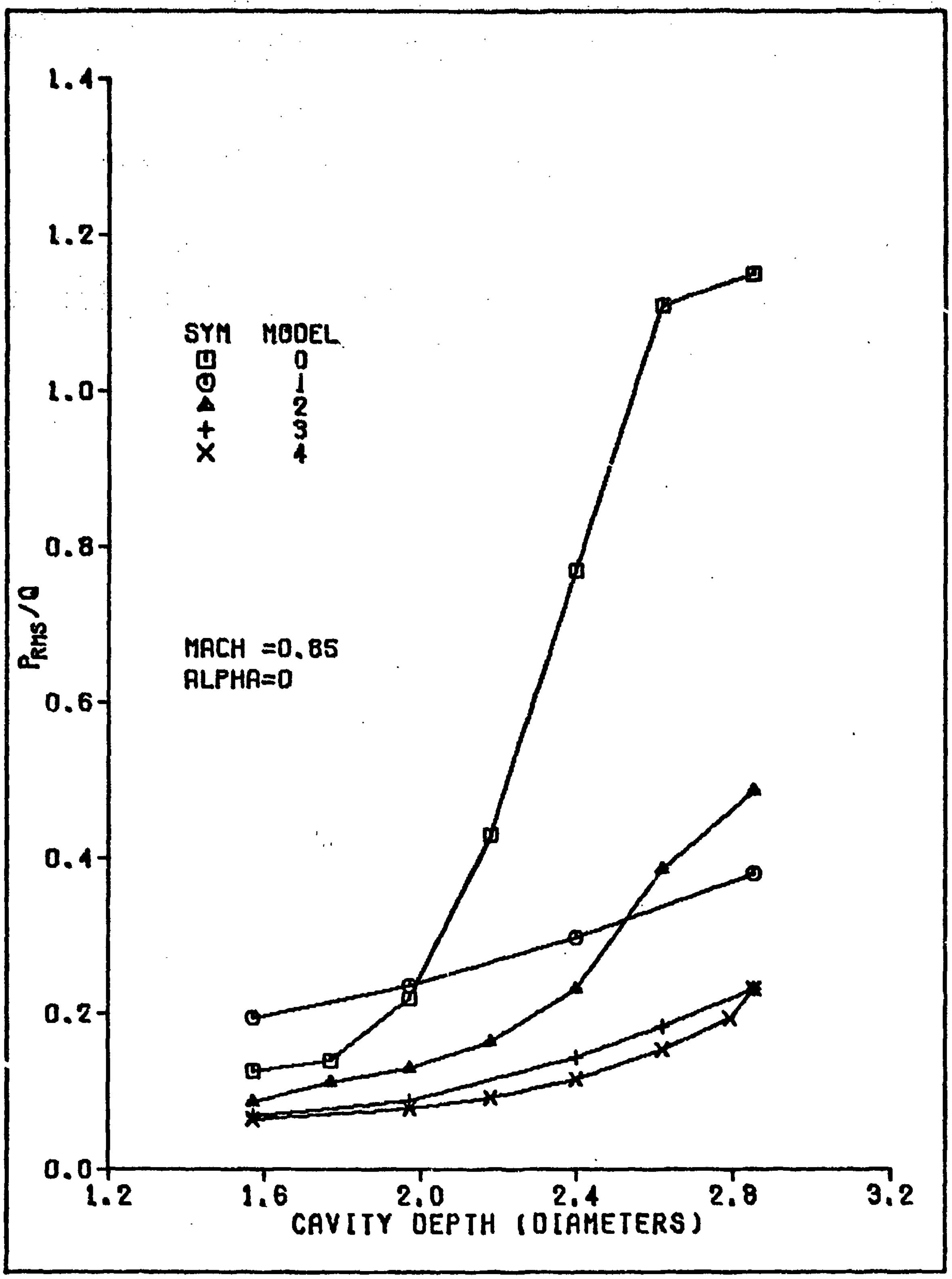

Fig. 21. Effectiveness of Models 1,2,3, and 4 in Reducing the RMS Pressure for Various Cavity Depths, Mach=0.85, Alpha = 0

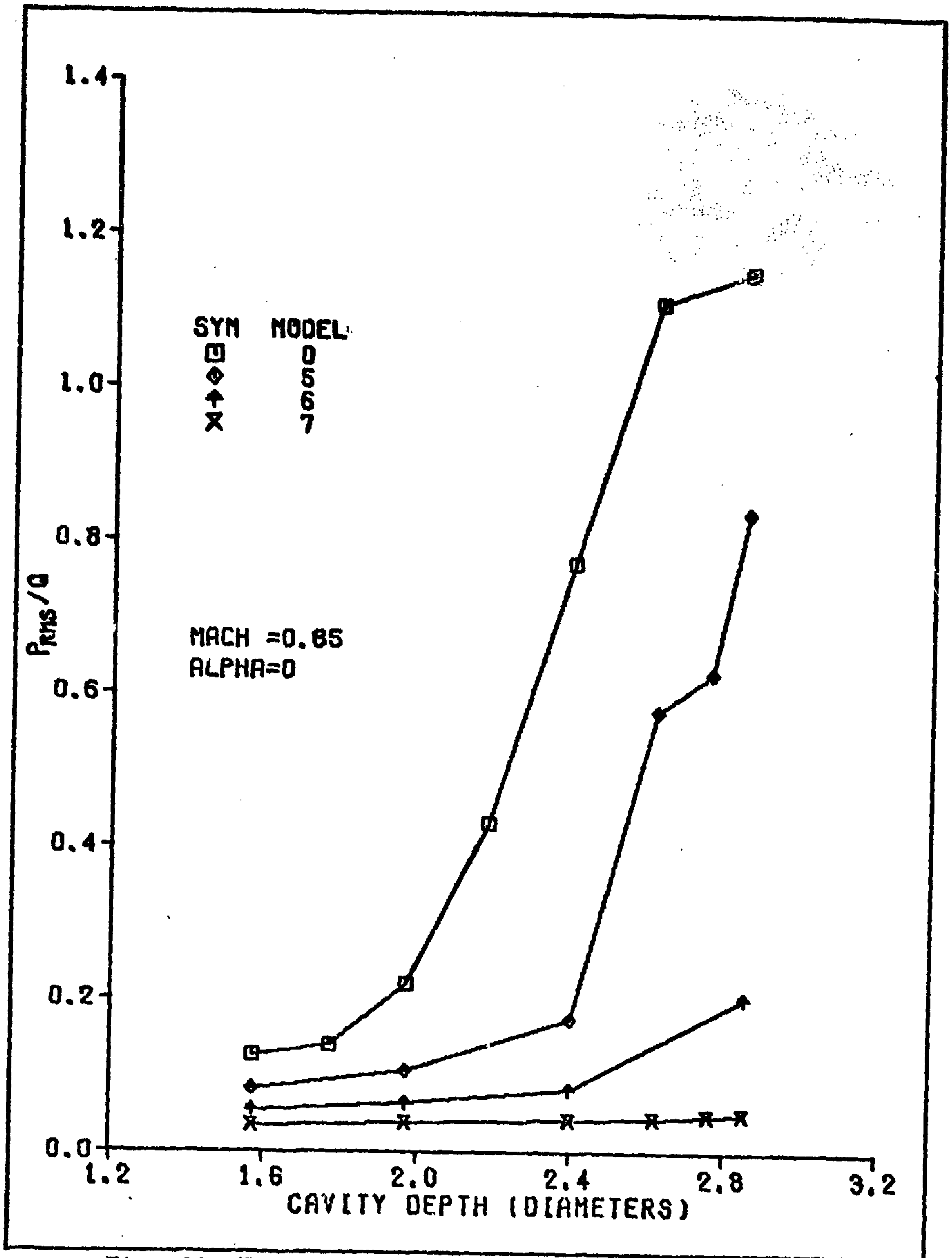

Fig. 22. Effectiveness of Models 5,6, and 7 in Reducing the RMS Pressure for Various Cavity Depths, Mach=0.85, Alpha = 0

to the combined effects of channeling flow across the resonant wave and reflecting back part of the incident wave, reduced the RMS pressure. Model 7, the side relief hole with the greatest diameter (.375 in.) reduced the P_{rms} level by a factor as great as 23 at the deepest cavity depth.

Figure 23 shows the effect of models 8,9, and 10 on the P_{rms} level. The porous fence insert (Model 10) was not effective and at some cavity depths even amplified the RMS pressure level. Model 8 (scoop attachment) and Model 9 (foam lining) reduced the RMS pressure significantly (by factors of 6 and 3 respectively at the deepest cavity position).

From Figs 21 thru 23 it can be seen that the Helmholtz resonators with the combined cylindrical annular and cylindrical-segment volumes (Models 3 and 4) and the side relief hole with the largest diameter (Model 7) were the most effective in reducing the resonance level. Model 11, a combination of the most effective side relief hole (Model 7) and the most effective Helmholtz resonator (Model 3), also reduced the resonance level significantly (factor of 13 at the deepest cavity position). A comparison of the most effective models (Models 3,7, and 11) is given in Fig 24. For every test condition, Model 7 (the side relief hole with the greatest diameter) was determined to be the most effective in reducing the RMS pressure fluctuations in the cavity. A complete set of figures for all test conditions, excluding the figures that were presented in this section, is given in Appendix C.

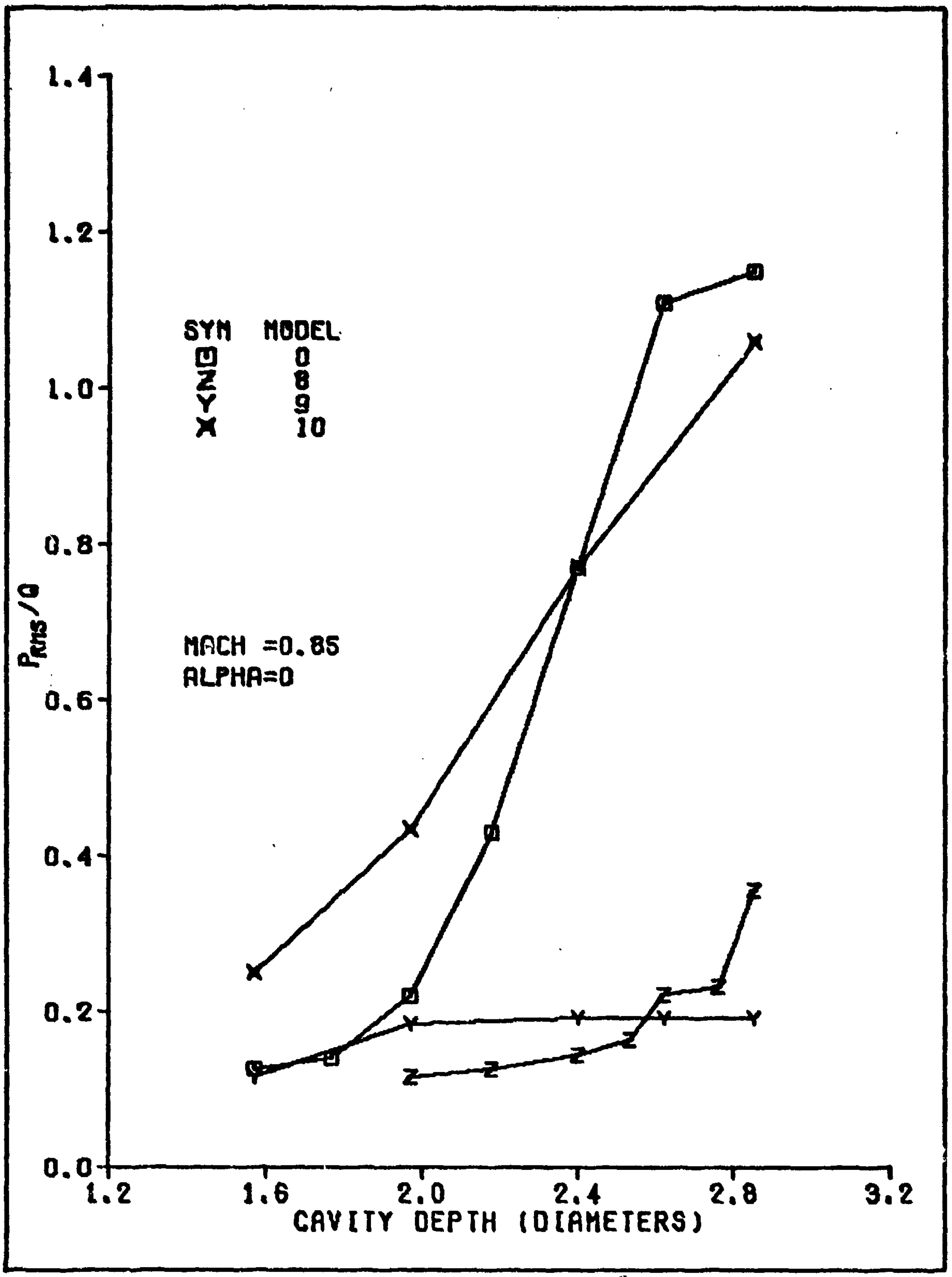

Fig. 23. Effectiveness of Models 8,9, and 10 in Reducing the RMS Pressure for Various Cavity Depths, Mach=0.85, Alpha = 0

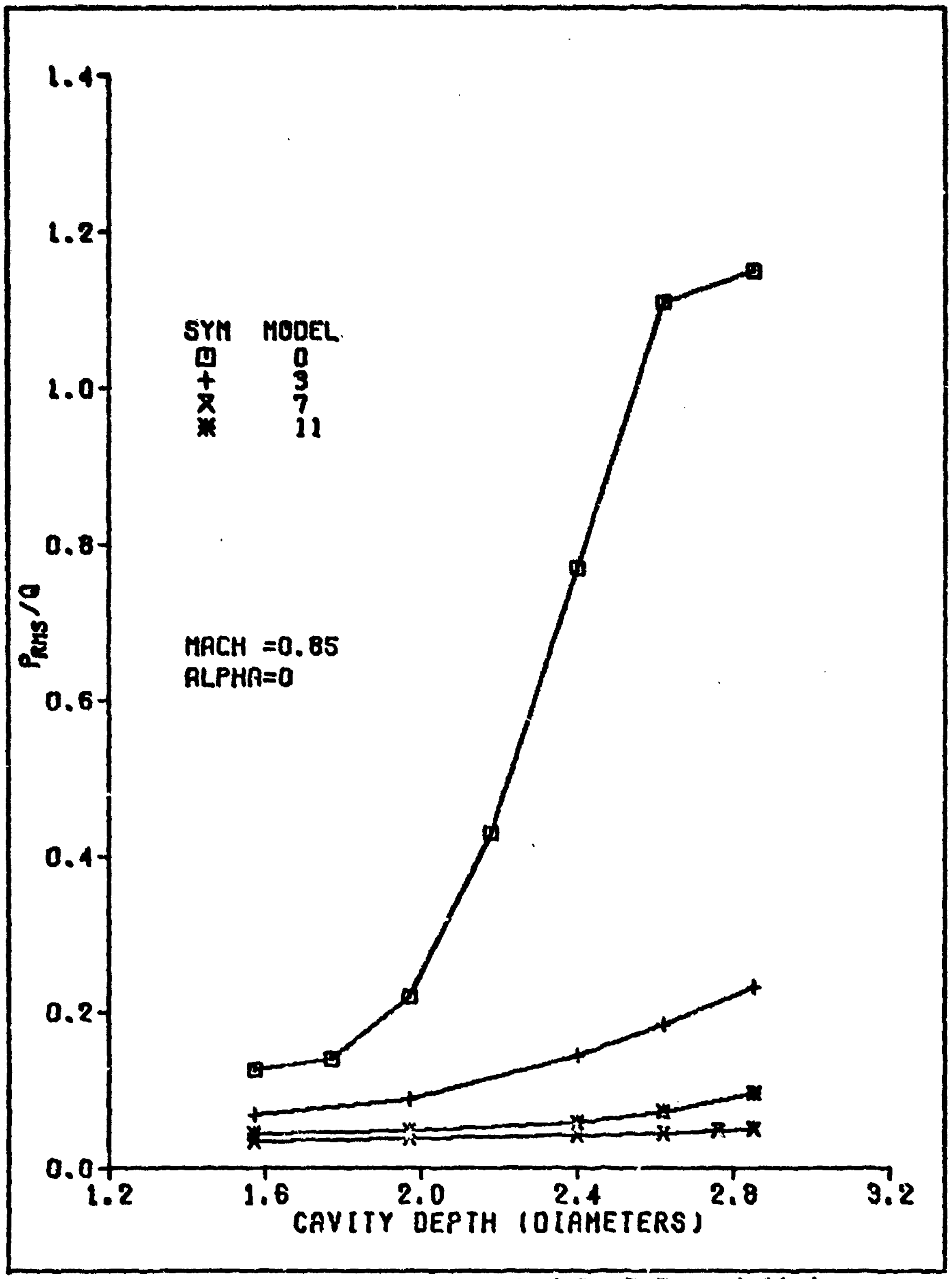

Fig. 24. Effectiveness of Models 3,7, and 11 in Reducing the RMS Pressure for Various Cavity Depths, Mach=0.85, Alpha = 0

Temperature Measurement. The results of the temperature measurements at the rear of the cavity are summarized in Fig 25. As the RMS pressure increased, the temperature also increased. This can be explained by the fact that at any resonant condition some of the accoustic energy contained in the standing waves present in the cavity was dissipated as heat due to viscosity effects. As the RMS pressure increased the amplitude of the standing waves increased and as a result a greater amount of acoustic energy was dissipated as heat. When this increase in heat was combined with the stagnated cavity the temperature increased as is shown in Fig 25.

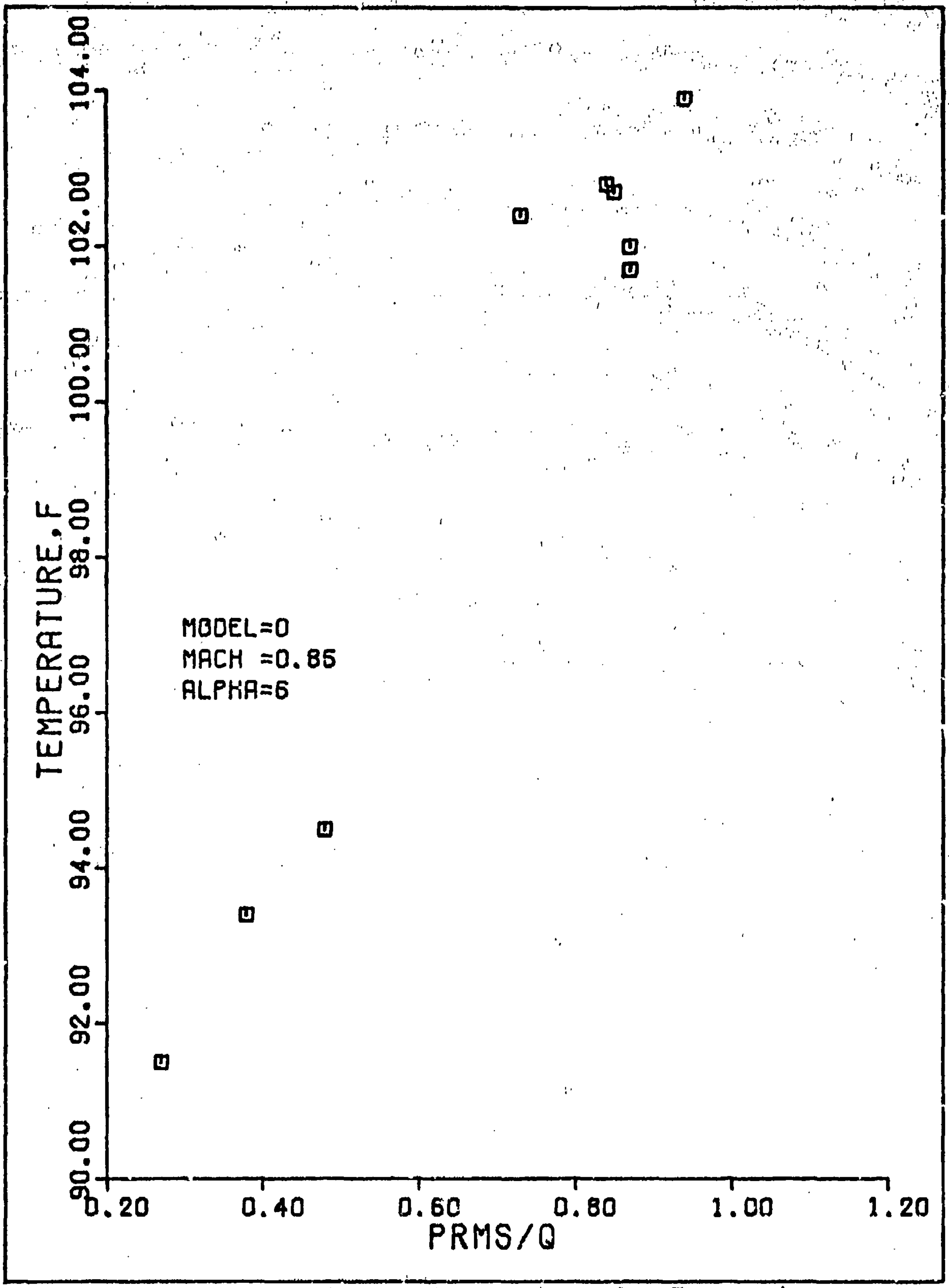

Fig. 25. Variation of Temperature for Increasing P_{rms}/q Level, Mach=0.85, Alpha = 6

VI. Conclusions

In the study the pressure gains and the resonant frequencies of a forward facing cylindrical cavity offset from the axis of an ogive cylinder were investigated. In addition the effectiveness of various anti-resonance devices in reducing the resonance level in the cavity was determined. The major conclusions of the investigation are as follows:

1. The airflow around the nose of the ogive cylinder excited the fundamental resonant frequency of the cavity. The second harmonic was present but at a level 30 to 40 dB lower than the fundamental mode frequency.

2. By adding a length correction to account for the skewed opening at the open end of the cavity, transmission line theory was applied to predict the pressure gains and resonant frequency when the flow was stagnated in the cavity and to predict at least the resonant frequency when there was flow in the cavity.

3. The RMS pressure in the cavity was reduced effectively with the anti-resonance devices. A relief hole, due to the combined effects of channeling flow across the resonant wave and reflecting back part of the incident wave, reduced the RMS pressure by a factor as great as 23. A Helmholtz resonator with combined cylindrical annular and cylindrical-segment volumes reflected back part of

the incident wave and reduced the RMS pressure level by a factor as great as 6.

4. The deeper the cavity depth the higher was the RMS pressure level. For the baseline model, at the deeper cavity positions the RMS pressure was consistantly on the order of the tunnel dynamic pressure q.

5. As the RMS pressure increased the temperature in the cavity increased significantly (as much as 20 degrees at the deepest position).

6. The most desirable configuration tested was the side relief hole due to the simplicity of the configuration and the model's extreme effectiveness in reducing the RMS pressure in the cavity.

VII. Recommendations

Applications

Transmission line theory is a very powerful tool and the fact that it does predict the frequency response of the cavity is of immeasurable importance. The theory can be used to predict what effect a particular configuration will have on the resonance, and more importantly, a preliminary investigation of this type can be done before any construction of materials is started.

Further Investigations

The side relief hole was shown to be very effective and the construction of such a device seems to be quite easy. The aerodynamics of such a relief hole needs to be investigated to determine what effect, if any, the relief hole would have on the overall aerodynamics of the airplane. In addition, transmission line theory does not predict the pressure gains of a side relief hole due to the high speed flow in the cavity. An attempt should be made to model the flow so that the theory could be applied accurately to this type of device. Finally, alternative methods of reducing the resonant pressure oscillations in the cavity should be considered. The use of mass injection has been shown to be successful

in reducing the resonance level in similar forward facing cavities (Ref 9). A study should be conducted to consider its application to this particular configuration.

Bibliography

1. Bird, Thomas. A Computer Program for Predicting the Frequency Response of Complex Pneumatic Line Networks. Unpublished thesis. Wright Patterson Air Force Base, Ohio: Air Force Institute of Technology, December, 1974.

2. Buell, Donald A. An Experimental Investigation of the Air Flow Over a Cavity with Antiresonance Devices. NASA Technical Note D-6205, Washington: National Aeronautics and Space Administration, March, 1971.

3. Franke, M.E., Malanowski, A.J., and Martin, P.S. Effects of Temperature, End Conditions, Flow and Branching on the Frequency Response of Pneumatic Lines, ASME Paper 71-WA/Aut-5, 1971.

4. Franke, M.E., Karam, J.T., Jr., and Lynburner, F.C. "Experimental Frequency Response of Fluidic Transmission Lines," Paper E1, Proceedings of the Fourth Cramfield Fluidics Conference, Coventry, England, 1970.

5. Icardi, Stephan E. An Experimental Investigation of Transonic Flow Around a Nose Section with an Off-Axis Longitudinal Cavity. Unpublished thesis. Wright Patterson Air Force Base, Ohio: Air Force Institute of Technology, December, 1973.

6. Kr'schnaiyer, R. and Lechner, T.J. "An Experimental Evaluation of Fluidic Transmission Line Theory," Advances in Fluidics, ed. Brown, F.T., ASME, New York, 1967.

7. Nichols, N.B. "The Linear Properties of Pneumatic Transmission Lines," Transactions of the Instrument Society of America, 1:5-14 (1962).

8. Troke, Robert W. "Tube-Cavity Resonance," Acoustical Society of America, 44:684-688 (April 1968).

9. VanKuren, James T. and William R. Conner. Acoustic Phenomena of Open Cavity Airborne Cassegrainian Telescopes. AFFDL TM-73-54. Wright Patterson Air Force Base, Ohio: Air Force Flight Dynamics Laboratory, June 1973.

10. White, H.L. Trisonic Gasdynamic Facility Users Manual. AFFDL TM-73-82 FXM. Wright Patterson Air Force Base, Ohio: Air Force Flight Dynamics Laboratory, June, 1973.

Appendix A

Cavity Resonance Devices

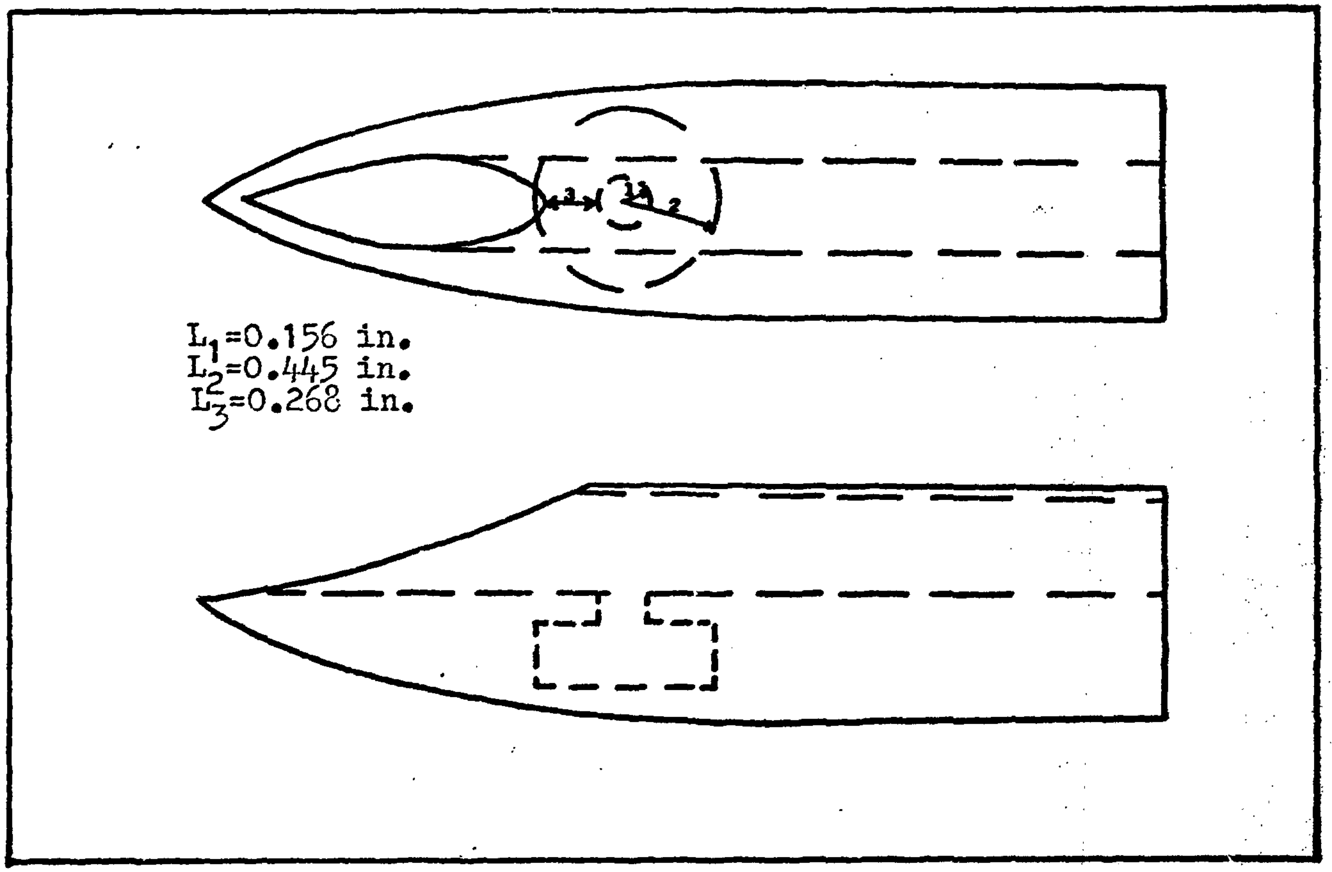

Fig. 26. Model 1, Conventional Helmholtz Resonator

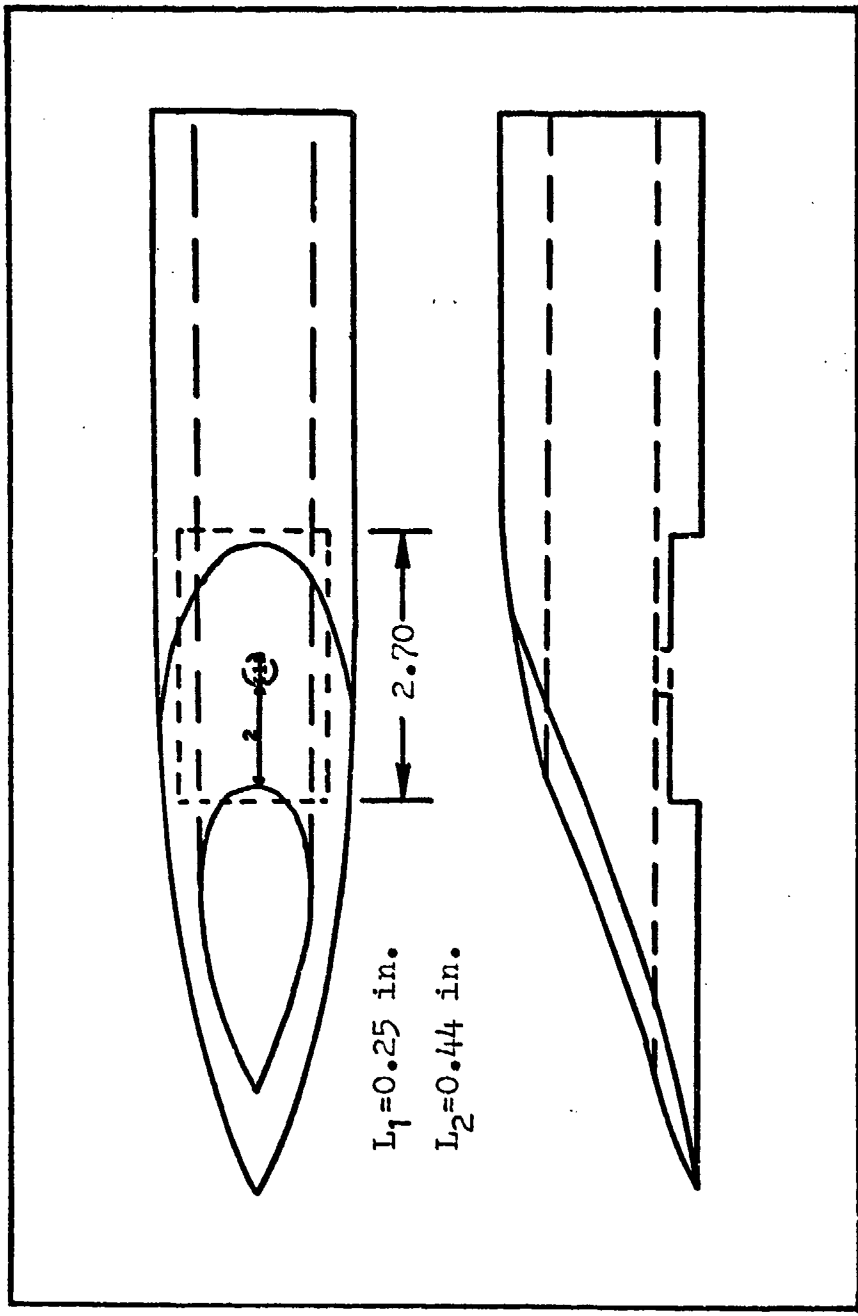

Fig. 27. Model 2, Helmholtz Resonator (Cylindrical-Segment Volume)

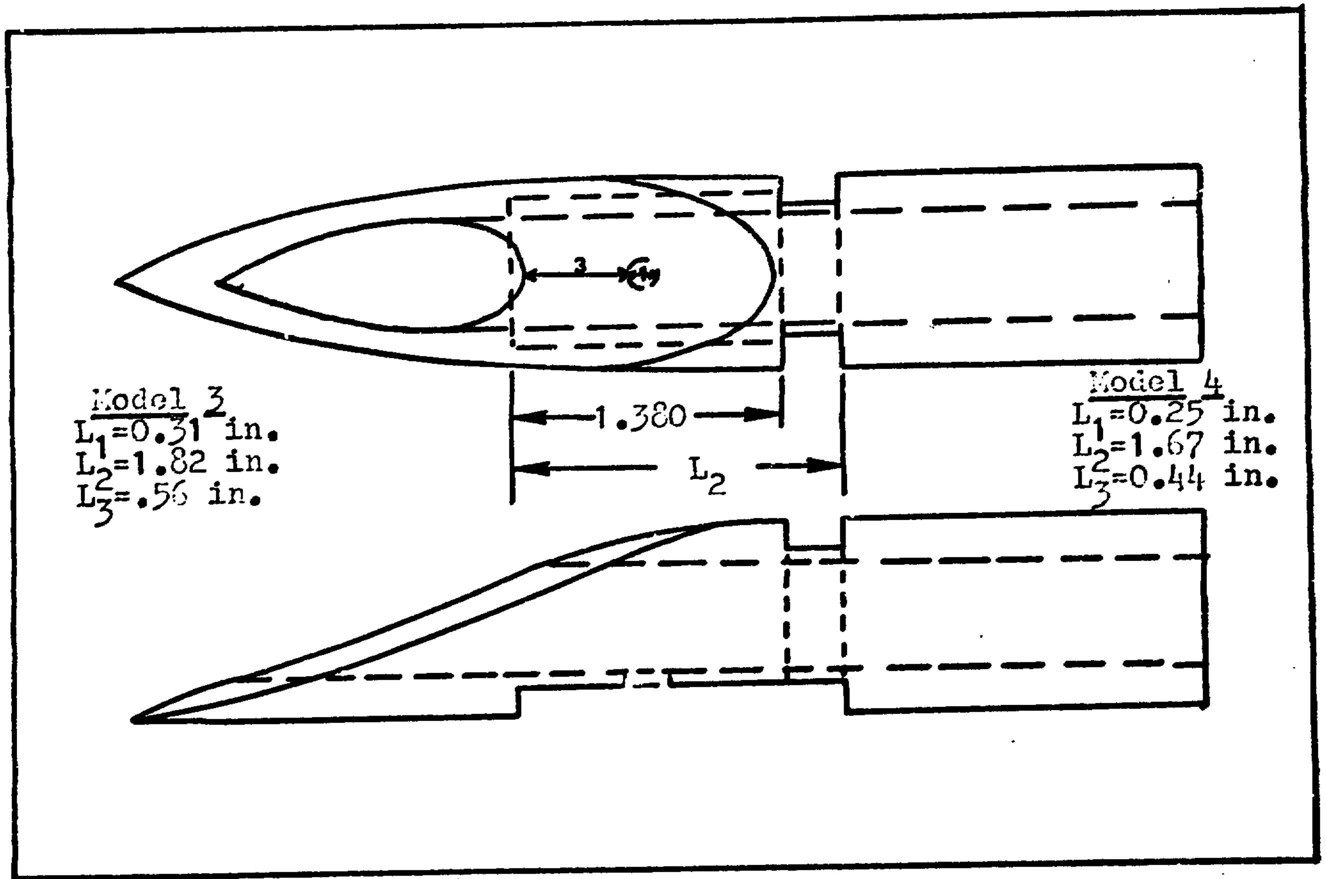

Fig. 28. Models 3,4, Helmholtz Resonators (Combined Cylindrical Annular and Cylindrical Segment Volume)

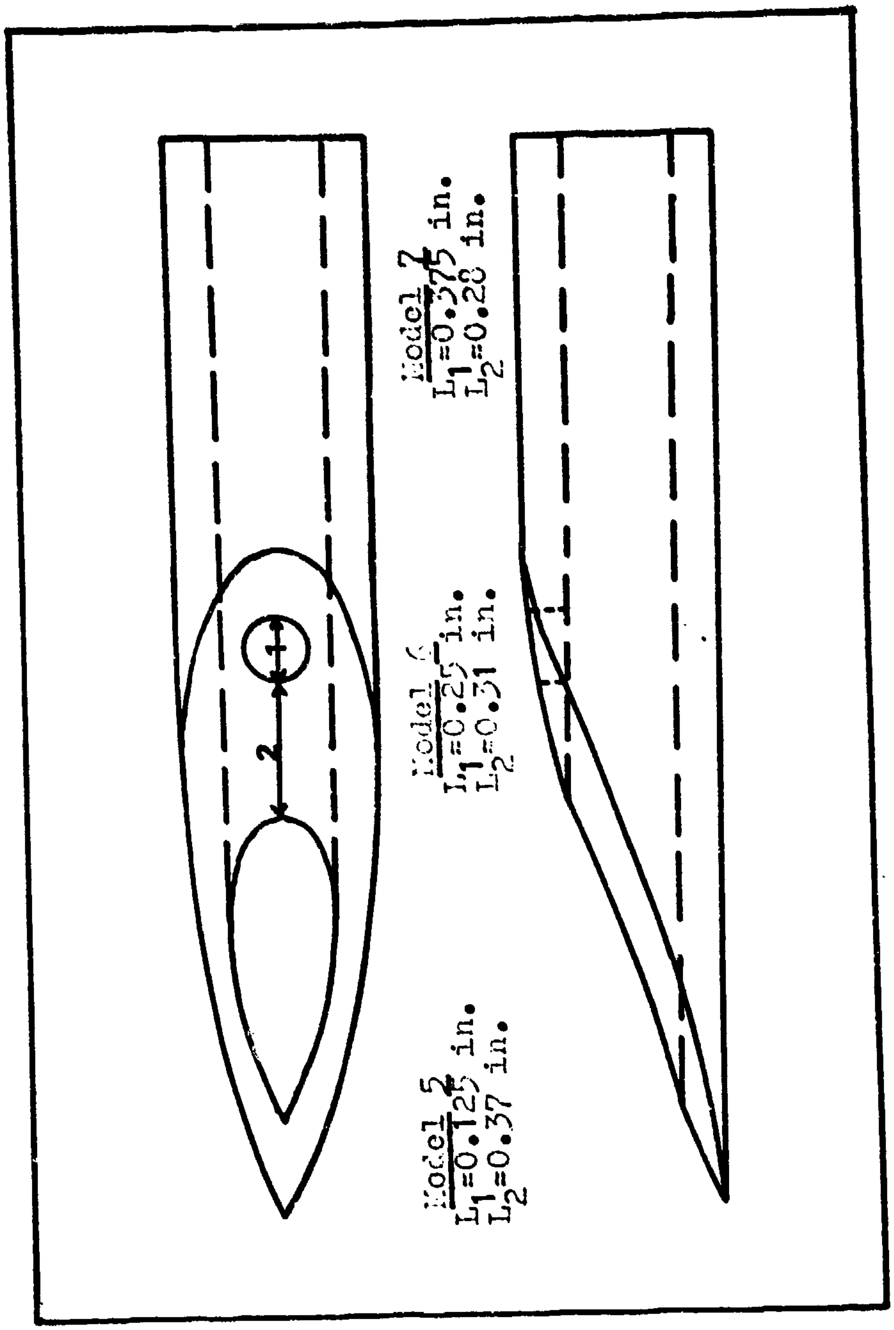

Fig. 29. Models 5,6,7, Relief Holes

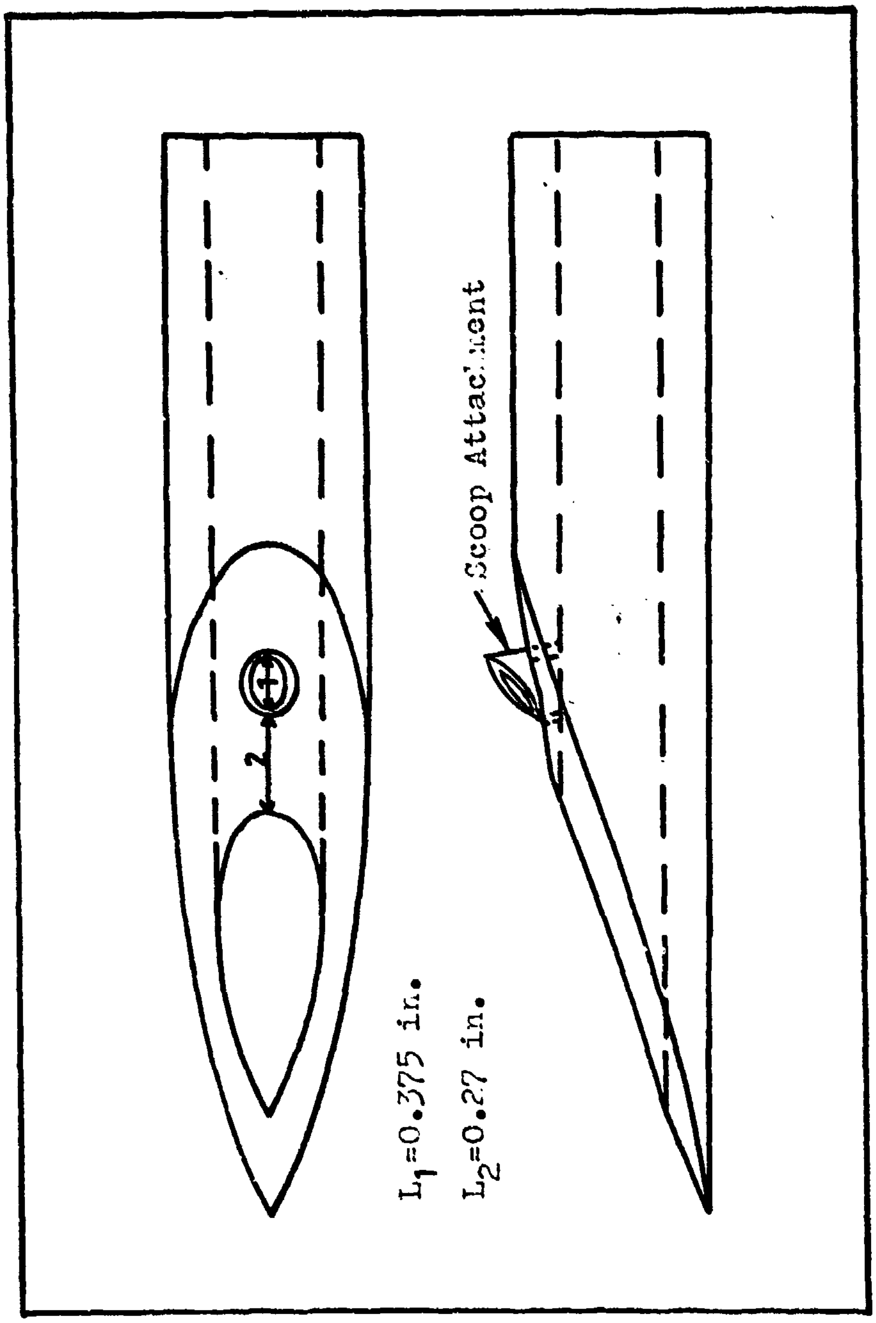

Fig. 30. Model 8, Scoop Attachment

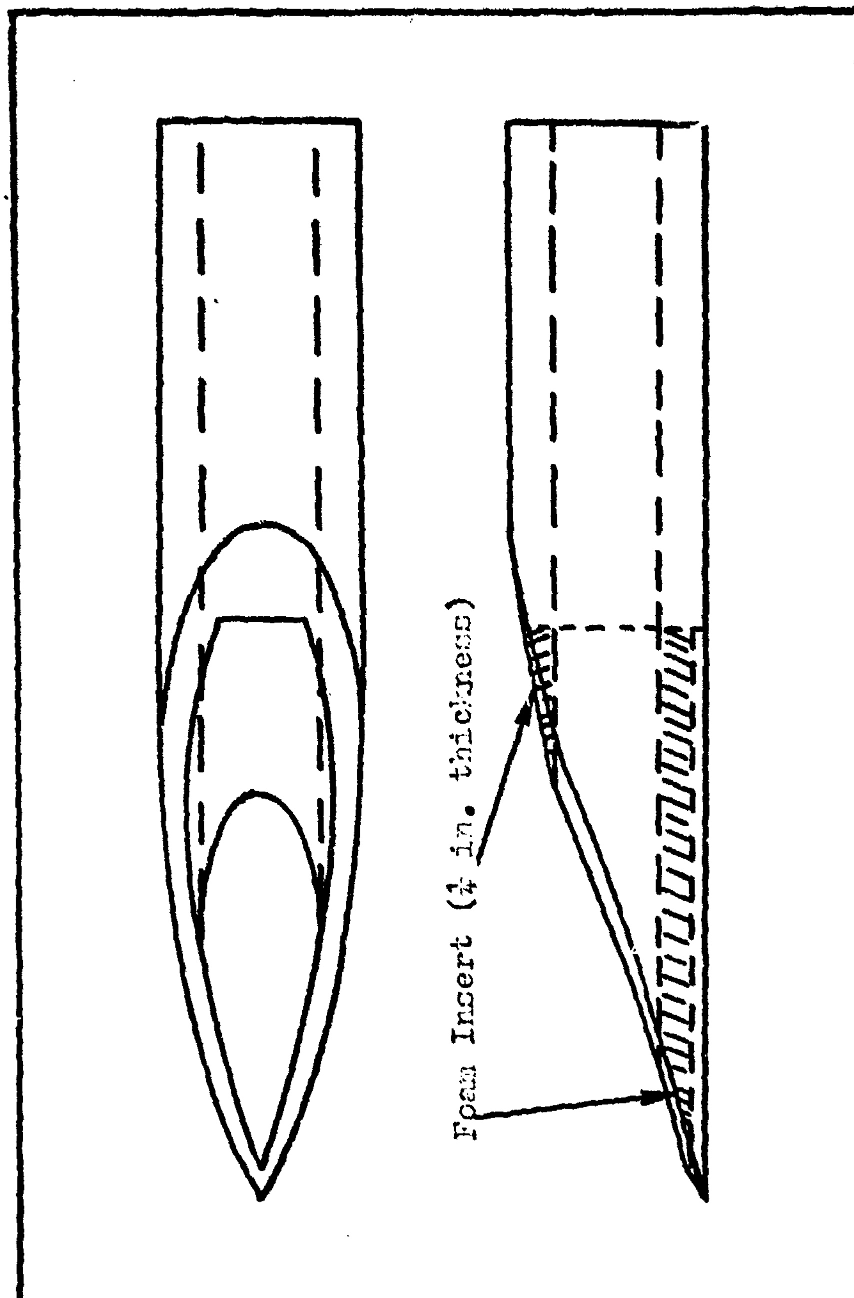

Fig. 31. Model 9, Polystyrene Foam Lining

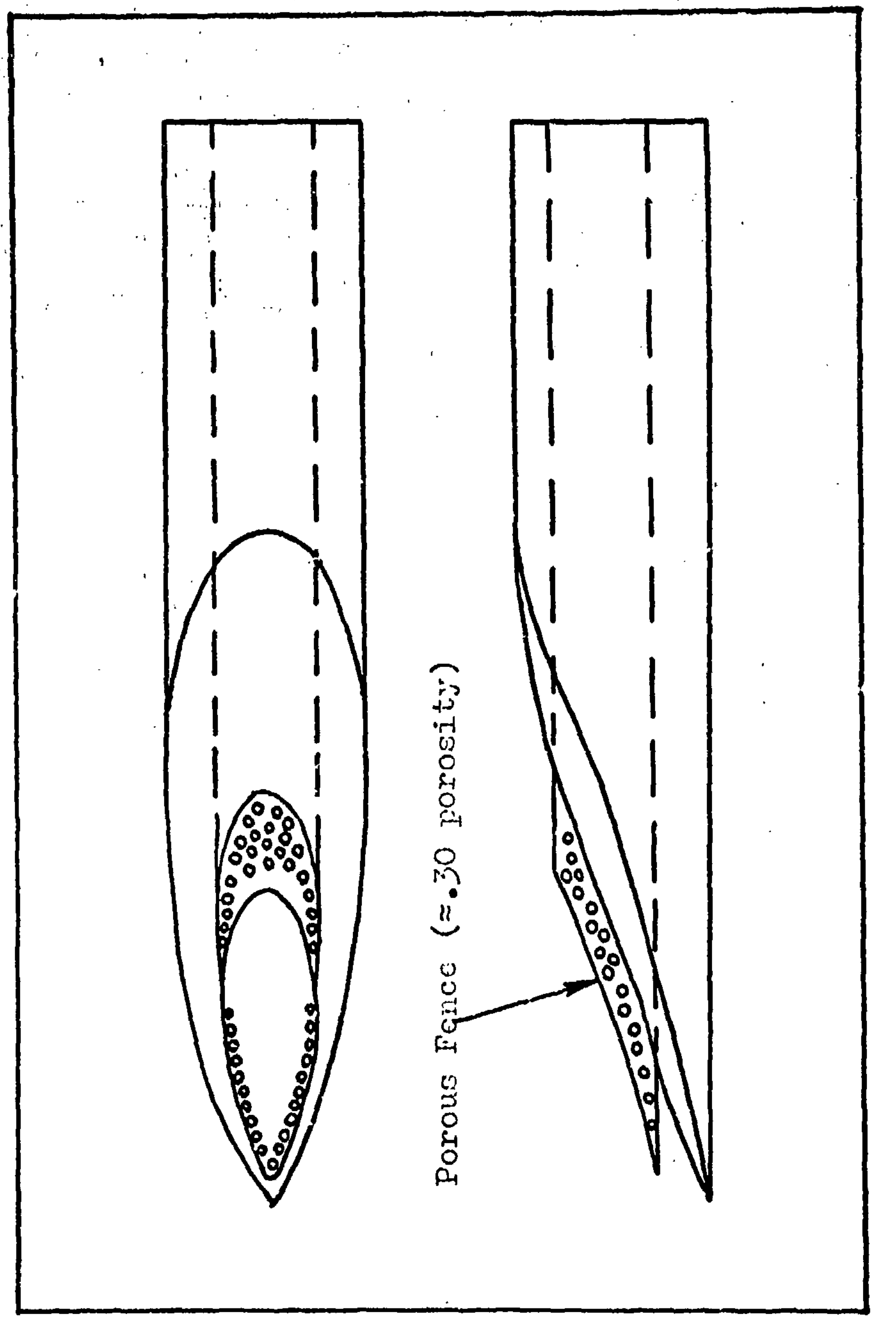

Fig. 32. Model 10, Porous Fence

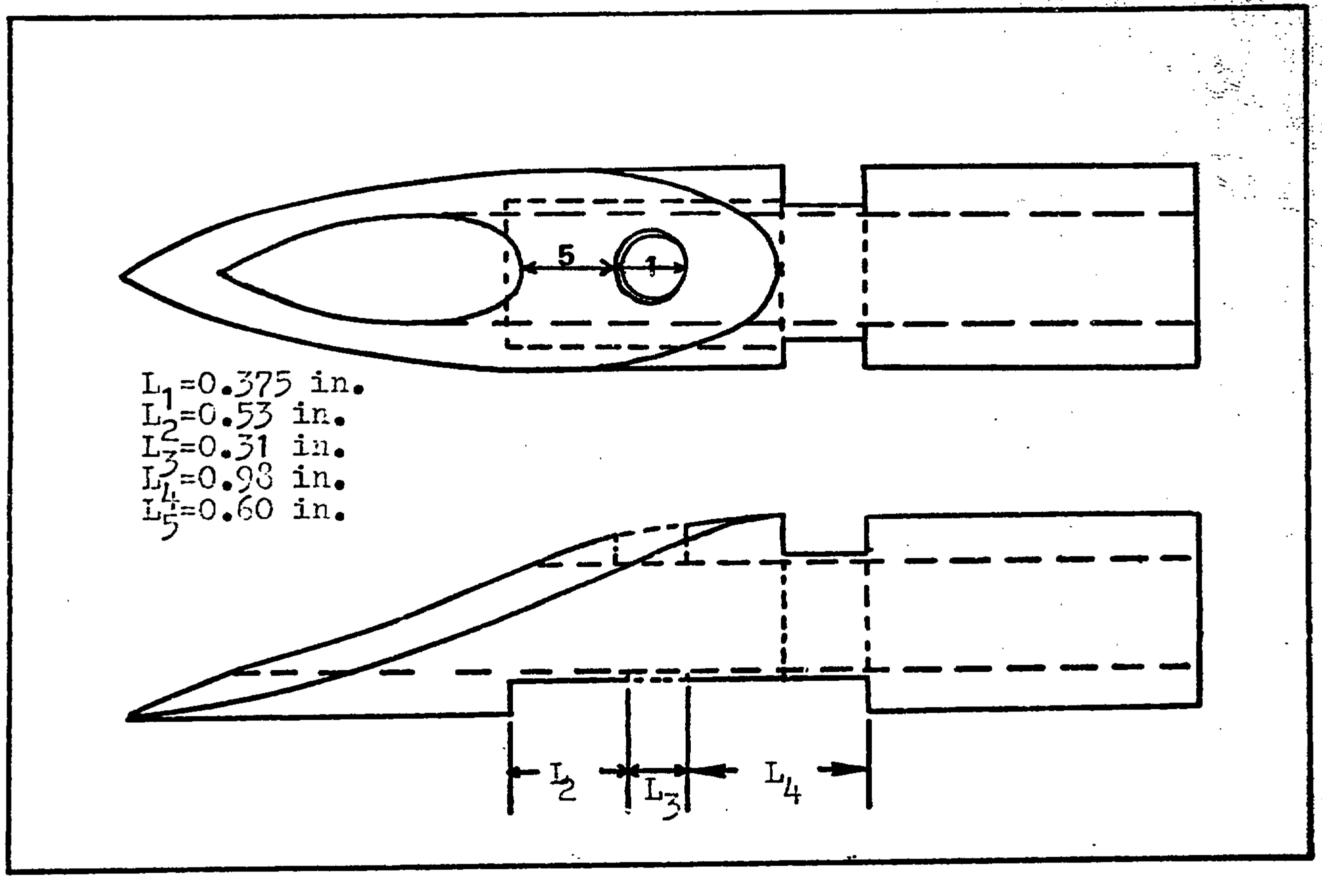

Fig. 33. Model 11, Helmholtz Resonator (Model 3) with a Relief Hole (Model 7)

Appendix B

Transmission Line Models

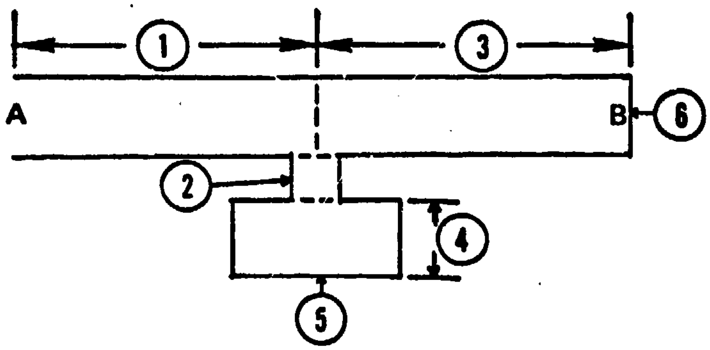

L_1=1.45 in.	D_1=.5625 in.
L_2=.1 in.	D_2=.3125 in.
L_3=X-.425 in.	D_3=.5625 in.
L_4=.35 in.	D_4=.89 in.
L_5=0	D_5=0
L_6=0	D_6=0

Fig. 34. Model 1 Pneumatic Line Configuration

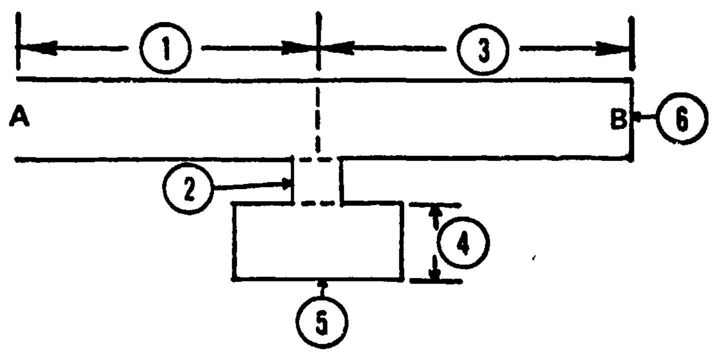

L_1=1.59 in.	D_1=.5625 in.
L_2=.05 in.	D_2=.25 in.
L_3=X-.565 in.	D_3=.5625 in.
L_4=.276 in.	D_4=.932 in.
L_5=0	D_5=0
L_6=0	D_6=0

Fig. 35. Model 2 Pneumatic Line Configuration

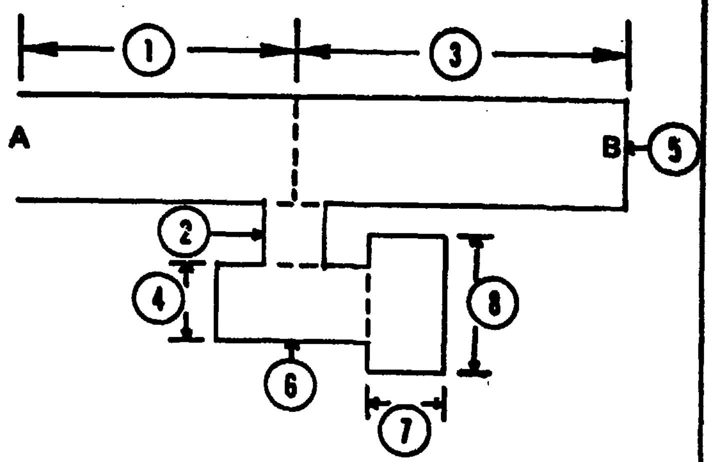

L_1=1.85 in.	D_1=.5625 in.
L_2=.075 in.	D_2=.3125 in.
L_3=X-.73 in.	D_3=.5625 in.
L_4=.218 in.	D_4=.85 in.
L_5=0	D_5=0
L_6=0	D_6=0
L_7=.435 in.	D_7=.564 in.
L_8=0	D_8=0

Fig. 36. Model 3 Pneumatic Line Configuration

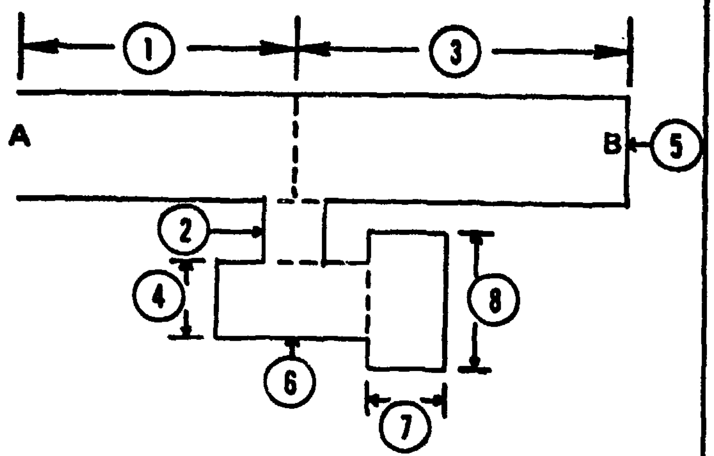

L_1=1.59 in.	D_1=.5625 in.
L_2=.075 in.	D_2=.25 in.
L_3=X-.565 in.	D_3=.5625 in.
L_4=.206 in.	D_4=.819 in.
L_5=0	D_5=0
L_6=0	D_6=0
L_7=.29 in.	D_7=.528 in.
L_8=0	D_8=0

Fig. 37. Model 4 Pneumatic Line Configuration

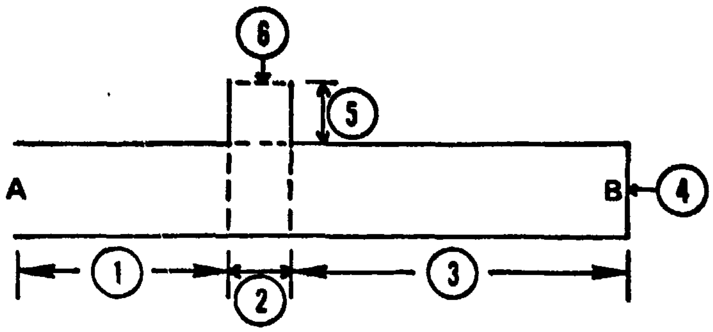

L_1=1.4 in.	D_1=.5625 in.
L_2=.125 in.	D_2=.5625 in.
L_3=X-.67 in.	D_3=.5625 in.
L_4=0	D_4=0
L_5=.1 in.	D_5=.125 in.
L_6=0	D_6=.125 in.

Fig. 38. Model 5 Pneumatic Line Configuration

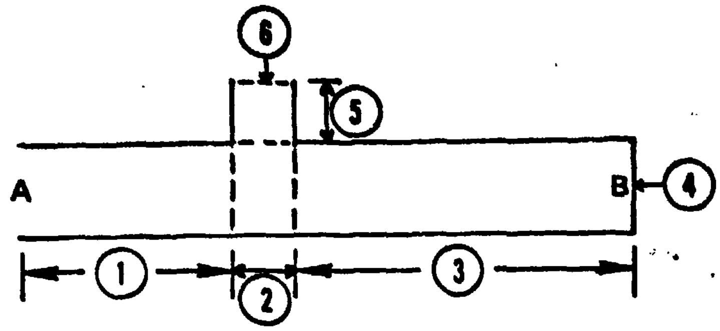

L_1=1.34 in.	D_1=.5625 in.
L_2=.25 in.	D_2=.5625 in.
L_3=X-.73 in.	D_3=.5625 in.
L_4=0	D_4=0
L_5=.1 in.	D_5=.25 in.
L_6=0	D_6=.25 in.

Fig. 39. Model 6 Pneumatic Line Configuration

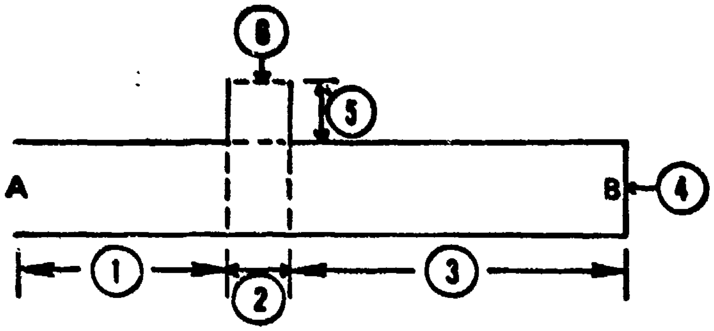

L_1=1.3 in.	D_1=.5625 in.
L_2=.375 in.	D_2=.5625 in.
L_3=X-.66 in.	D_3=.5625 in.
L_4=0	D_4=0
L_5=.156 in.	D_5=.375 in.
L_6=0	D_6=.375 in.

Fig. 40. Model 7 Pneumatic Line Configuration

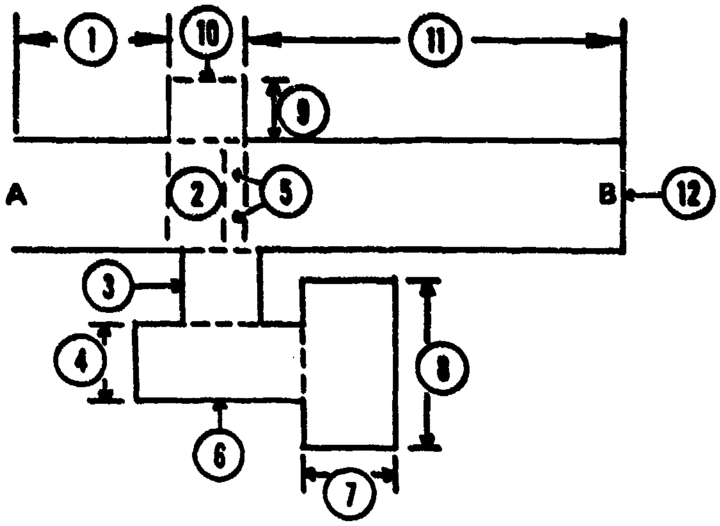

L_1=1.63 in.	D_1=.5625 in.
L_2=.275 in.	D_2=.5625 in.
L_3=.075 in.	D_3=.3125 in.
L_4=.218 in.	D_4=.85 in.
L_5=.1 in.	D_5=.5625 in.
L_6=0	D_6=0
L_7=.435 in.	D_7=.564 in.
L_8=0	D_8=0
L_9=.156 in.	D_9=.375 in.
L_{10}=0	D_{10}=.375 in.
L_{11}=X-.98 in.	D_{11}=.5625 in.
L_{12}=0	D_{12}=0

Fig. 41. Model 11 Pneumatic Line Configuration

Appendix C

Experimental Data
(P_{rms}/q versus X/D)

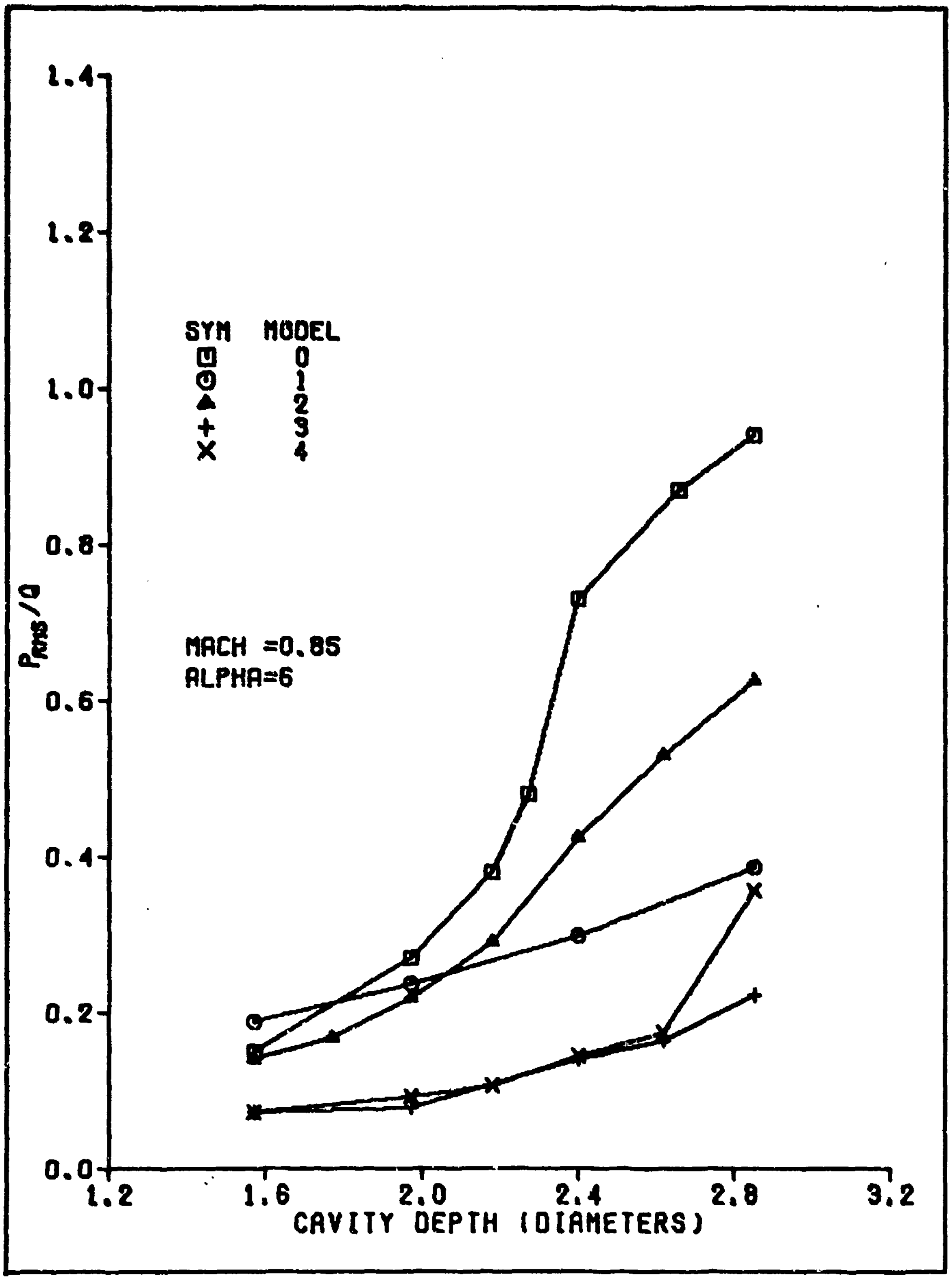

Fig. 42. Effectiveness of Models 1,2,3, and 4 in Reducing the RMS Pressure for Various Cavity Depths, Mach=0.85, Alpha = 6

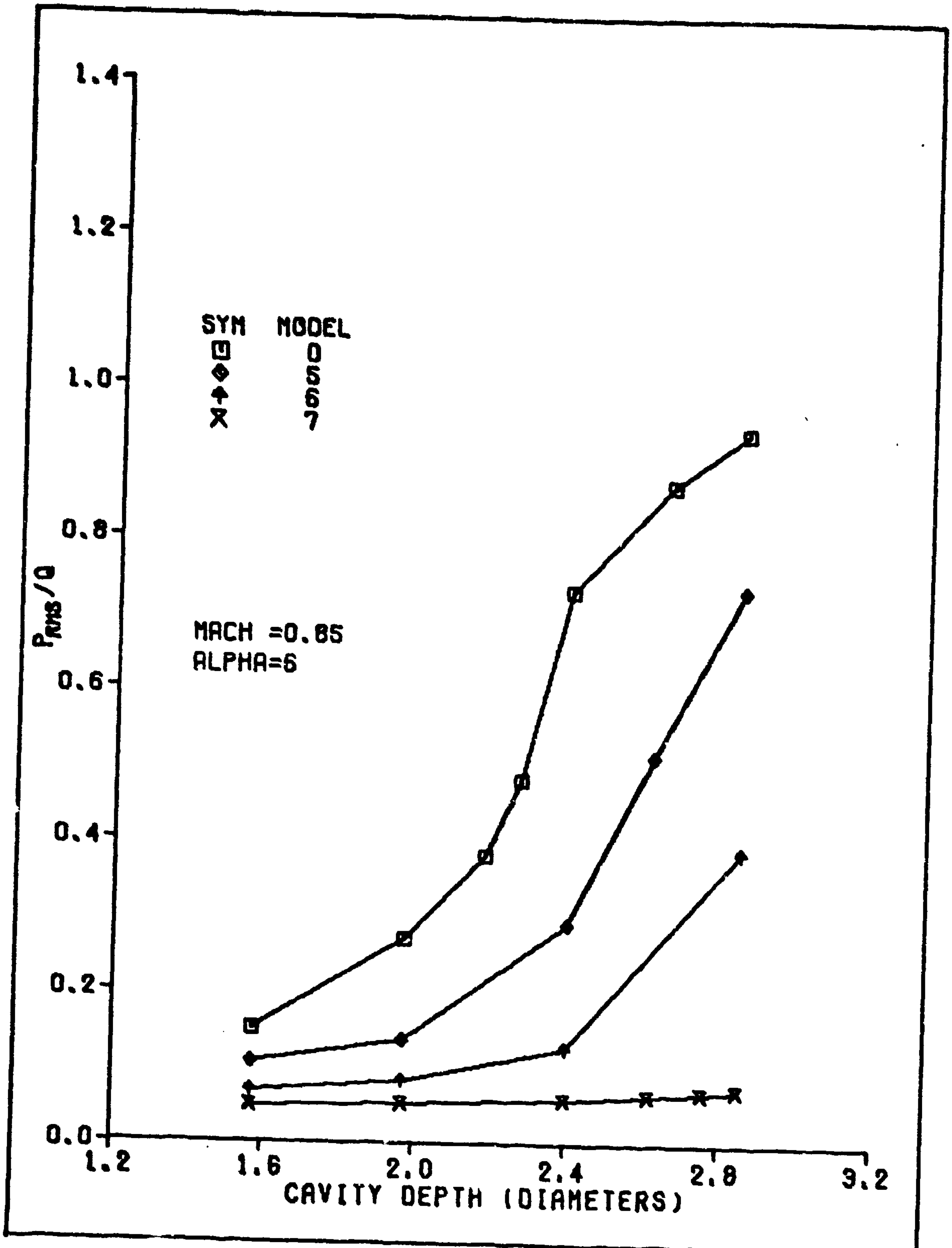

Fig. 43. Effectiveness of Models 5,6, and 7 in Reducing the RMS Pressure for Various Cavity Depths, Mach=0.85, Alpha = 6

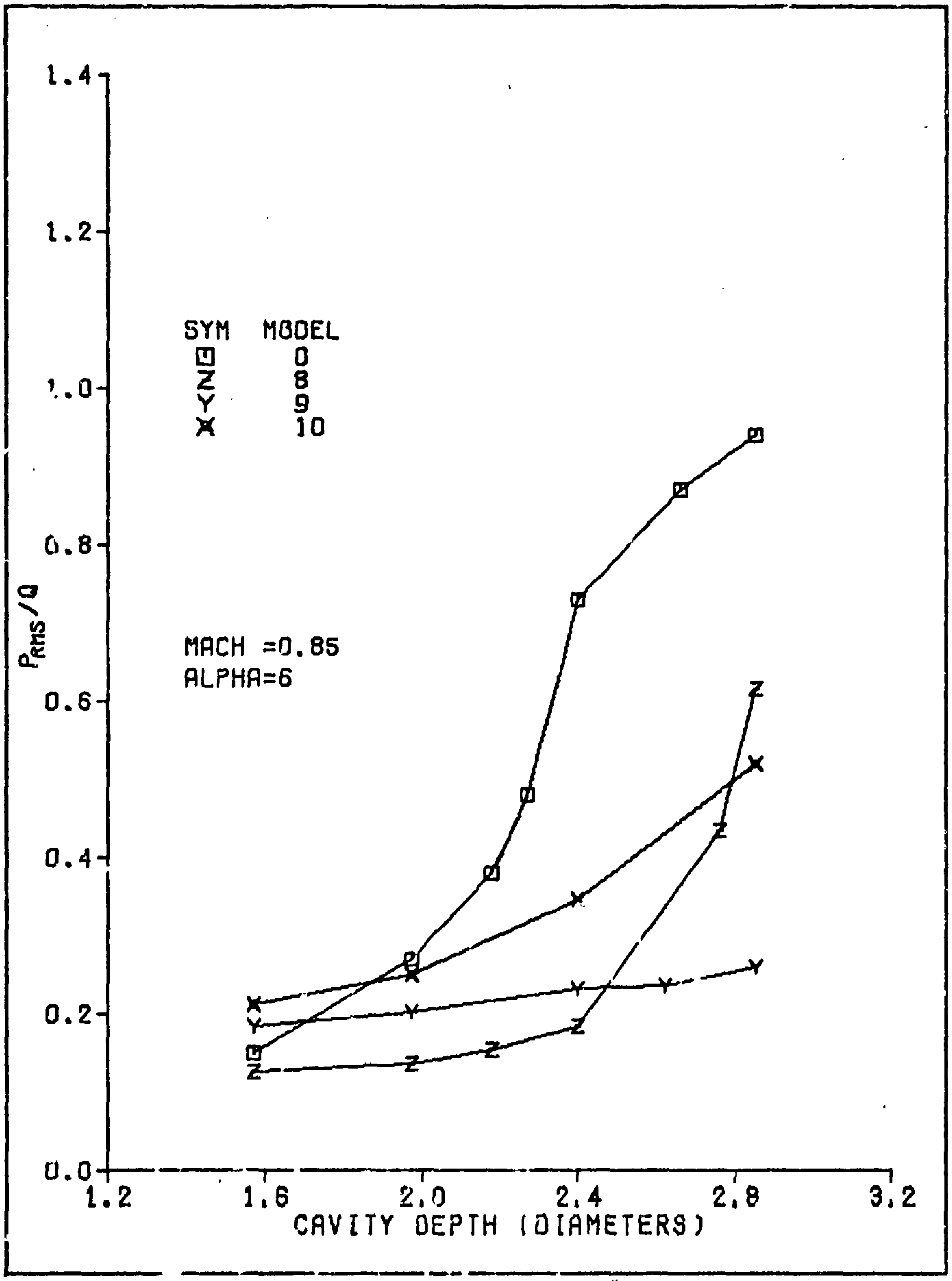

Fig. 44. Effectiveness of Models 8,9, and 10 in Reducing the RMS Pressure for Various Cavity Depths, Mach=0.85, Alpha = 6

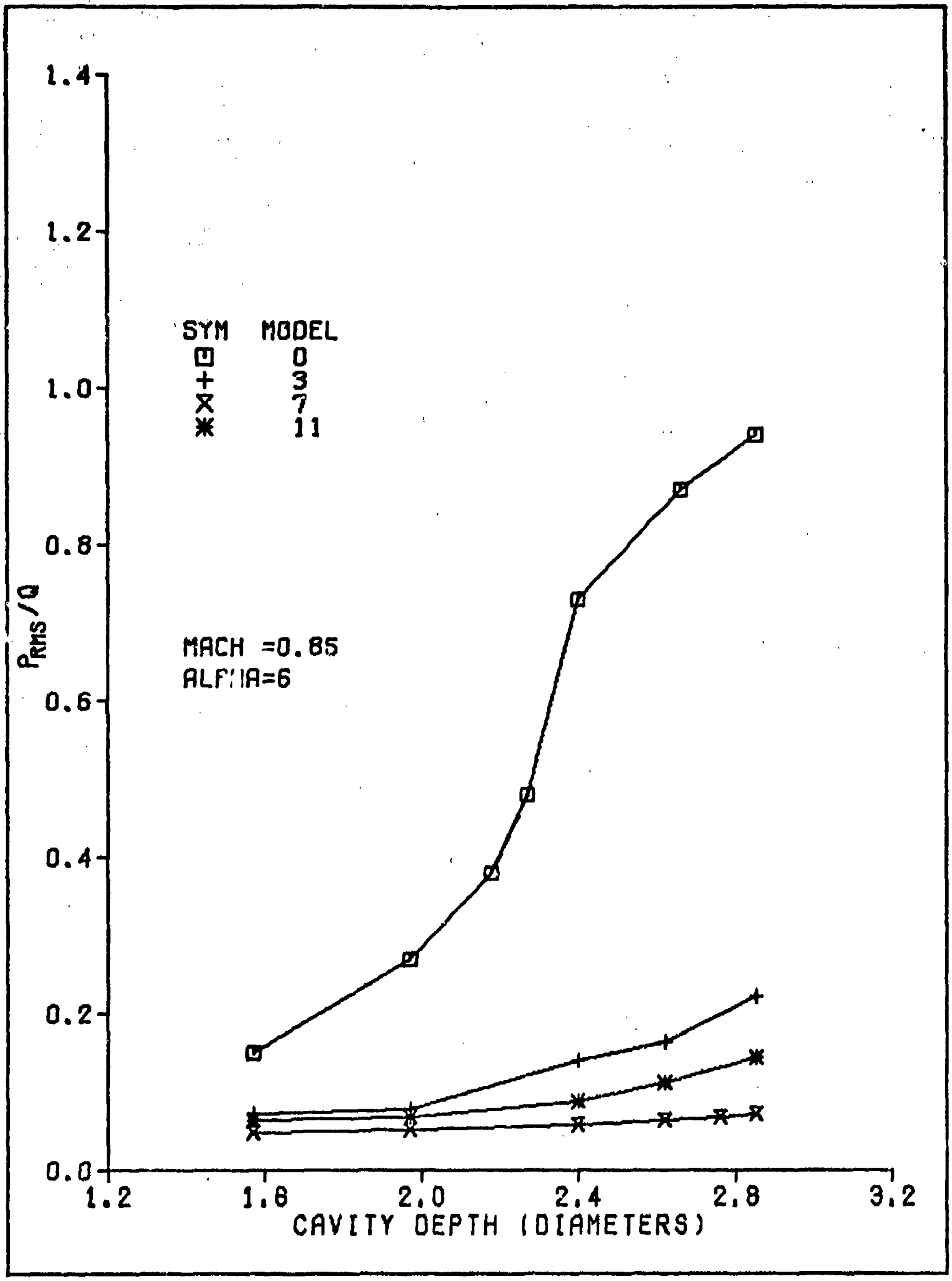

Fig. 45. Effectiveness of Models 3,7, and 11 in Reducing the RMS Pressure for Various Cavity Depths, Mach=0.85, Alpha = 6

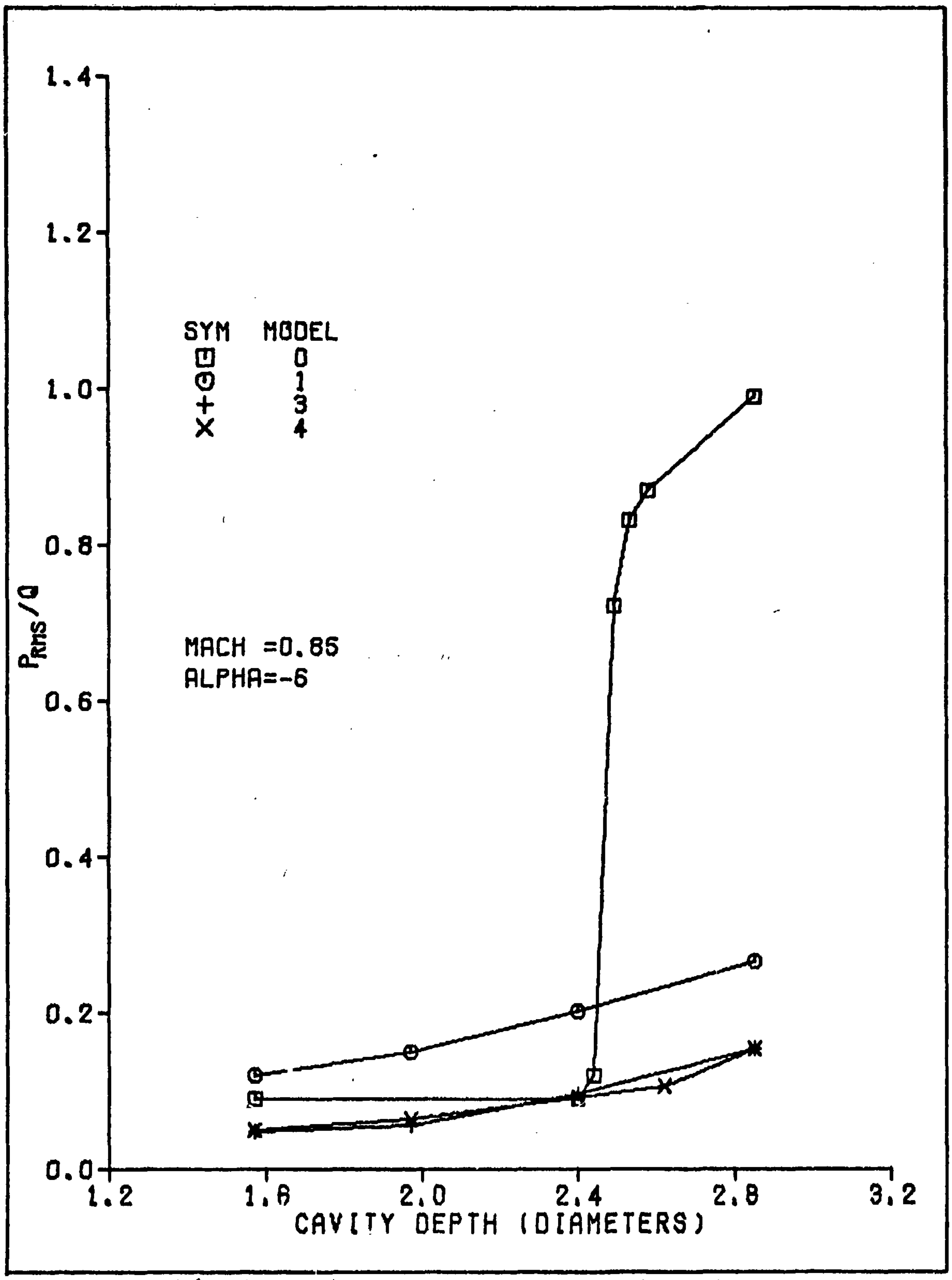

Fig. 46. Effectiveness of Models 1,3, and 4 in Reducing the RMS Pressure for Various Cavity Depths, Mach=0.85, Alpha =-6

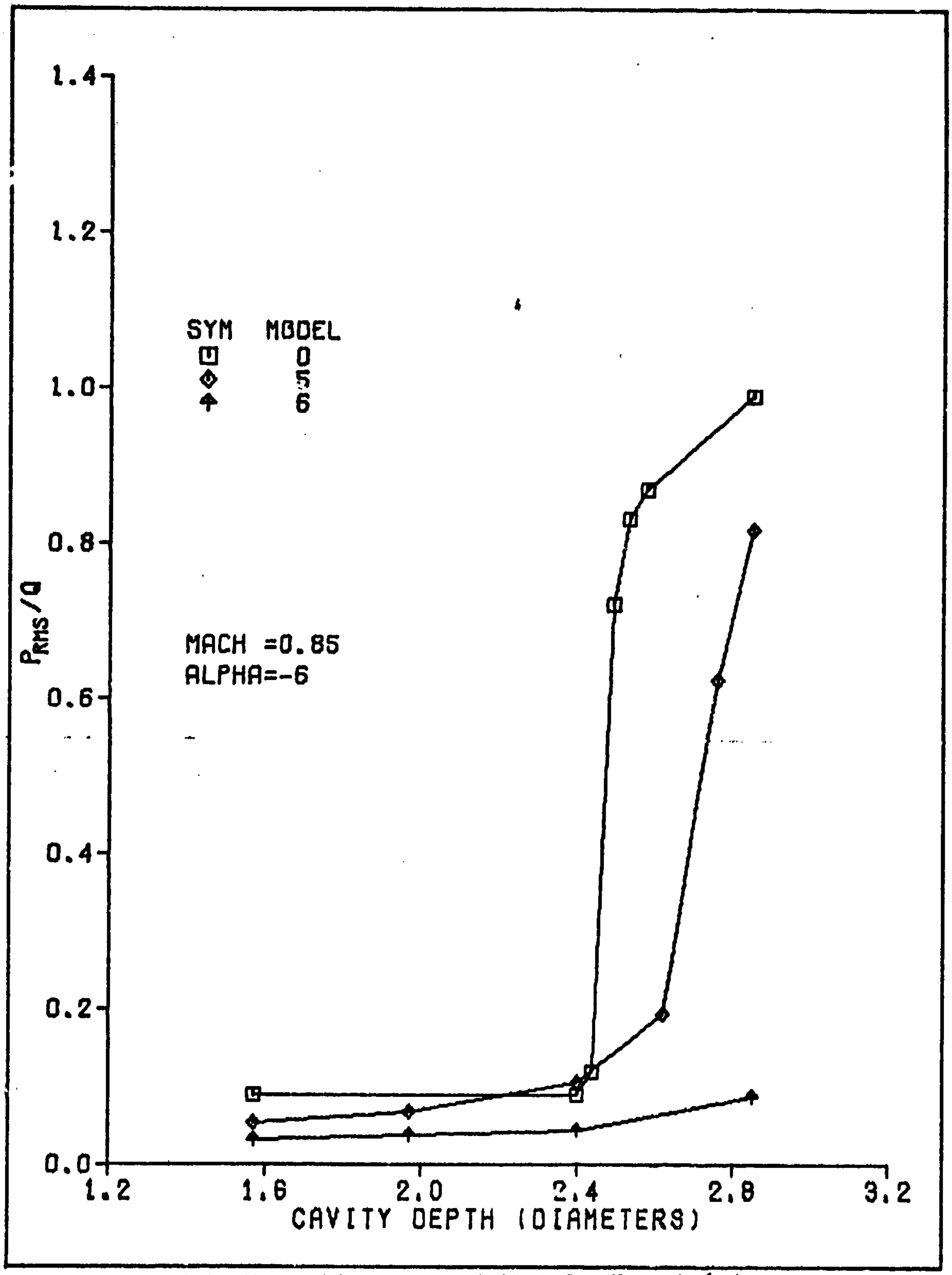

Fig. 47. Effectiveness of Models 5 and 6 in Reducing the RMS Pressure for Various Cavity Depths, Mach=0.85, Alpha =-6

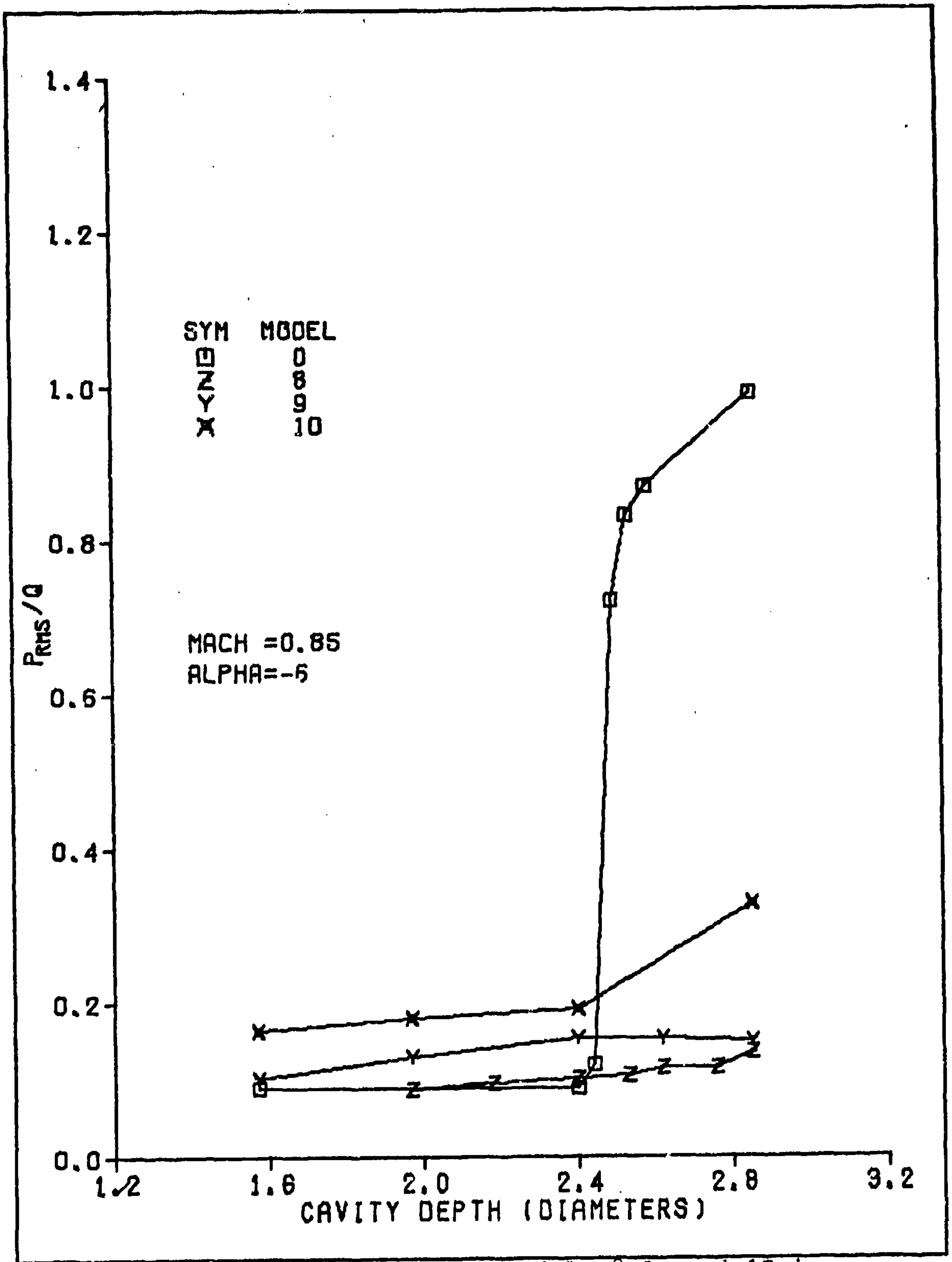

Fig. 48. Effectiveness of Models 0,9, and 10 in Reducing the RMS Pressure for Various Cavity Depths, Mach=0.85, Alpha =-6

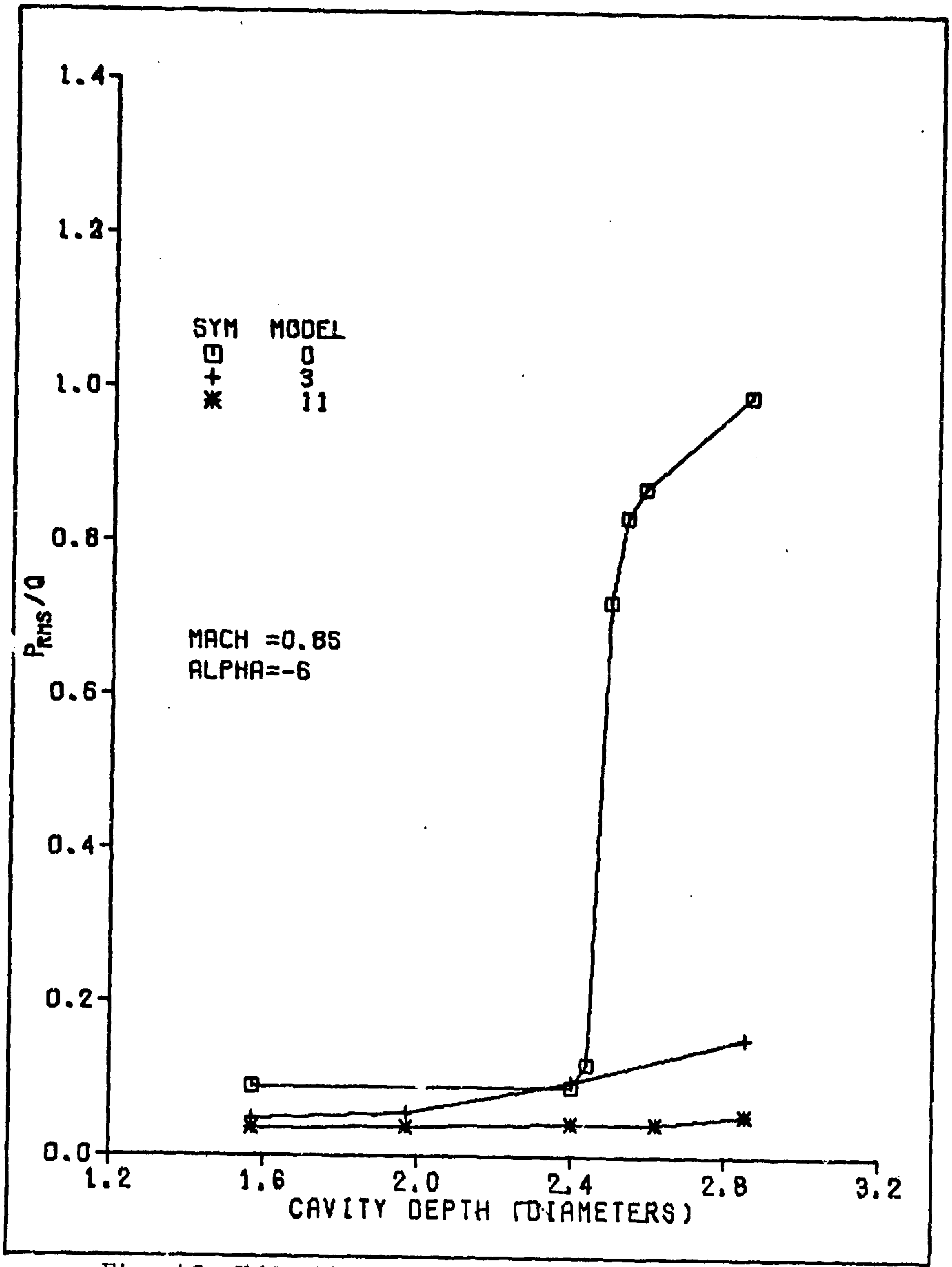

Fig. 49. Effectiveness of Models 3 and 11 in Reducing the RMS Pressure for Various Cavity Depths, Mach=0.85, Alpha =-6

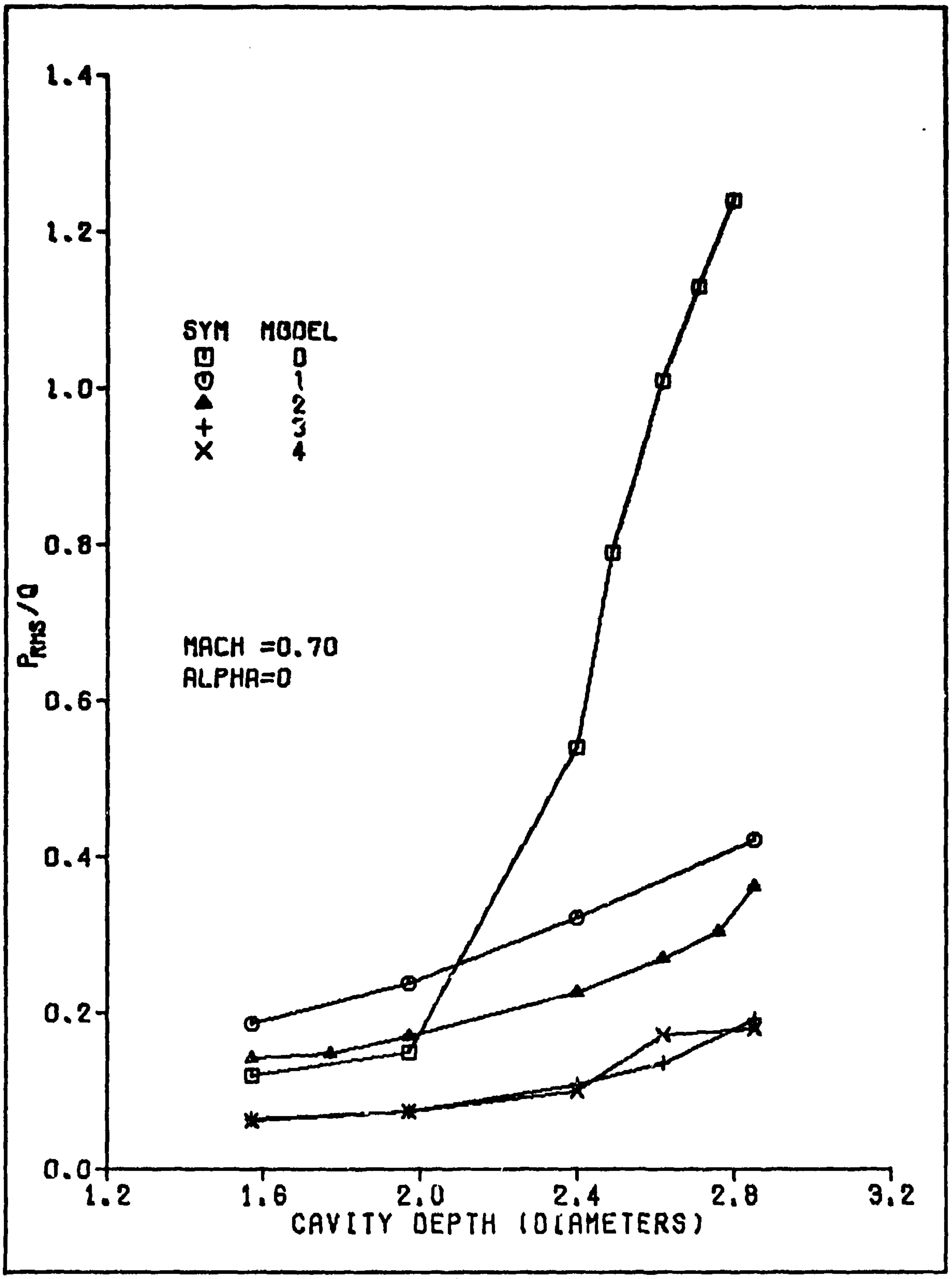

Fig. 50. Effectiveness of Models 1,2,3, and 4 in Reducing the RMS Pressure for Various Cavity Depths, Mach=0.70, Alpha = 0

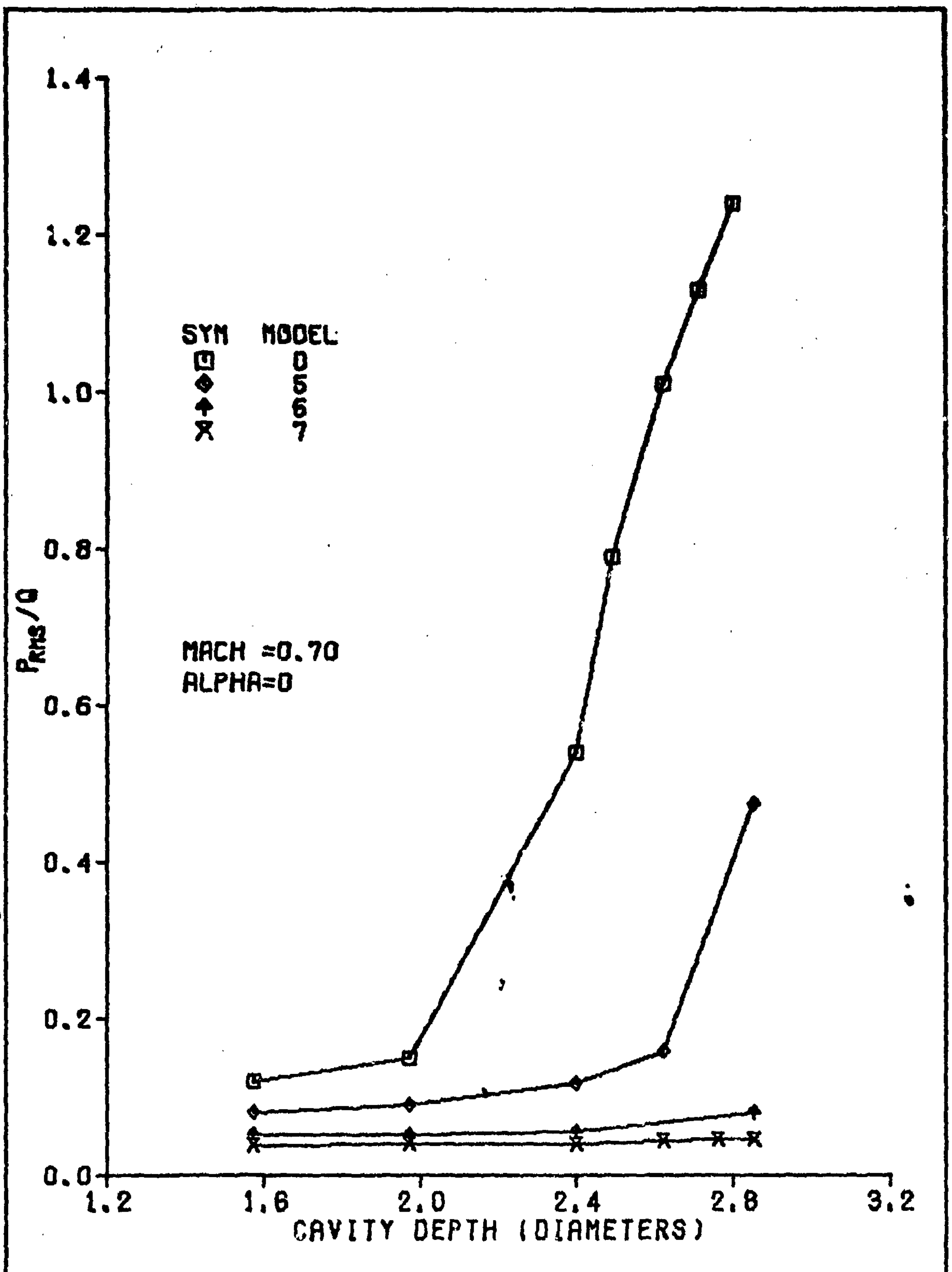

Fig. 51. Effectiveness of Models 5,6, and 7 in Reducing the RMS Pressure for Various Cavity Depths, Mach=0.70, Alpha = 0

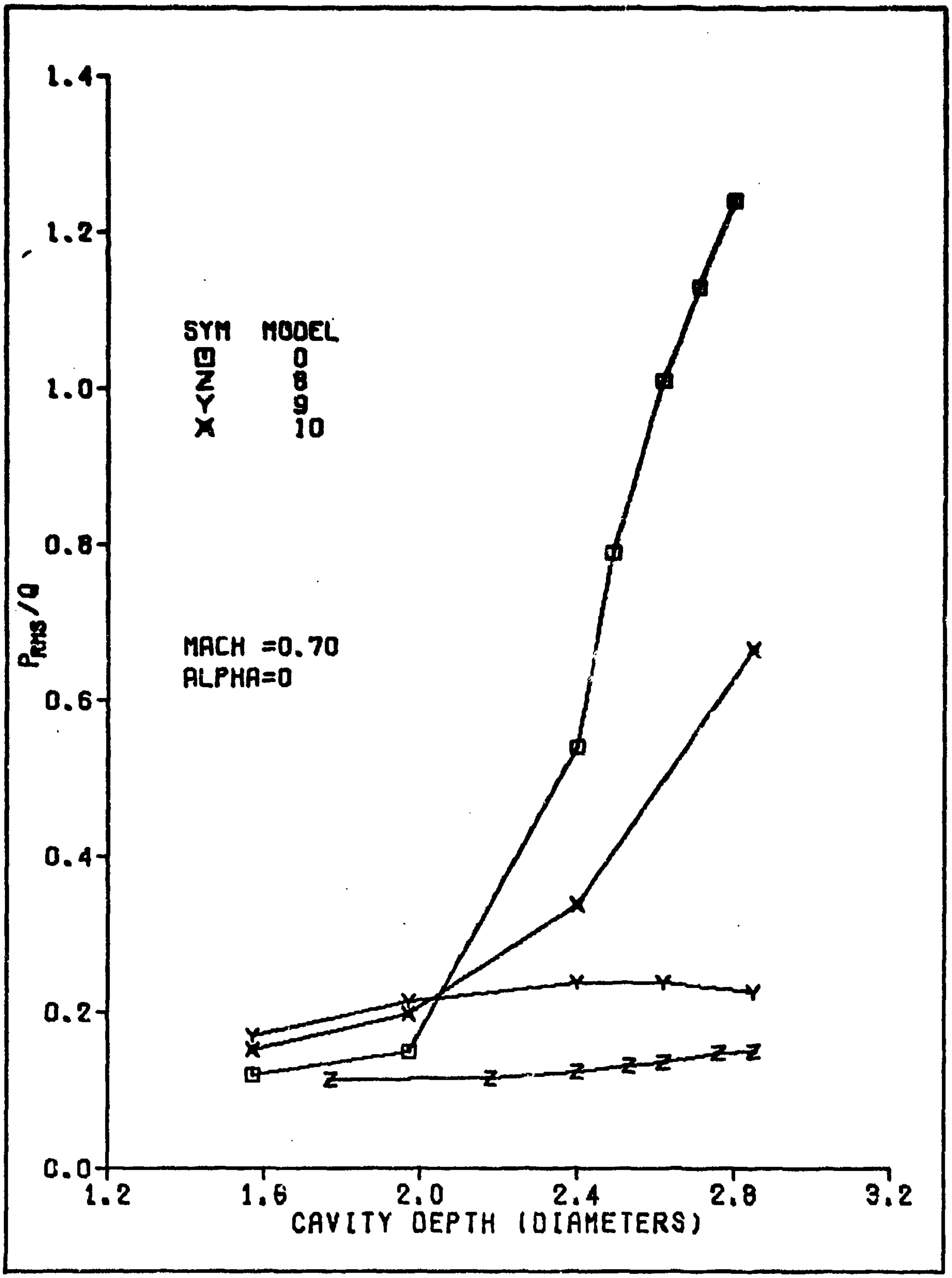

Fig. 52. Effectiveness of Models 8,9, and 10 in Reducing the RMS Pressure for Various Cavity Depths, Mach=0.70, Alpha = 0

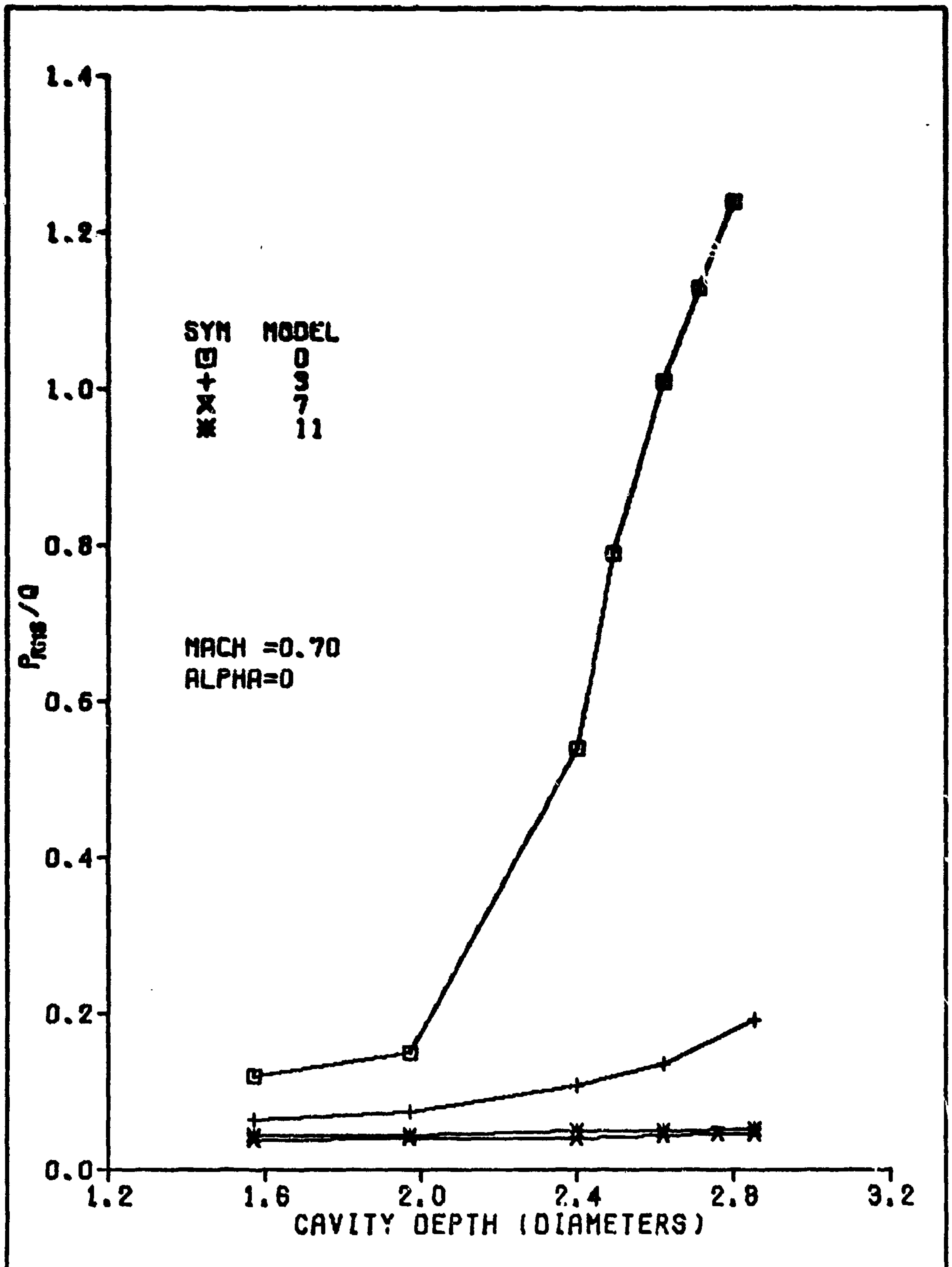

Fig. 53. Effectiveness of Models 3,7, and 11 in Reducing the RMS Pressure for Various Cavity Depths, Mach=0.70, Alpha = 0

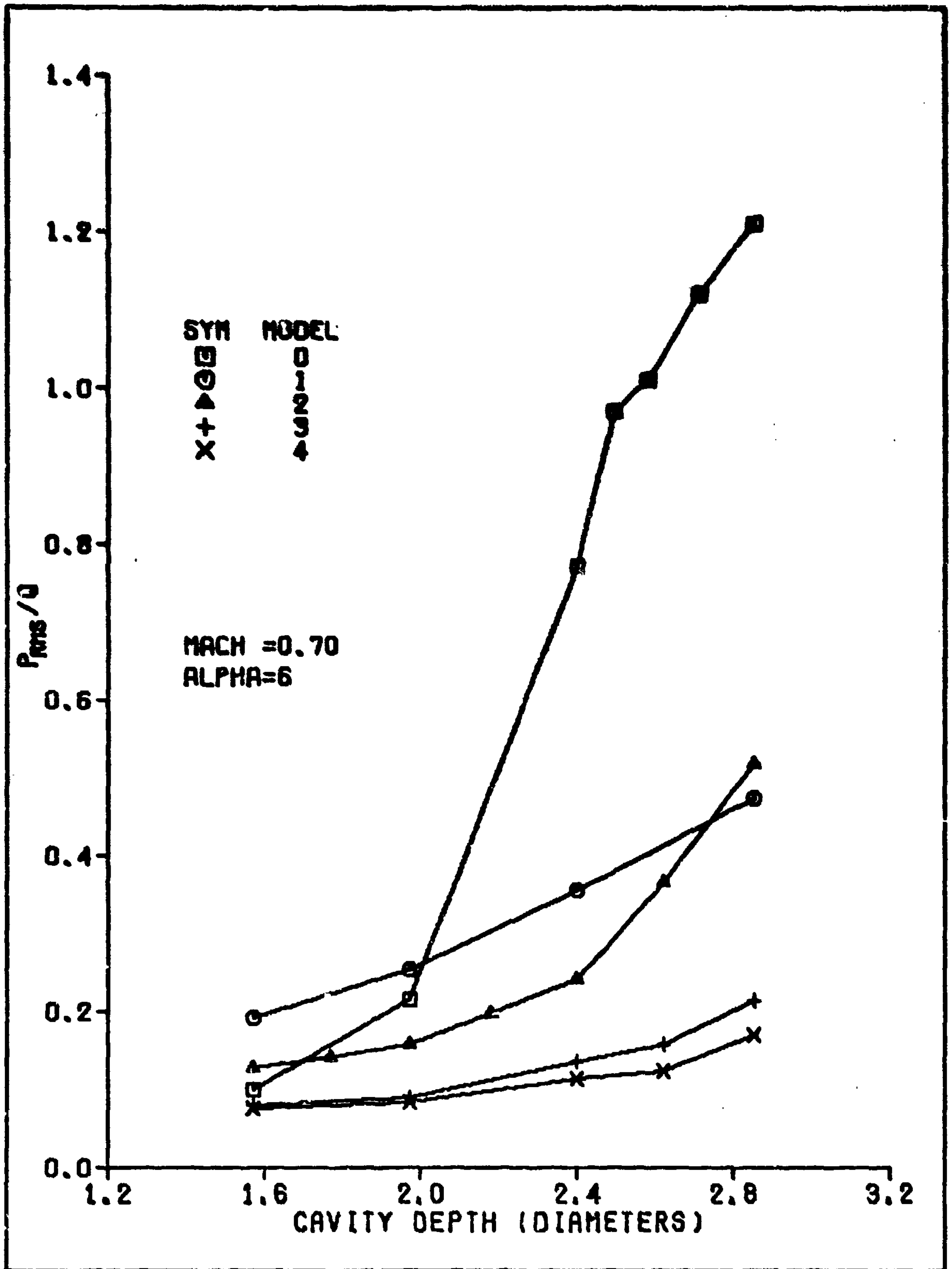

Fig. 54. Effectiveness of Models 1,2,3, and 4 in Reducing the RMS Pressure for Various Cavity Depths, Mach=0.70, Alpha = 6

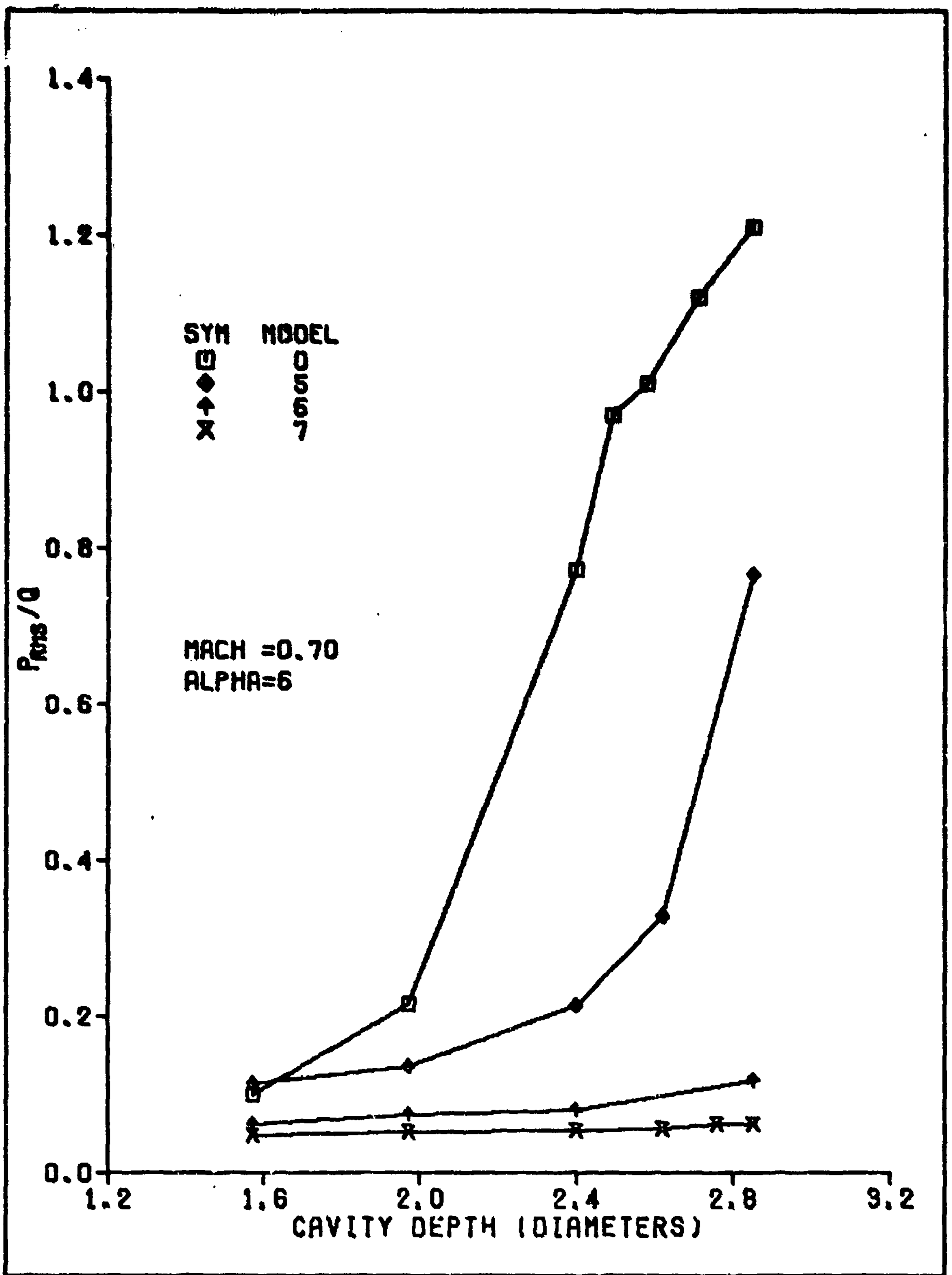

Fig. 55. Effectiveness of Models 5,6, and 7 in Reducing the RMS Pressure for Various Cavity Depths, Mach=0.70, Alpha = 6

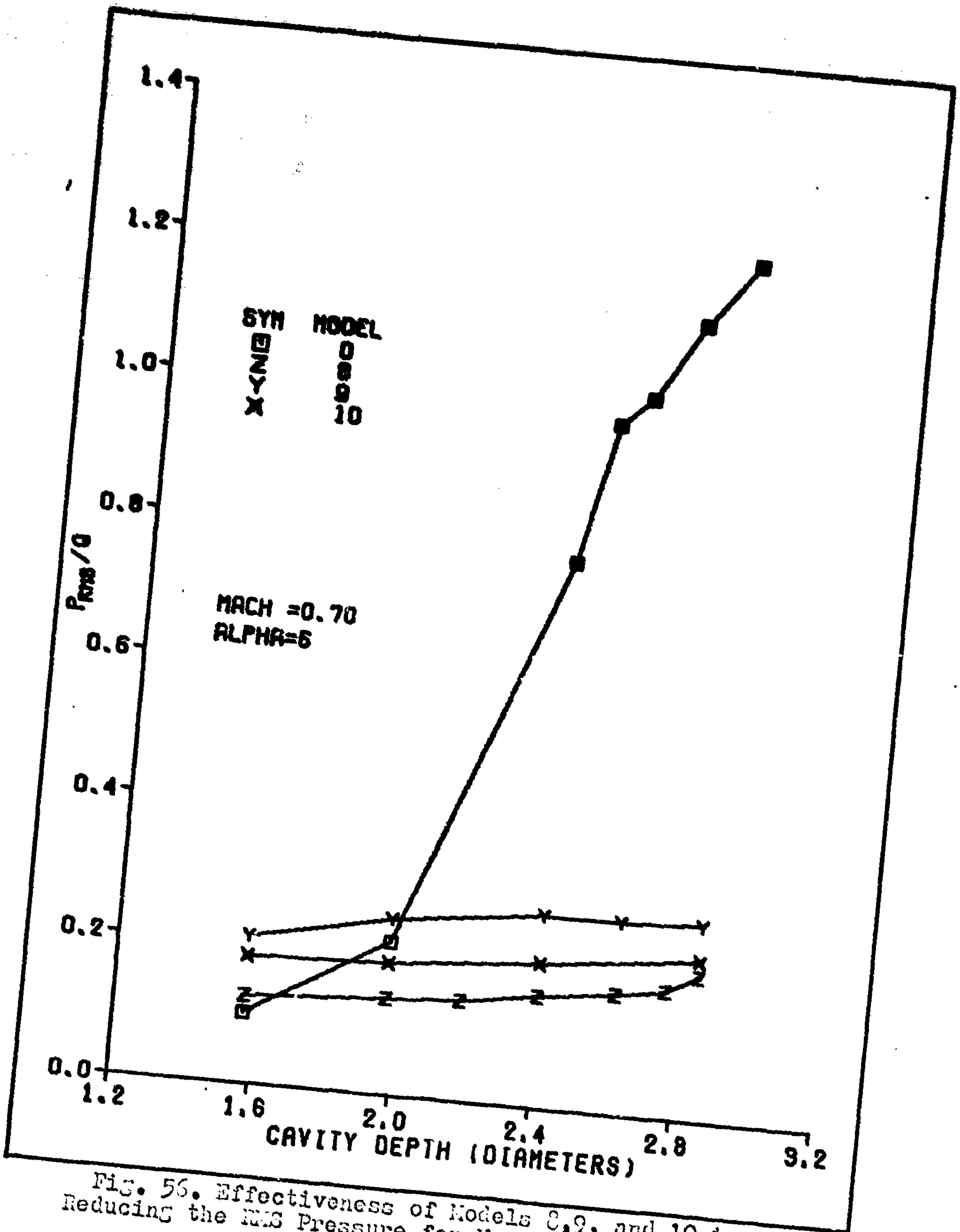

Fig. 56. Effectiveness of Models 8,9, and 10 in Reducing the RMS Pressure for Various Cavity Depths, Mach=0.70, Alpha = 6

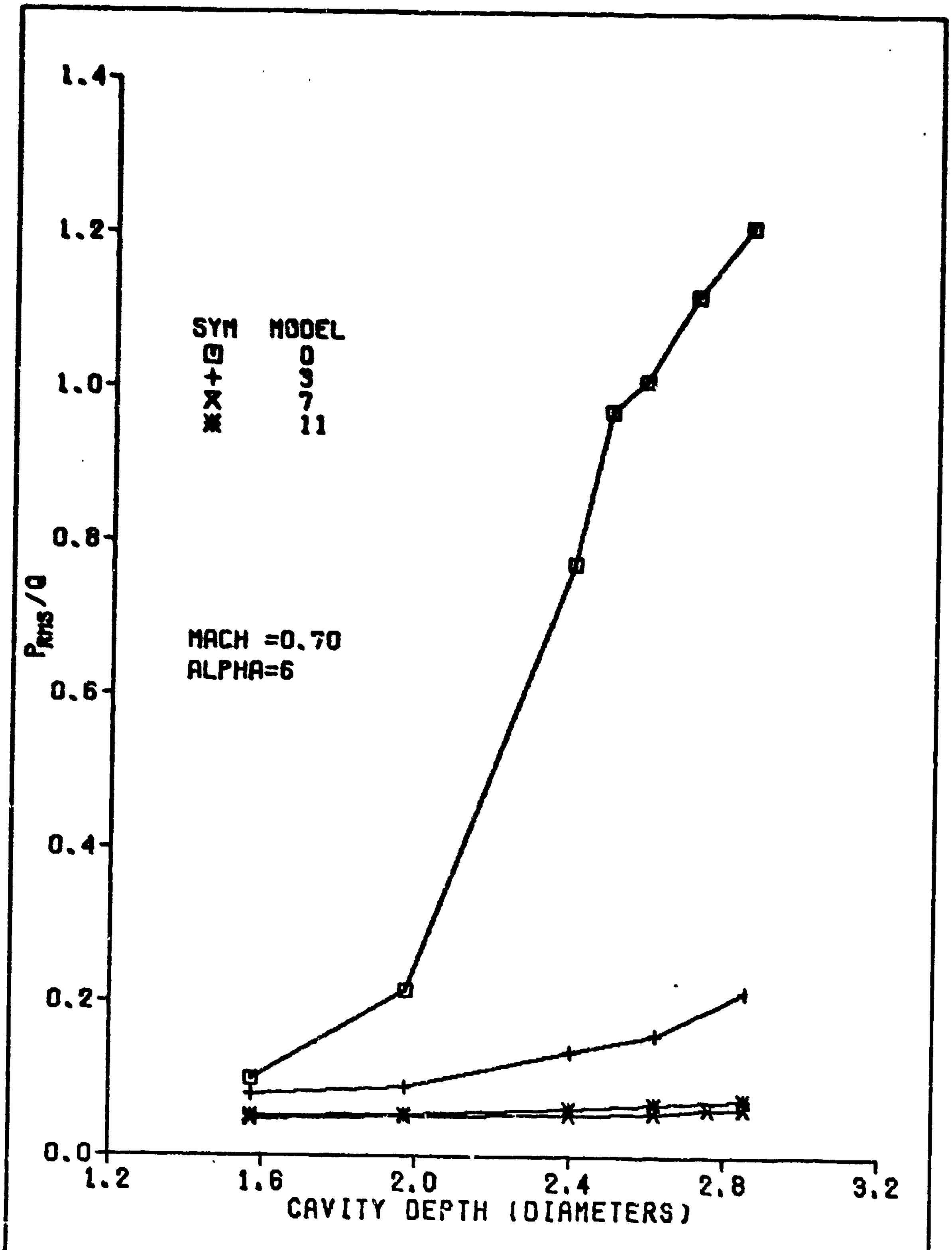

Fig. 57. Effectiveness of Models 3,7, and 11 in Reducing the RMS Pressure for Various Cavity Depths, Mach=0.70, Alpha = 6

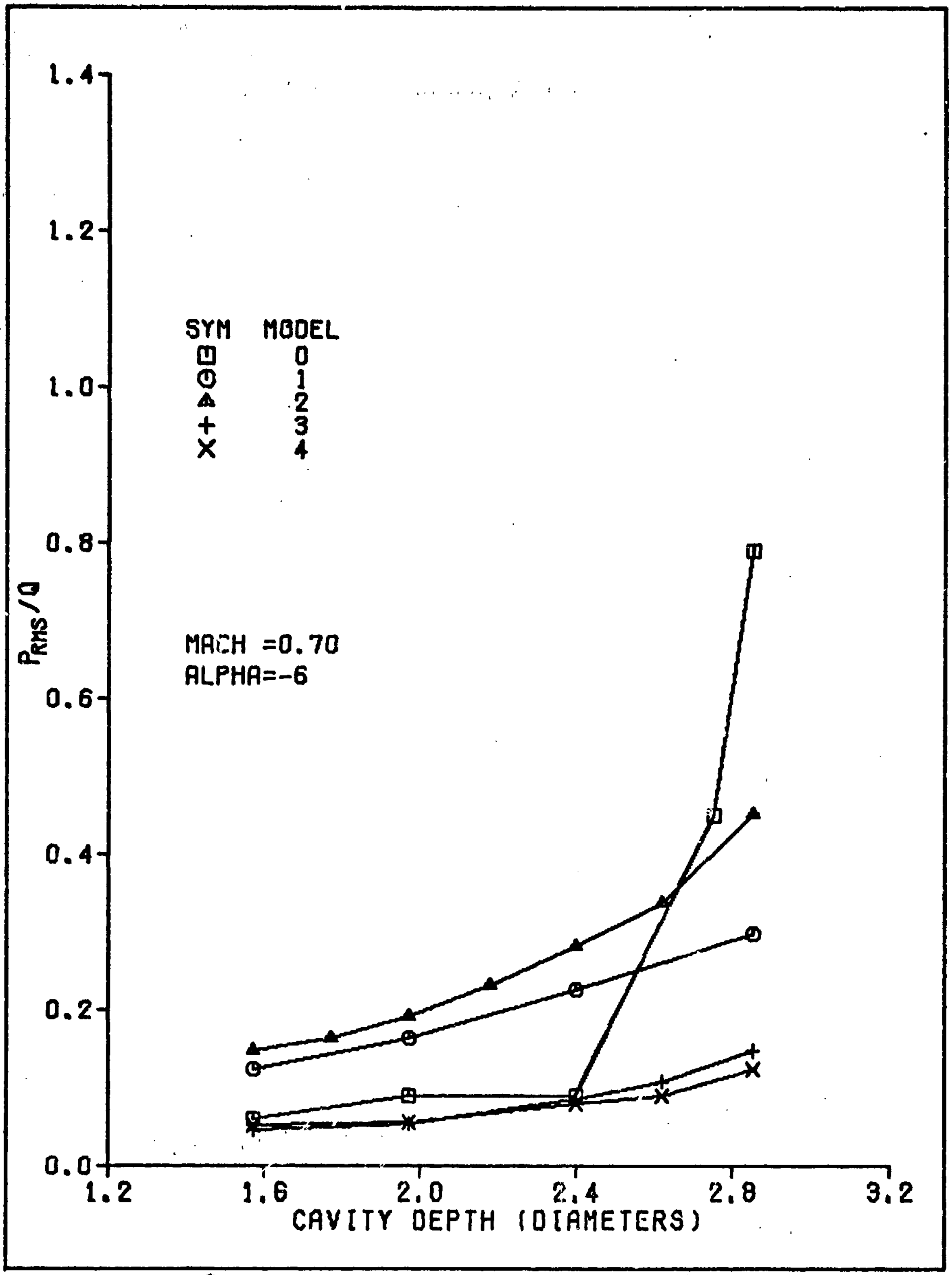

Fig. 58. Effectiveness of Models 1,2,3, and 4 in Reducing the RMS Pressure for Various Cavity Depths, Mach=0.70, Alpha =-6

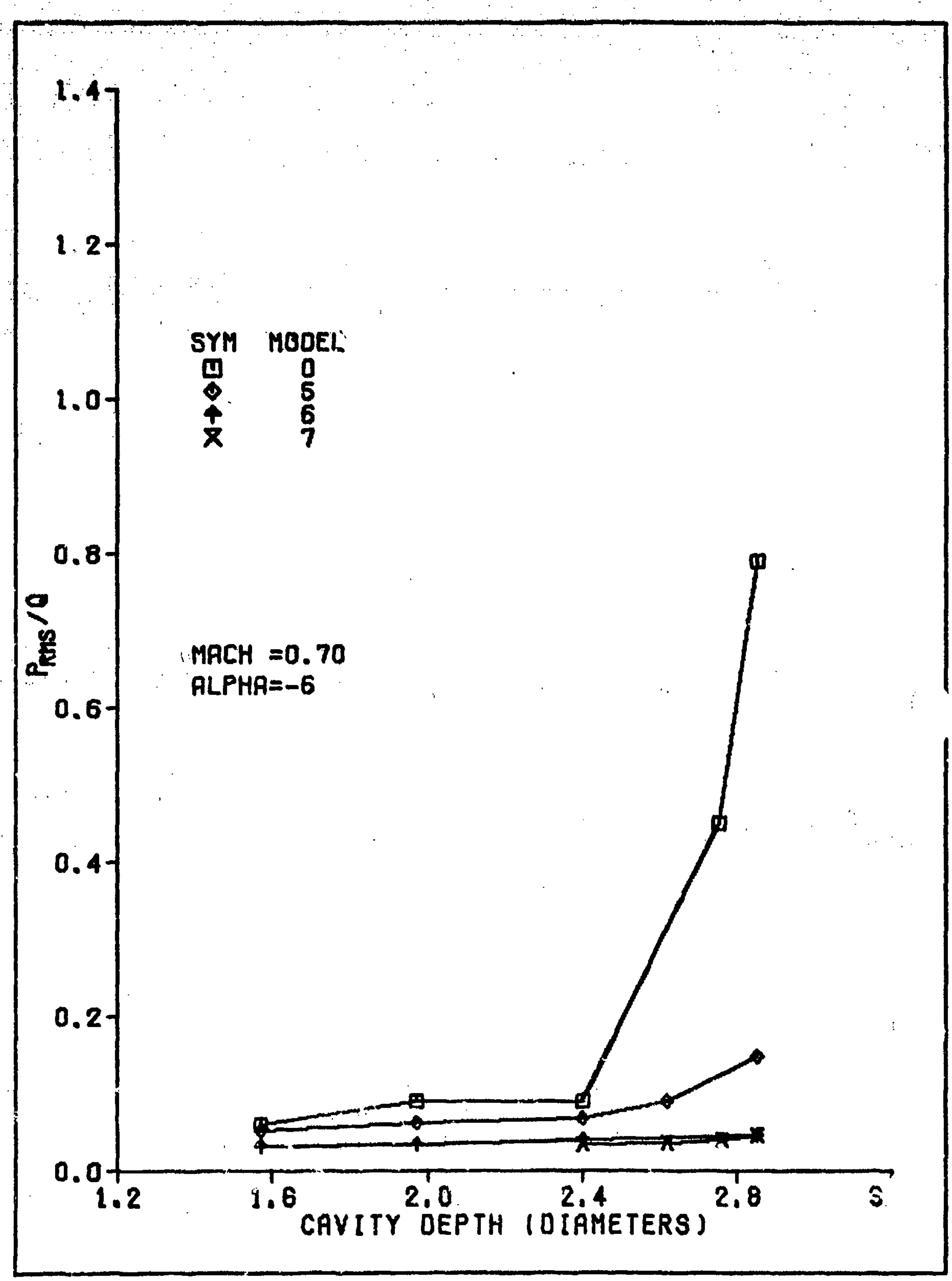

Fig. 59. Effectiveness of Models 5,6, and 7 in Reducing the RMS Pressure for Various Cavity Depths, Mach=0.70, Alpha =-6

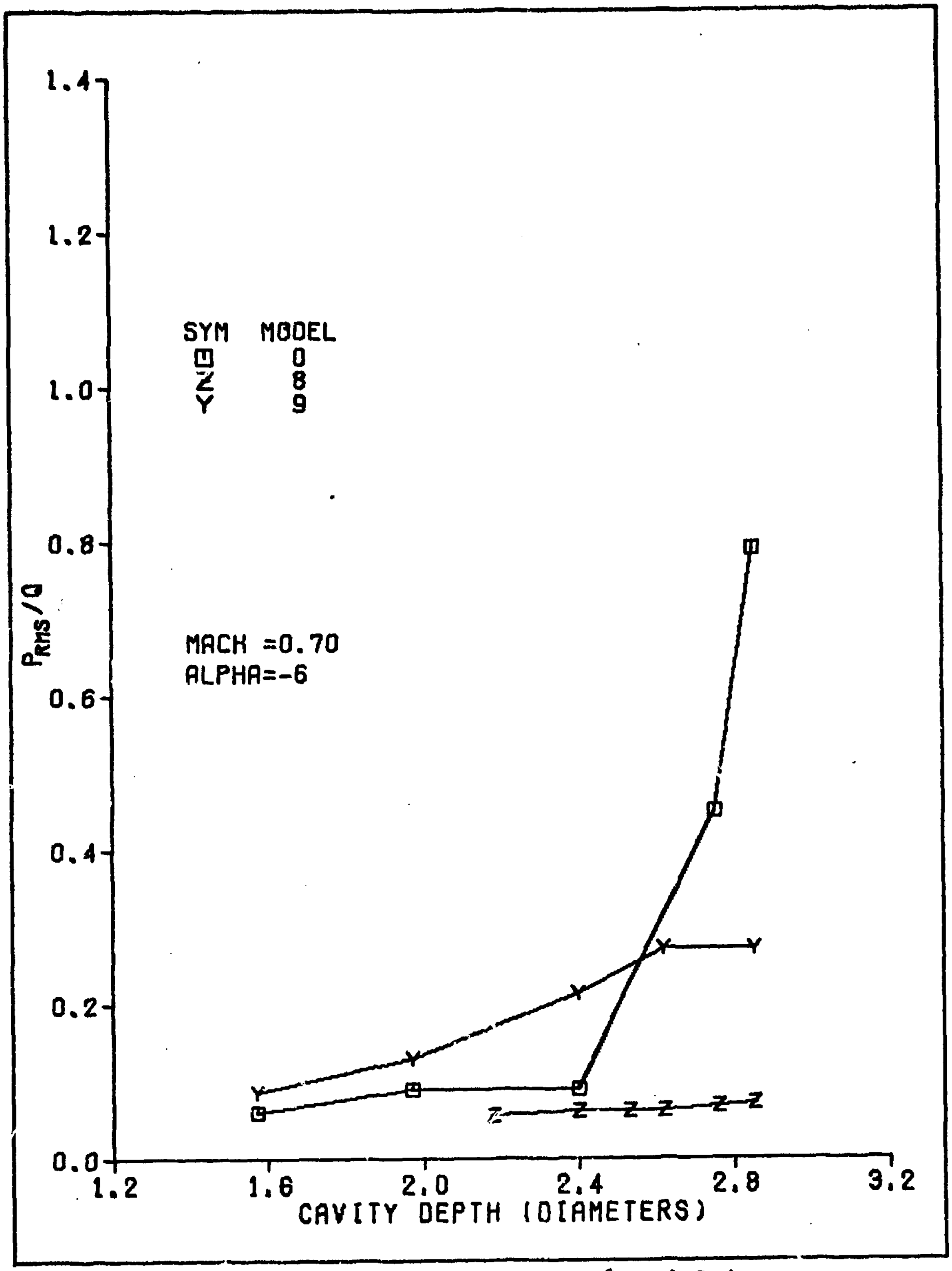

Fig. 60. Effectiveness of Models 8 and 9 in Reducing the RMS Pressure for Various Cavity Depths, Mach=0.70, Alpha =-6

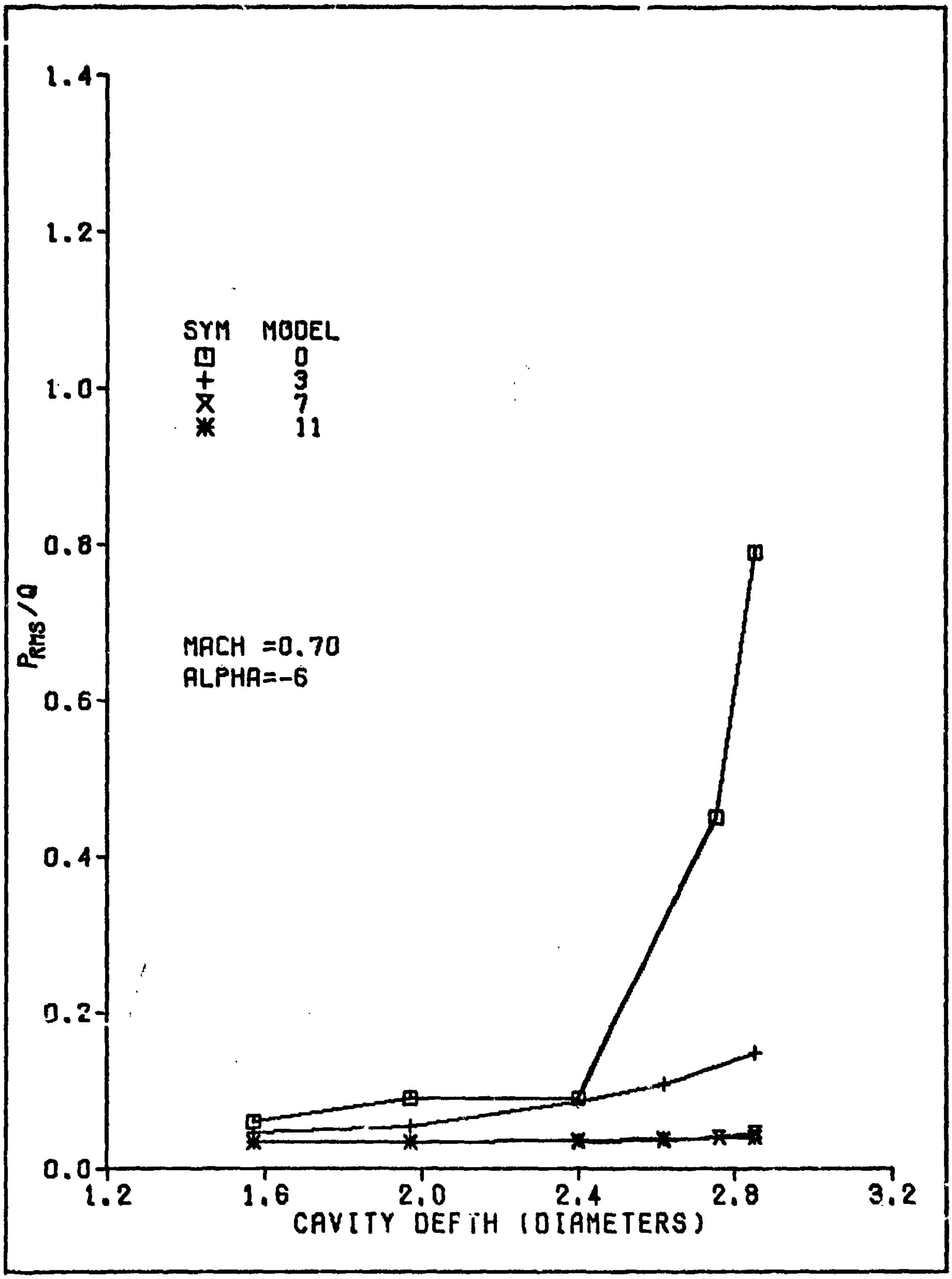

Fig. 61. Effectiveness of Models 3,7, and 11 in Reducing the RMS Pressure for Various Cavity Depths, Mach=0.70, Alpha =-6

Vita

Kenneth Vaccaro was born on 29 November 1951 in Rome, New York. Graduating in 1969 from Washingtonville High School, Washingtonville, New York, he then attended the United States Military Academy at West Point, New York, where he received the degree of Bachelor of Science in 1973. He accepted his commission as a Lieutenant in the USAF in June, 1973, and his initial assignment was to the Air Force Institute of Technology.

Permanent address: 347 Mohawk St.
Rome, New York
13440

This thesis was typed by Miss Sharon Bjurstrom.